View metadata, citation and similar papers at core.ac.uk

brought to you by CORE

provided by DCU Online Research Access Service

Analysis of Oxidative Damage to DNA Mediated by Transition Metal-Fenton Reactions

by

Michele Kelly B.Sc.
51431447

Thesis submitted for the degree of Doctor of Philosophy.

Supervisors:

Prof. Malcolm R. Smyth

Dr. Blánaid White

Dublin City University **September 2008**

DECLARATION

I hereby certify that this material, which I now submit for assessment is entirely my own work and has not been taken from the work of others save and to the extent that such work has been cited and acknowledged within the text of my work. I make this declaration in the knowledge that a breach of the rules pertaining to project submission may carry serious consequences.

I am aware that the project will not be accepted unless this form has been handed in along with the project.

Signed: _____

ID No.: _____

Date: _____

TABLE OF CONTENTS

ABBREVIATIONS

$^1O_2$	singlet oxygen
3,4-DHBA	3, 4-dihydroxybenzoic acid
4-HBA	4-hydroxybenzoic acid
5'-dGMP	2-deoxyguanosine-5'-monophosphate
8-OHdG	8-hydroxy-2'-deoxyguanosine
8-OHG	8-hydroxyguanine
8-oxoA	8-oxoadenine
8-oxoG	8-oxoguanine
ACN	acetonitrile
A	adenine
Ag/AgCl	silver/silver chloride (reference electrode)
ATP	adenosine tri-phosphate
BER	base excision repair
bp	base pairs
BZ	Belousov-Zhabotinskii
C	cytosine
Cd	cadmium
CE	capillary electrophoresis
ct DNA	calf thymus DNA
Co	cobalt
Cu	copper
Cy	cyanuric acid
dA	2'-deoxyadenosine
dC	2'-deoxycytidine
DCF	dichlorofluorescin
dG	2'-deoxyguanosine
dT	2'-deoxythymidine
dU	2'-deoxyuridine
DMPO	5,5-dimethyl-1-pyrroline N-oxide

DMSO	dimethyl sulfoxide
DNA	deoxyribonucleic acid
ds DNA	double-stranded DNA
e^-	electron
ECD	electrochemical detection
EDTA	ethylenediaminetetraacetic acid
EI	electron ionisation
EIC	extracted ion chromatogram
ELISA	enzyme linked immunosorbent assay
EOF	electroosmotic flow
ESI	electrospray ionisation
ESR	electron spin resonance
FAB	fast atom bombardment
FapyG	2,6-diamino-4-hydroxy-5-formamidopyrimidine
Fe^{2+}	ferrous iron
Fe^{3+}	ferric iron
FPG	formamidopyrimidine DNA glycosylase
G	guanine
GC	gas chromatography
Gh	guanidinohydantoin
H	hydrogen
H^+	proton
H_2O_2	hydrogen peroxide
HOGG1	human 8-oxoG DNA glycosylase
HPLC	high performance liquid chromatography
I^-	iodide
I_2	iodine
Iz	2,5-diaminoimidazolone
LOD	limit of detection
m/z	mass to charge ratio
MALDI	matrix assisted laser desorption/ionisation

MeOH	methanol
Mg	magnesium
Mn	manganese
MS	mass spectrometry
NADH	nicotinamide adenine dinucleotide
NaOH	sodium hydroxide
NER	nucleotide excision repair
NHE	normal hydrogen electrode
NP	normal phase
Oa	oxaluric acid
·OH	hydroxyl radical
oxGh	oxidised guanidinohydantoin
Oz	2,2,4-triaminooxazalone
ROS	reactive oxygen species
RP	reversed phase
RSD	relative standard deviation
SOD	superoxide dismutase
SSB	single strand break
S/N	signal to noise ratio
Sp	spiroiminodihydantoin
SPE	solid phase extraction
ss DNA	single-stranded DNA
SWV	square wave voltammetry
T	thymine
TLC	thin layer chromatography
TMS	trimethylsilane
U	uracil
UV	ultra violet
X	xanthine
Zn	zinc

ABSTRACT: ANALYSIS OF OXIDATIVE DNA DAMAGE MEDIATED BY TRANSITION METAL-FENTON REACTIONS

Oxidative damage to DNA is implicated in numerous diseases and disorders including, but not limited to cancer, neurodegeneration and inflammation. There are many ways in which this type of damage can be caused *in vivo*, including radiation, chemical oxidation and oxidation mediated by transition metals. Oxidative damage to DNA can cause single point mutations which, when undetected and unrepaired by enzyme repair systems, can lead to transversion mutations, and errors in the DNA sequence. It is for this reason that this damage is very significant *in vivo*. It is important to determine the mechanism and the extent to which oxidative stress occurs in order to fully understand its role in both the initiation and the propagation of mutations, which are implicated in disease.

This research focused specifically on oxidative damage to guanine (G) induced by transition metals to which the human body is exposed. G is the most easily oxidised of the DNA bases, and so G oxidation products are primarily investigated as potential biomarkers. The transition metals Ni, Co, Mn, Zn and Cd, which had previously not been investigated in detail as potential Fenton catalysts *in vivo,* were examined by HPLC with UV, ECD and MS detection. Existing methodologies were improved by exploiting monolithic column technology, reducing analysis time by 90%. Coupling monolithic columns to ECD detection, not achieved previously, allowed rapid, specific and sensitive detection of oxidative damage products. This enabled a comprehensive comparison of oxidative product formation over time for a range of transition metals.

All metals showed an erratic formation of G oxidation product 8-oxoG with oscillatory-type patterns over time. This highlighted 8-oxoG's inadequacies as a biomarker of oxidative damage to DNA, and more stable biomarkers were investigated as a result. Ni, Co and Mn were all shown to provoke the formation of 8-oxoG oxidation product oxidised guanidinohydantoin (oxGH), when a solution of G was analysed, and guanidinodihydantoin (GH) from G within the DNA backbone. Zn and Cd did not mediate appreciable formation of any 8-oxoG oxidation products above control levels. These results are significant for a number of reasons. They establish that 8-oxoG is merely an intermediate in the oxidation of G, and its ease of further oxidation means that it is not suitable as a biomarker of oxidative damage to DNA. The further oxidation products oxGH and GH do form in steady increasing patterns over time, and therefore would be more suitable for use as biomarkers. Differences between transition metal mediation of oxidative damage to DNA were also emphasized at this stage.

This research then examined the nature of the ROS involved for these transition metals, using hydroxyl radical (˙OH) scavenger 4-hydroxybenzoic acid (4-HBA). Fe is known to generate ˙OH from the Fenton reaction, though there is extremely limited research to date on the other transition metals. It was observed that none of the metals Cu, Ni, Co, Mn, Cd or Zn behaved similarly to Fe, suggesting they did not generate ˙OH. However, Ni, Co, Cu and Cd all appeared to react in a similar fashion, generating a reactive species which did consume the radical scavenger. Mn and Zn, the two essential dietary metals, also showed similarities to each other, with neither metal resulting in ROS formation detectable by 4-HBA.

ACKNOWLEDGEMENTS

First and foremost, I would like to extend my deepest thanks to Prof. Malcolm Smyth for his guidance, support and his help over the course of my research. I would also like to thank Dr. Blánaid White, not only a fantastic mentor but a great friend. Her support and encouragement was unending throughout and her friendship invaluable. I thank the rest of the members of my research group: the Sensors and Separations Group (SSG!) past and present: Gill, Kyriaki (my mommy), Laura, Jeremy, Tony, Aoifs, Ewa, Karl, Fu-Qiang, Adriano, Xiliang, Ciarán, Eimer, Geoff, Amy, Ciara, Aaron and Combs for their friendship and support. Thanks also to the DCU technical staff and faculty for their help with random queries.

Thank you to my manager and team lead at Bristol-Myers' Squibb during my part-time-student years, Dr. Augusta Conway and Dr. Keith Hanlon, for their help and encouragement, and also to my fellow MT colleagues and shift buddies, thanks for the support!

I wish to thank all of my friends in DCU for keeping my spirits high: Stephen "Riddled with Gorgeous" Finn, my little buttercup and my robotic dance partner; thanks for keeping me sane and keeping me laughing; Colm "Molm" Mallon, for your many years of friendship; Emmet "Smemmet" O'Reilly, thanks for the coffee breaks, chats and high fives; Eoin "Dodgy Knee" Sheridan, for being a good listener; Rob Groarke, for letting me be your bass player despite my lack of talent and bass guitar. Also thanks to Lynda Cosgrave, Claudio "Donkey" Zuliani, Andrea McNally, Elaine Spain, Bincy Jose, Anita V., Giovanni "Gi-Gi" Valenti, Lynn Dennany, and Fadi Hatoum for being the most fun bunch of people in the world.

An honourable mention should also go to the Starbucks Corporation for supplying me with my sometimes more than twice-daily fix of caffeine, without which I would be a cranky, irate, sarcastic and horrible person and would not have had any of these friends to thank.

Thank you to my oldest friends; my extended family; Francesca Murray, thanks for the good times and the great times ever since I've known you!!! Thanks to Stuart Clarke; my brother from another mother. To Phil Howlett, Donal Campion, Mark Keogh and Jennifer Egan; thanks for all the fun and frolics over the years.

An enormous thank you to Seán Somers for everything over the years and especially for the last few months, for keeping me smiling, and for all of the hugs and kind words that always make me see that nothing is as bad as it seems.

And finally, but most importantly, to my family; my parents, Patricia and Michael, who have supported me and have never stopped encouraging me throughout my life. To my siblings, Lilian, Brian and Michael, my family-in law Jess and Ian and my baby niece Aoife; I thank you all with all of my heart for your guidance and encouragement over the last few years, for supporting me through this epic battle and for always standing by me and my decisions. Thank you for your unconditional love for me and for each other, without which I wouldn't be where I am today.

This thesis is dedicated to my parents, Patricia and Michael Kelly.

1 OXIDATIVE DAMAGE TO DNA: A LITERATURE SURVEY

1.1 INTRODUCTION

1.1.1 Introduction to DNA

Even before the discovery of deoxyribonucleic acid (DNA) and the genetic code, it has always been common knowledge that we inherit certain traits from our parents. It was shown that chromosomes, and later that certain genes on these chromosomes, provided the genetic information that gives us our distinguishing traits, an idea proposed by Gregor Mendel that was later confirmed T.H. Morgan [1]. The debate subsequently centred on whether it was DNA or proteins that were the actual genetic material. These are both present in the chromosome, and both appeared to have active functions in the body. Substantial research was carried out on DNA in bacterial cells during the early half of the 1900s. The three dimensional molecular structure of double helix DNA was then proposed by Watson and Crick in 1953 [2]. DNA is comprised of hydrogen bond paired nucleotides: bases, connected to ribose sugar moieties and phosphate groups, arranged in a helical structure. The four bases of DNA are Adenine (A), Cytosine (C), Guanine (G) and Thymine (G), the structures of which are shown below in Scheme 1.1.

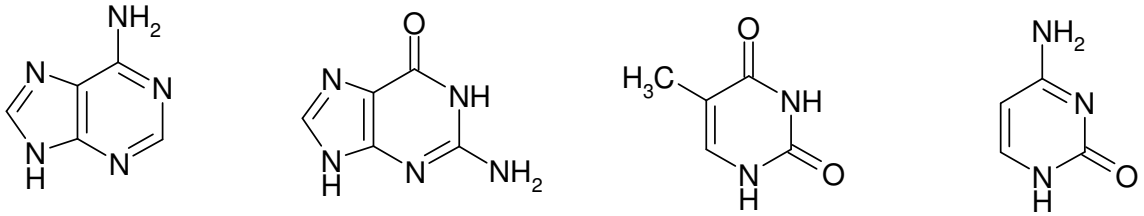

Scheme 1.1: Structures of DNA bases Adenine, Guanine, Thymine and Cytosine.

A and G are substituted purines and T and C are substituted pyrimidines. The base pairs consist of one purine and one pyrimidine base; A is paired with T, and G with C [2, 3]. The base pairs and double helix structures are illustrated in Fig. 1.1 and 1.2.

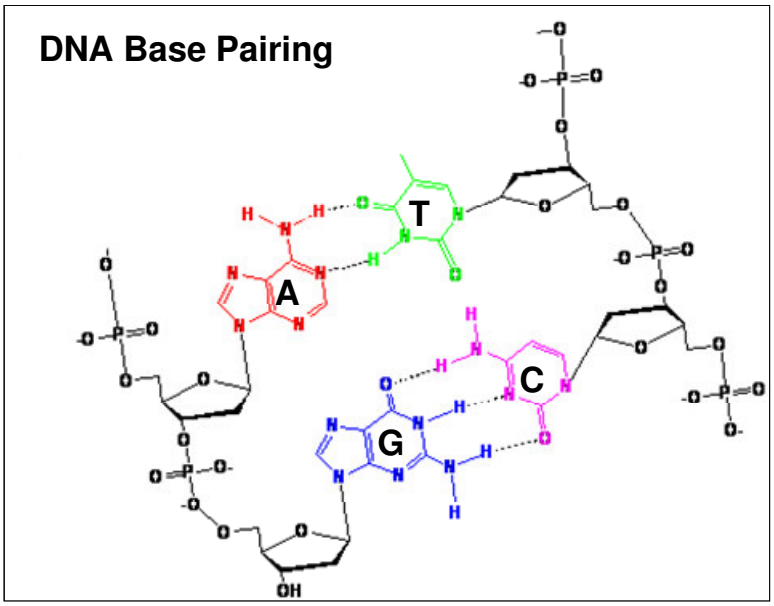

Fig. 1.1: Base pairs A-T and G-C in DNA. (Reproduced from Matthews and Van Holde [3]).

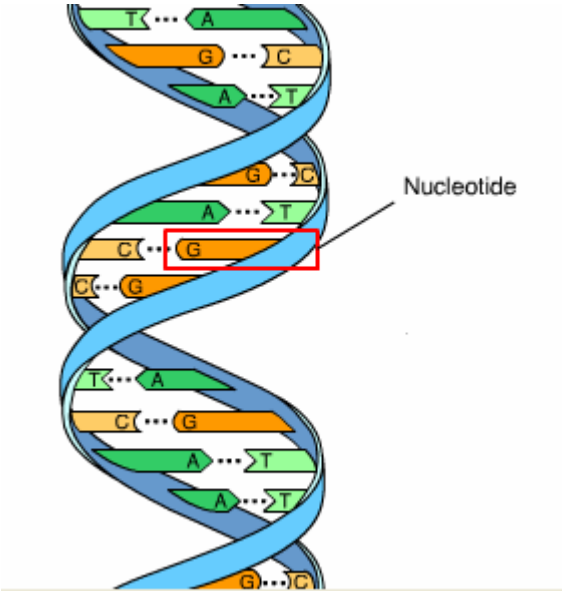

Fig 1.2: The double helix structure of DNA illustrating base pairing of A-T and G-C. (Reproduced from Campbell, Reece and Mitchell [1]).

1.1.2 Implications of DNA damage

When DNA is damaged, the damage can cause adverse effects, inducing various diseases and disorders. DNA is the control centre that codes protein synthesis and genetic traits. Therefore damage that changes its composition by causing base mutations or strand breaks can obviously have great implications. Damage to DNA can cause a transversion mutation, causing for example G:C to be incorrectly replaced by T:A during replication, as discussed in Section 1.2.2 [2,3]. DNA damage is implicated in a wide spectrum of clinical conditions including lethal and incurable disorders such as cancer, neurodegeneration and heart disease among others [4, 5]. Heart disease and cancers are the two primary causes of death in the western world [6-8].

1.1.3 Oxidative damage to DNA

Cells are constantly exposed to oxidants from various physiological processes such as mitochondrial respiration, and pathological processes such as inflammation, ischemia, foreign compound metabolism and radiation [5, 9]. Oxidative damage to DNA has been very widely studied, due to the implications discussed previously. The mechanisms of oxidative DNA damage have yet to be fully elucidated. Oxidative damage to DNA is caused by a range of exogenous and endogenous factors. Exogenous causes of oxidative damage to DNA include UV and ionising radiation, and endogenous agents of oxidative damage to DNA include free radical reactive oxygen species (ROS) and transition metals, which will be discussed in subsequent chapters [5].

1.2 DNA OXIDATION

1.2.1 How easy is it to oxidise DNA?

Of the four DNA bases, G, C, A and T; G is the easiest to oxidise. The oxidation potentials of each of the four bases are shown in Table 1.1. G is an electron rich DNA base moiety [10, 11], and so will attract electron scavengers such as hydroxyl radicals, singlet oxygen and other reactive oxygen species (ROS).

Oxidation products of the other bases have also been studied, but not to the same extent as G oxidation [12, 13]. The ease of oxidation of G accounts for the abundance of its oxidation products.

Oxidation Potentials of DNA Bases	
Base	*Potential (V) vs. NHE*
Cytosine	1.7
Thymine	1.6
Adenine	1.42
Guanine	1.29
8-Oxoguanine	0.74

Table 1.1: Oxidation Potentials of the DNA bases and 8-oxoGuanine [10, 11].

1.2.2 Guanine Oxidation

The structure of G, illustrating the available spots for oxidation is shown in Scheme 1.2. G undergoes a H^+ coupled, e^- oxidation and can be oxidised at the C4, C5 or C8 position [11, 14]. On oxidation at either the C4 or C5 position, radical 4- and 5- hydroxyguanine species are generated. These are very reactive and can regenerate the G moiety by an autocatalytic regeneration process, serving as catalysts for the regeneration of G [15].

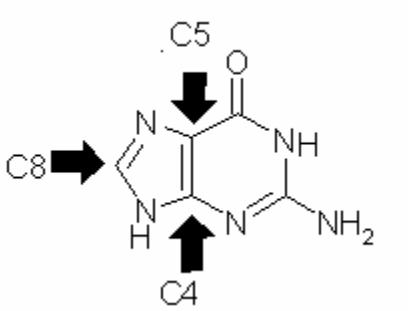

Scheme 1.2: Susceptible sites for G oxidation [14].

However, when G undergoes oxidation at the C8 position, the resulting product, redox ambivalent G-8-OH, can go on to form 8-oxoG, as well as being

reduced to form a formamidobipyrimidine derivative (Fapy-G), discussed below. 8-oxoG has been studied as a biomarker of DNA damage, and is the most studied of the DNA oxidation products [14]. The structure of 8-oxoG is shown below in Scheme 1.3.

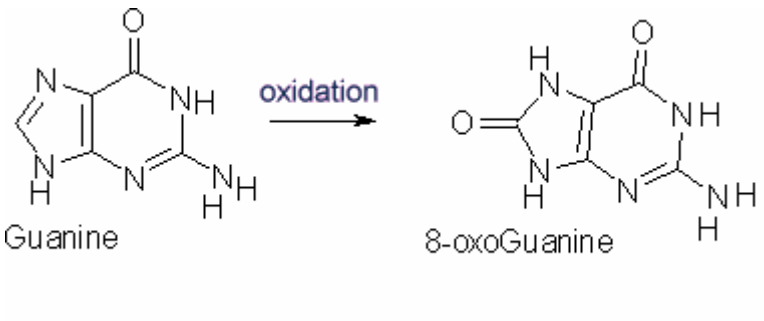

Scheme 1.3: G is oxidised to form 8-oxoGuanine (8-oxoG) [3].

The first step of G oxidation is an outer sphere one electron oxidation, or oxo transfer [16]. An outer-sphere electron transfer is a reaction in which the electron transfer takes place with weak or no (4 -16 kJ mol^{-1}) electronic interaction between reactants in the transition state. An inner-sphere electron transfer would occur when there is strong electronic coupling between reactants [17]. Oxo-transfer occurs when an oxo- group or double bonded oxygen is transferred from one moiety to another. This has been implicated in chromium-mediated oxidative DNA damage. This oxo-group transfer from oxo-Cr(V) does not involve an activated oxygen species such as the reactive oxygen species that are discussed later, but rather a direct atom transfer reaction [16].

Similarly, the nucleoside, 2'-deoxyguanosine (dG) can be oxidised to 8-oxo-2'deoxyguanosine (8-oxodG) [18, 19]. In 1999, Cadet *et al.* described the

mechanisms of hydroxyl radical (˙OH) induced formation of 8oxodG [18]. This mechanism illustrates the formation of a guanyl radical, 8-OH-$G^{\bullet+}$ on oxidation of dG, which is quickly reduced or oxidised to either the formamidopyrimidine dG (Fapy-dG) derivative or 8-oxodG, respectively. A study by Crespo-Hernandes and Arce showed opening of the imidazole ring of the G base moiety to result in the formation of the Fapy-G product [19].

8-oxoG is now widely accepted as an intermediate in the overall oxidation of G, and not a stable biomarker of oxidative DNA damage, because it is so easily further oxidised [10]. Many further oxidation products of 8-oxoG have been identified in the literature, some of which are illustrated in Scheme 1.4. Oxidation products of 8-oxoG that have been identified to date include guanidinohydantoin (GH), oxidised-guanidinohydantoin (oxGH), spiroiminodihydantoin (Sp), iminoallantion (Ia), cyanuric acid, oxaluric acid (Oa) and parabanic acid (Pa) [20-23]. Imidazolone (Iz) and 2, 2, 4- triaminooxazolone (Oz), are formed from the deprotonation of the G radical and not from 8-oxoG [24].

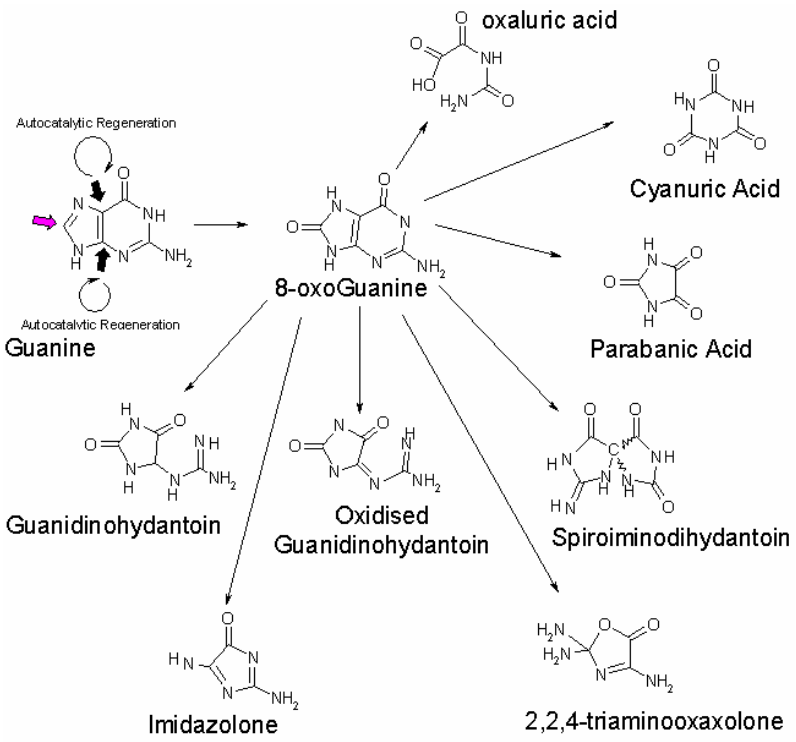

Scheme 1.4: Summary of Oxidation products of 8-oxoG as outlined in the literature [20-24].

The formation of these further oxidation products is highly dependent on the conditions to which G and 8-oxoG are subjected. The formation of GH, ox-GH, Iz, Oz, Ia and Sp from various oligomers and nucleosides, subjected to different conditions was summarised by White *et al.* [25]. It was noted that the factors determining the products formed were: pH, temperature, the oxidising agent or reactive species involved, and the source of these species, as well as the nature of the substrate: whether it is in a double stranded or single stranded DNA backbone, or studied as a free nucleoside or base [25].

These further oxidation products have been implicated as mutagenic lesions, therefore causing cancer. Henderson *et al.* illustrate this by demonstrating the mutagenic potential of hydantoin lesions. GH and both stereoisomers of Sp can cause G to C transversions, and Sp can also cause G to T transversions in DNA [26]. The mutagenicity of the 8-oxoG oxidation products is also illustrated by Burrows *et al*., who found that the oxidised lesions caused a G:C to T:A transversion mutation. The frequency of this mutation is not generally as high as that of G:C to A:T transversions, which is the most common transversion mutation, but it is relative to that of a G:C to C:G transversion [21].

1.2.3 Oxidation products of thymine, cytosine and adenine

In a review by Dizdaroglu *et al.* [27] it was evident that, although G is the most easily oxidised of the four bases, it is not always the only oxidation target. The formation of 2-OH-Adenine was investigated by Kasai *et al.* [12]. It was found that adenine triphosphate (ATP) in the nucleotide pool could be oxidised to 2-OH-ATP, which could then be incorporated as a base lesion on DNA synthesis. The 2-OH-ATP lesion was also incorporated opposite T and C, causing G:C to A:T conversions. In the same study, it was also noted that 5-hydroxy-2'cytosine caused a high frequency of C:G to T:A transversions.

Cadet *et al.* [18] reviewed the reactions of the reactive ·OH, and discussed its oxidation of T as well as G. T was oxidised to form a range of products including 5,6-dihydroxy-5-6-dihydrothymine, 5-hydroxy-5-methylhydantoin and 5-(hydroxymethyl)-2'-deoxyuridine.

1.2.4 Protection against oxidation of DNA

The cell has a vast array of preventative and repair mechanisms to prevent the destruction of DNA and other vital biomolecules from oxidative stress, among other stresses. Repair systems include nucleotide excision repair (NER), which involves the removal of bulky adducts; Mismatch repair, involving repair of mismatched bases; recombinational repair, which tackles cross-links and strand breaks [28] and base excision repair (BER), which involves the action of DNA glycosylases upon base or lesion specific enzymes such as G lesion specific human 8-oxoG DNA glycosylase (hOGG1), T and Uracil (U) specific NTH1, Fapy-lesion specific NEIL1 and hydantoin lesion specific NEIL2 [29]. The cell also has a number of protective mechanisms. Various important antioxidant enzymes including superoxide dismutase, glutathione peroxidase, and catalase, are present and can sequester various ROS before they cause oxidative stress. Superoxide dismutase (SOD) can exist in three forms Cu-Zn-SOD, Mn-SOD and EC-SOD, which exist in the cytoplasm, the mitochondria and extracellularly, respectively [30]. Superoxide dismutase works by catalysing the dismutation of superoxide anion to produce H_2O_2 and O_2 [31]. Catalase has the ability to detoxify H_2O_2, as does glutathione peroxidase as well as converting lipid hydroperoxides into non-toxic alcohols [32]. Factors affecting the concentration and activity of these enzymes include age, sex, weight and general health [33].

Dietary antioxidants are also a key factor in influencing the affect of oxidants and oxidative stress on a cell or organism by preventing the oxidation of important biomolecules. The most thoroughly researched antioxidants are Vitamin

C, Vitamin E, selenium and carotene. Vitamin C, or ascorbic acid, has been known to enhance the activity of Fe dependent enzymes and increase Fe absorption from the diet. It has, however, also been linked with promoting the Fenton reaction *in vitro* by acting as a reductant and recycling Fe(III) back to Fe(II). Its mode of antioxidant activity is by scavenging free radicals [34] and reacting to form a weakly reactive ascorbyl radical [35]. It has functions in preventing lipid peroxidation [36].

Vitamin E is comprised of 4 variants of tocopherol and 4 of tocotrienol. The most potent of these in humans is α-tocopherol, though the relative reactivities are essentially similar [37]. Dietary Vitamin E acts as a peroxyl radical scavenger and can thus prevent oxidation [38]. Selenium is used in many multivitamin supplements and in infant nutrition products. It can prevent the formation of the $^{\cdot}OH$ from H_2O_2 by enzymes [39]. It is also an important co-factor for various proteins and enzymes including glutathione peroxidase and selenoproteins [40]. Beta-Carotene is also a very important antioxidant, which acts by free radical and singlet oxygen ($^1O_2$) scavenging/quenching [41].

The bioavailability of various toxins, dietary trace elements, and drugs are also of interest when examining the effect of oxidative stress on a cell. This type of interference cannot be examined accurately *in vitro*.

1.3 THE ROLE OF REACTIVE OXYGEN SPECIES IN OXIDATIVE DAMAGE TO DNA

1.3.1 Introduction to reactive oxygen species

Free Radicals, including ROS, have been implicated in "Free Radical Theory of Aging". ROS and their mechanisms of oxidative stress on the human body are a significant cause of the degeneration of an organism over time [42]. Accumulation of products of oxidation of DNA and rates of production of ROS in organisms, as well as dietary intake of anti-oxidant and pro-oxidant species, are all determining factors in the aging of a species [42].

Free radicals, including, but not limited to, ROS, have been identified as causes of oxidative DNA damage. $^{\cdot}OH$, superoxide radicals ($O_2^{\cdot-}$) and singlet oxygen ($^1O_2$) are all examples of such species that have all been implicated in DNA damage [5].

ROS can be grouped as radical ROS, non-radical ROS, lipid peroxidation products and secondary ROS [43]. Aging is itself a degenerative disease and oxidative stress by ROS has been also implicated in other degenerative diseases. These include, but are not limited to, neurodegenerative disorders such as Dementia, Alzheimer's and Parkinson's diseases, as well as cancer and heart diseases [44-46].

Though oxygen itself is a radical species, its reactivity is not as high as the "reactive oxygen species" as its two unpaired electrons have parallel spins. These electrons are located in π anti-bonding orbitals. For oxygen to accept two electrons,

they must both have anti-parallel spins, and as this not usually accomplished in a pair of electrons, it will generally take one at a time [5]. The electron configuration illustrating the unpaired, parallel spinned electrons of molecular oxygen is shown in Fig. 1.3 below.

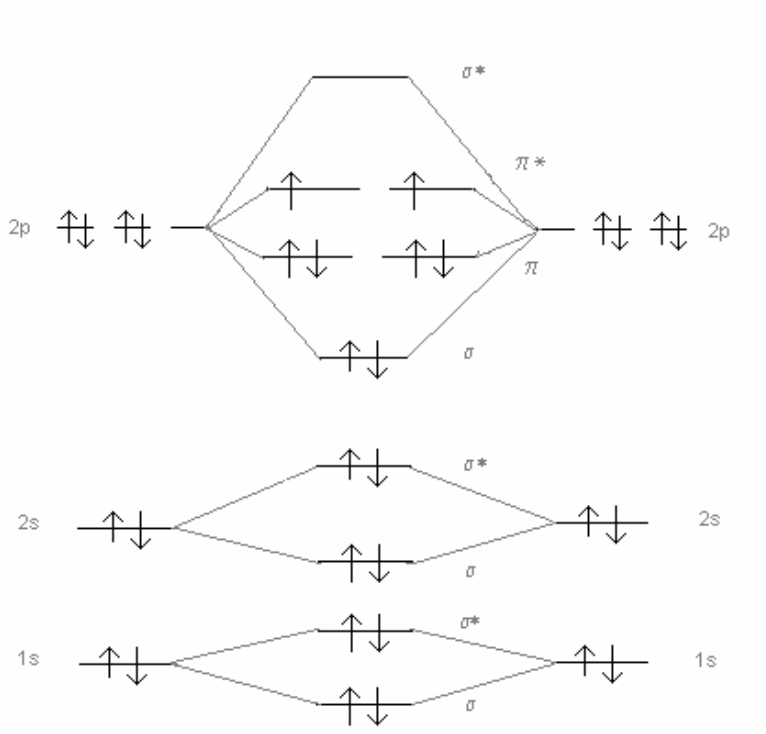

Fig. 1.3: Molecular orbital diagram showing the electron configuration of molecular O_2 [5].

The single electron reduction of oxygen yields $O_2^{\cdot -}$, which has one unpaired electron. The electron configuration of the $O_2^{\cdot -}$ is shown in Fig. 1.4. $^1O_2$ is produced from the input of energy to the oxygen molecule. A double electron acceptance

leads to the formation of the peroxide ion (O_2^{2-}), which is usually protonated and in the form of H_2O_2.

The O-O bond in this case is relatively weak compared to that of molecular oxygen, and therefore H_2O_2 can decompose easily, yielding the ·OH, by homolytic fission, where each of the oxygen atoms take one electron from the O-O bond. Equation 3.1 shows the formation of the ·OH from H_2O_2.

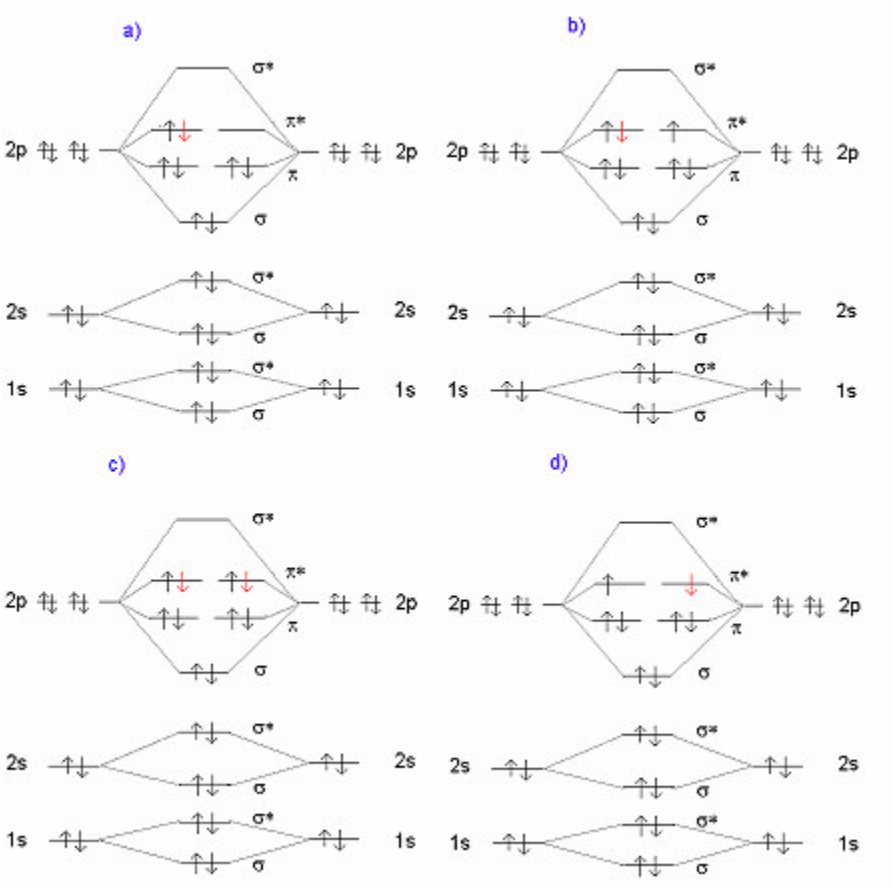

Fig. 1.4: Molecular orbital diagram showing the electron configurations of each type ROS. a) Singlet O_2 ($^1\Delta gO_2$), b) Superoxide ($O_2^{\cdot-}$), c) Peroxide Ion (O_2^{2-}), and d) singlet oxygen ($^1\Sigma g^+O_2$) [5].

ROS can be generated by the homolytic breaking of the strong double bond in molecular O_2 by heat or ionising radiation, as shown in Eqn. 1.1 [5].

$$H_2O_2 \xrightarrow{Energy} 2^{\bullet}OH \qquad \textbf{Eqn. 1.1}$$

1.3.2 Superoxide

$O_2^{\bullet-}$, are also implicated in oxidative damage to DNA [47]. $O_2^{\bullet-}$ itself does not have a high reactivity towards DNA, but instead is involved in other biochemical reactions involving the production of ROS and H_2O_2, as well as reacting with transitions metals, such as iron, copper and nickel, for example [18]. The presence of the enzyme superoxide dismutase (SOD), which acts to break down $O_2^{\bullet-}$, is evidence that the presence of $O_2^{\bullet-}$ has the potential to cause harm in aerobic organisms [5]. $O_2^{\bullet-}$ is formed in cells by the autooxidation of a variety of reduced electron carriers and redox enzymes. It can also be produced from the redox cycling of quinone and semiquinone [48].

$O_2^{\bullet-}$ was thought to act as a reductant for iron, resulting in Fe(II), which subsequently was involved in the production of the $^{\bullet}OH$ via the Fenton reaction [5]. However, recently role of the $O_2^{\bullet-}$ in iron mediated oxidative damage to DNA, was disputed [5, 47].

The production of the Fe(II) state by $O_2^{\bullet-}$ from Fe(III) has a half time of 10 hours, which was argued too long to support the rate of DNA damage observed to occur in cells with H_2O_2. Instead, it was proposed that the conversion of $O_2^{\bullet-}$ by SOD into hydrogen peroxide and oxygen further contributed to the Fenton mediated production of $^{\bullet}OH$ [5].

It has also been suggested that NADH could act as a reductant of Fe(III) to produce Fe(II) [31]. This reaction occurs at a faster rate than that of $O_2^{\cdot-}$, due to the abundance of NADH *in vivo* [5]. It was then suggested that $O_2^{\cdot-}$ was involved in increasing the cellular concentration of another of the species involved in the reaction. As $O_2^{\cdot-}$ was more likely to diminish the concentration of NADH in the cell, it was suggested that it was involved in increasing the levels of free Fe in the cytosol. Increased free Fe levels in the cell would increase cell susceptibility to H_2O_2 induced damage, and hence to oxidative damage to DNA [5].

1.3.3 Singlet oxygen $^1O_2$

$^1O_2$, can be produced by the reaction of $O_2^{\cdot-}$ with $^{\cdot}OH$ or H_2O_2 as well as from the disproportionation of $O_2^{\cdot-}$ [5]. $^1O_2$ and its implication in oxidative damage to DNA are most important when looking at radiation induced oxidative damage to DNA [24]. $^1O_2$ is formed from photosensitisation of endogenous photosensitisers. It has been suggested by Ravanat *et al.* that $^1O_2$ may be produced from the reaction of molecular oxygen with the triplet states of purine and pyrimidine bases [24].

$^1O_2$ is an electrophile, reacting with electron rich biomolecules, like G. It can be formed via a photosensitisation reaction as described above, or by chemical generation, via H_2O_2 oxidation, by the thermolysis of naphthalene endoperoxidases and via the Russell mechanism, a biomolecular reaction of the peroxyl radical involving a cyclic mechanism from a tetraoxide intermediate [20].

Martinez *et al.* [20] examined at the action of $^1O_2$ in oxidative damage to DNA. It was observed that the action of $^1O_2$ was much more specific than that of

·OH, acting preferentially on the G moiety over the other DNA bases and with the oxidised lesion 8-oxoG.

Ravanat *et al.* [49] suggested a mechanism for the oxidation of dG by $^1O_2$, as outlined in Scheme 1.5.

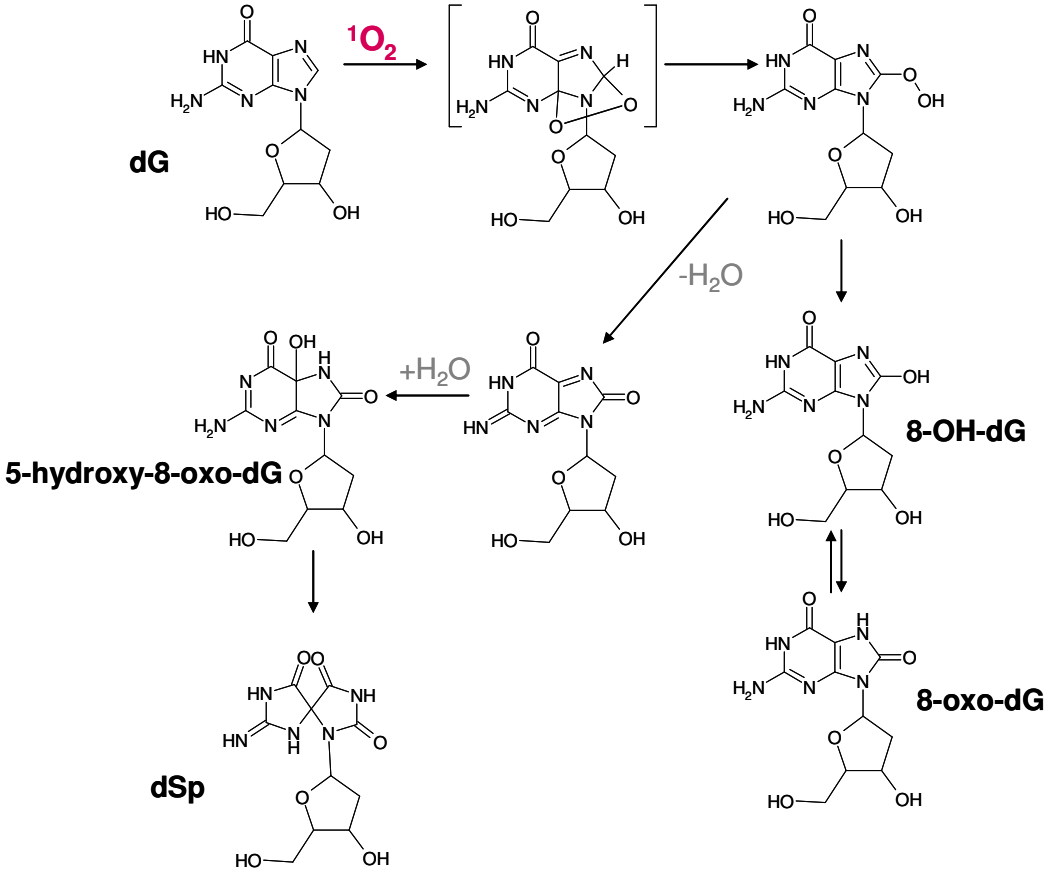

Scheme 1.5: The mechanism of oxidation of G nucleoside, dG, by $^1O_2$ as proposed by Ravanat et al. [49]

1.3.4 The hydroxyl radical, ·OH

·OH is an electrophilic and highly reactive radical, which can abstract hydrogen atoms and rapidly add to double bonds. It reacts with all known biomolecules at diffusion controlled rates. It reacts preferentially with the π-bonds of DNA bases, but can also interact with the sugar units by hydrogen abstraction [50].

H_2O_2 is ubiquitously present in the cell, as a by-product of aerobic respiration, namely $O_2^{\cdot-}$ molecules are converted into molecules of H_2O_2 and O_2 by the enzyme superoxide dismutase (SOD) [5]. One means by which ·OH can be generated is by the transition metal mediated Fenton reaction from H_2O_2. Eqn. 1.2 below shows the Fenton reaction [5].

$$H_2O_2 + M^n \rightarrow M^{n+1} + {}^{\bullet}OH + OH^- \qquad \textbf{Eqn. 1.2}$$

where, M^n indicates a transition metal of oxidation state, n. The metal is oxidised to a higher oxidised state. One electron is donated to the H_2O_2, resulting in the formation of a ·OH and a hydroxyl ion [17].

·OH is known to react with T and G, resulting in lesions. The mechanism of action of ·OH oxidation of G is outlined in Scheme 1.6 as proposed by Cadet *et al.* [18].

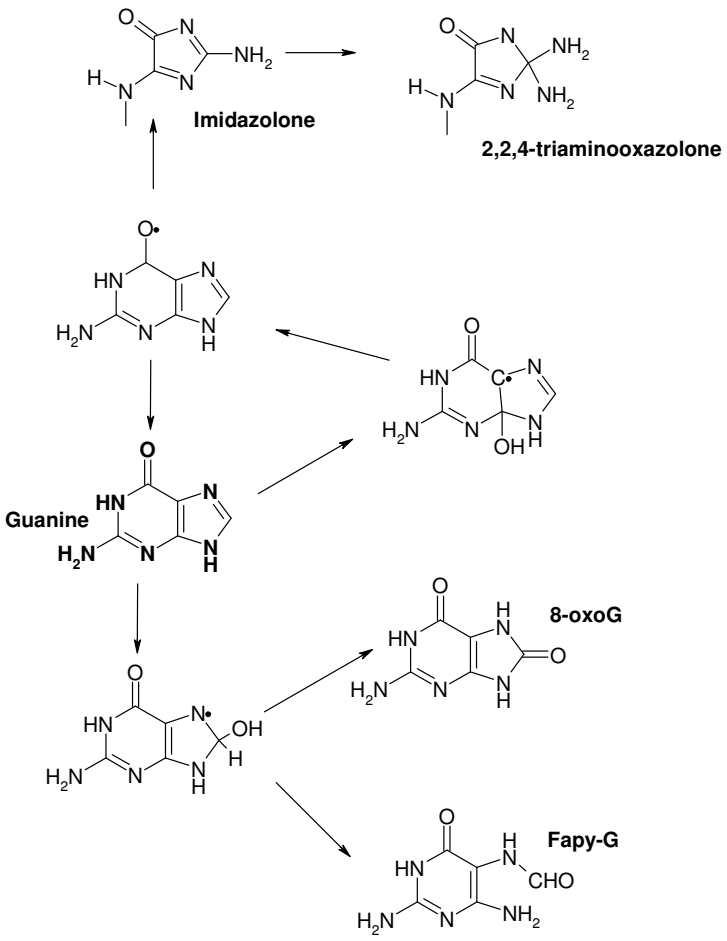

Scheme 1.6: Mechanisms of ·OH-mediated decomposition of G to form 8-oxoG, Fapy-G, Imidozolone and Oxozolone. (Reproduced from Cadet et al. [18]).

The ·OH, attacks the G moiety at the C4, C5 or the C8 position. The addition of the radical to the C4 position is in greater yield (60%) than the C8 position (25%) [14]. The formation of radicals is seen initially. On C8 oxidation, the resulting 8-hydroxy-7,8-dihydroguanyl radical is redox ambivalent and can be oxidised or reduced to form 8-oxoG and Fapy-G respectively. The 4- or 5- OH-G$^{\bullet}$ can be dehydrated to form a further oxyl radical which is then converted to final oxidation

products, imidazolone (Iz) and oxazolone (Oz) derivatives. 8-oxoG is the most abundant oxidation product of ·OH oxidation of G, with a 50% yield. Fapy-G had a reported yield of 20%. Cadet *et al.* also implicated the ·OH in tandem DNA base damage [18].

As well as from the Fenton reaction, ·OH can be produced by the radiolysis of water by ionising radiation or other chemical sources, as discussed by Breen *et al.* [50]. In a comprehensive study, the role and consequences of ·OH in DNA damage was discussed [50, 51]. ·OH is known to react with all biomolecules, and as a result its damage is not limited to the nucleobases of DNA. ·OH can cause SSBs by attacking the ribose sugar unit, whereas DSBs are caused only by an onslaught of multiple ·OH attacks to this moiety. It was determined that 20% of hydroxyl radical attack is directed at the ribose sugar. ·OH attack to G, resulting in 8-oxoG, leads to transversion mutations (G to T) and, upon insufficient repair, may cause mutagenesis.

Significant damage to DNA can also be caused by reactive nitrogen species, but these are outside the scope of this thesis.

1.4 MEASUREMENT OF OXIDATIVE DAMAGE

1.4.1 Considerations for accurate measurement

In order for sensitive and accurate detection of oxidative damage products, a number of precautions should be taken. This is to ensure that data obtained is reliable, accurate and reproducible. Kasai has studied the application of numerous

methods of analysis to oxidative damage to DNA [12, 52]. The levels of 8-oxodG and 8-oxoG are found to vary greatly from method to method, from 10-1000 fold. The lowest levels of these oxidation products were found in biology-based analyses, which identified levels of approximately 0.8 adducts per 10^5 unmodified bases. Chemistry-based methods generally show higher levels of oxidised base lesions; high performance liquid chromatography with electrochemical detection (HPLC-ECD) gave levels of 25 lesions per 10^5 bases, and gas chromatography with mass spectrometric detection (GC-MS) identified levels of up to 700 modified bases per 10^5 unmodified bases. The variance in results between these three methods was of three orders of magnitude. Clearly unacceptable, this indicates the possibility of artifact formation, or inaccurate detection between methods.

ESCODD, the European standards committee on oxidative DNA damage, has investigated the baseline levels of 8-oxoG in HeLa cells by studying the levels of 8-oxoG that were obtained by numerous laboratories on similar samples. It is agreed that the baseline level of 8-oxoG is 1-5 lesions per 10^6 G bases. In this study it was recognised that GC-MS gave results of a higher magnitude than HPLC-ECD, which in turn was slightly higher than enzymatic biology-based methods [53].

Artifactual oxidation is a major issue facing the analyst when determining oxidative damage to DNA. ESCODD have also investigated the extent to which artifactual oxidation occurs. HPLC-ECD, GC-MS and ^{32}P-Postlabelling, which have been used for this type of analysis for many years, were investigated by Cadet *et al.* [54]. GC-MS and ^{32}P-Postlabelling were to give results up to 50 times higher than those obtained with methods such as HPLC-MS/MS and HPLC-ECD as well

as biological methods. It is important that the extraction method, for extracting DNA from cells and the hydrolysis of DNA is not detrimental to the accuracy of the methods. In methods where there is a generation of artifactual oxidation it has been suggested that large samples are used to minimise artefact interference. In real biological sample analysis, however, it can prove difficult to achieve sample sizes of up to 30μg of DNA and as a result standardised DNA extraction methods are required to minimise artifact formation [55]. Other steps to reduce artifact formation include the use of metal chelators or antioxidants during sample preparation [56].

Kasai discussed a number of precautions in sample preparation to ensure more reliable data is obtained. These included avoiding the use of phenol and organic solvents, which may contain photosensitisers, ensuring that no UV-induced oxidation is inflicted. Timely analysis, as soon as possible after sample preparation, was also recommended, as the samples can degrade, or form artifacts quickly. Performing and analysing controls on the same day, and as soon as possible after hydrolysis was also recommended [52].

Because of the relatively low amounts of oxidative damage lesions present, oxidative damage to DNA is quite difficult to measure *in vivo*. The analytical methods that are applied to the detection of this damage must, therefore, be very sensitive. Ravanat *et al.* [24] discussed three approaches to the determination of DNA damage. The first of these involved the extraction of DNA bases or nucleosides by hydrolysis or enzyme digestion, respectively, followed by separation of the mix of bases and lesions with subsequent detection. This approach involved

primarily the use of chemistry-based separation methods such as high performance liquid chromatography (HPLC) and gas chromatography (GC) with detection methods such as ultra-violet spectroscopy (UV), electrochemical (EC) and mass spectrometry (MS) detection [24, 57]. The sensitivity and accuracy of this approach depends, therefore, on the separation and detection method used post DNA extraction.

The second approach involves the combined use of repair glycosylases, which nick the DNA at the site of modified bases and an analytical method of detection, which allows the determination of strand break frequency. This approach will generally require biology-based assays, which will determine the sensitivity and accuracy of the detection. Biology-based methods, discussed in section 1.4.3, are generally more sensitive, but lack the robustness and calibration of chemistry-based analyses. The third biochemical approach involves the analysis of mutation spectra by obtaining DNA sequences and determining the frequency of mutations, such as G to T transversions. The mutation spectra approach not a quantitative tool. However, it is a good qualitative tool beneficial in comparing damage caused by various sources.

1.4.2 Application of chemistry-based methods to the detection of oxidative damage to DNA

1.4.2.1 Gas chromatography-mass spectrometry (GC-MS)

GC can be coupled to a variety of detectors including flame ionization detectors, electron capture detectors and thermal conductivity detectors [57]. These

detection methods, however, do not give the structural data that is accomplished by the coupling of GC to MS [58]. GC-MS was used widely as a method of detection of DNA damage in the earlier studies. The use of GC-MS was pioneered for the detection of oxidative damage to DNA when Dizdaroglu used it for detection of the four DNA bases as well as a range of damage adducts including thymine glycol, 5-methylcytosine, 8-oxoAdenine, Fapy-Adenine, 8-oxoG and Fapy-G. The method by which the DNA was oxidised was via γ-irradiation [59]. The power of GC-MS to sensitively detect such small quantities of a range of oxidation products meant it was promising for the determination of oxidative damage to DNA.

The limitations of GC-MS, as a detection method for oxidative damage lesions such as 8-oxoG, however, have come into light more recently in the literature. The main limitations to the method are its harsh conditions of sample preparation and derivatisation steps that are needed [60]. GC-MS requires derivatisation of the modified bases or nucleosides, after they have been obtained by either enzymatic digestion or by acid hydrolysis in order to make them suitably volatile for the separation and their detection. Electron capture negative ion MS requires off-line alkylation of DNA bases as well as prior isolation using HPLC. This HPLC isolation is thought to minimize some of this artifactual damage [61,62]. Trimethylsilane (TMS) is another common derivative for the GC-MS analyis of 8-oxo-G. This derivative was also shown to cause artifactual oxidation [63-65].

This artifactual oxidation of DNA, especially of G, can cause the formation of high levels of 8-oxoG, leading to the overestimation and hence the

misinterpretation of background levels of DNA damage. The artifactual oxidation via GC-MS significantly increases the limit of detection of the method, which means that it cannot perform to its potential sensitivity [61, 62].

Jenner *et al.* proposed a method of reducing the generation of oxidative DNA artefacts, using lower sample treatment temperatures, in anaerobic conditions, and a reducing agent, ethanethiol [66]. The use of the enzyme guanase as part of a pre-treatment step also showed a reduction in the concentration of 8-oxoG levels giving the GC-MS method results comparable with the HPLC-ECD analysis [66]. The amount of artifactual oxidation was minimized here, but to achieve this, extra sample preparation steps are required. In this study, samples were taken at lengthy intervals, and a general increase in 8-oxoG concentration was observed, though there was some erratic pattern observed, and the formation did not appear stable. Without minute by minute samples, it is impossible to determine if these were due to experimental error or were due to oscillations of 8-oxoG formation, similar to those reported by White *et al*. [67].

In a study by Collins *et al.* in 2004 [68], each of the methods of detection of DNA damage were critically reviewed. It was noted that GC-MS could not detect a dose-response of induced 8-oxodG, nor was it reliable for the detection of DNA damage at low levels, due to artifactual oxidation. Oxidative damage to DNA, determined by a range of laboratories by measuring the levels of 8-oxodG, indicated the highest levels obtained were using the GC-MS method. This indicates that the level of artifact 8-oxodG produced might overshadow actual oxidative G oxidation, and hence may cause great inaccuracies in results. An advantage that this method

has over other methods, such as HPLC-ECD or ^{32}P-Postlabelling, however, is the selectivity of MS in detection of particular compounds and its ability to give structural information [60, 69].

1.4.2.2 Liquid chromatography-mass spectrometry (LC-MS)

The specificity of MS detection, however, can still be obtained by the use of an LC-MS method, without the inaccuracy of the high levels of artifactual oxidation as obtained in the GC-MS method. HPLC allows for the separation of analytes without pre-derivatisation, based on their hydrophobic properties [70]. Dizdaroglu *et al.* reviewed the use of LC-MS methods, including the use of a LC-tandem MS (LC-MS/MS) method [71]. An acid hydrolysis preparation step was used by Dizdaroglu *et al.* for DNA base analysis and the authors concluded that this sample preparation did not cause artifact formation. The measurement of just a single damage adduct, 8-oxoG or 8-oxodG, can misrepresent the level of damage caused to the DNA structure, as a much wider spectrum of oxidative damage products have been identified. MS can be used for qualitative, structural determinations for a wider range of products. LC-MS has a detection limit of as low as picomolar levels. The sensitivity of LC-MS/MS, with selective ion monitoring was just 10 lesions per 10^6 bases per 1 mg of DNA; this is in the fmolar range, and close to baseline levels of DNA damage. Using LC instead of GC can minimise the formation of artifactual lesions, and coupled with MS can allow for specific and sensitive detection of a wider range of damage products. Tandem Mass Spectrometry (MS/MS) can increase this selectivity and sensitivity further. HPLC-MS/MS is fast becoming one of the most prominent methods of analysis of oxidative damage to DNA, with

accurate and sensitive determination of all oxidative DNA adducts, thus providing and insight to a wider spectrum of DNA damage. Its artifactual oxidation can be minimised, assuming it has not occurred during sample preparation and by ensuring the use of soft ionisation techniques such as electrospray ionization (ESI) [61-62, 72] which allows the ions to be formed in solution and thus is ideal for coupling to HPLC [73].

1.4.2.3 Liquid chromatography-electrochemical detection (LC-ECD)

This method of analysis of DNA damage is the most commonly used for the selective and sensitive detection of the important G oxidation product, 8-oxoG [68]. The ECD method used is achieved by use of a flow through ECD cell as illustrated in Fig 1.5 where the eluent and sample flow through a small area close to the the auxillary and working electrodes. The analysis is usually carried out at constant potential with the current measured as a function of time.

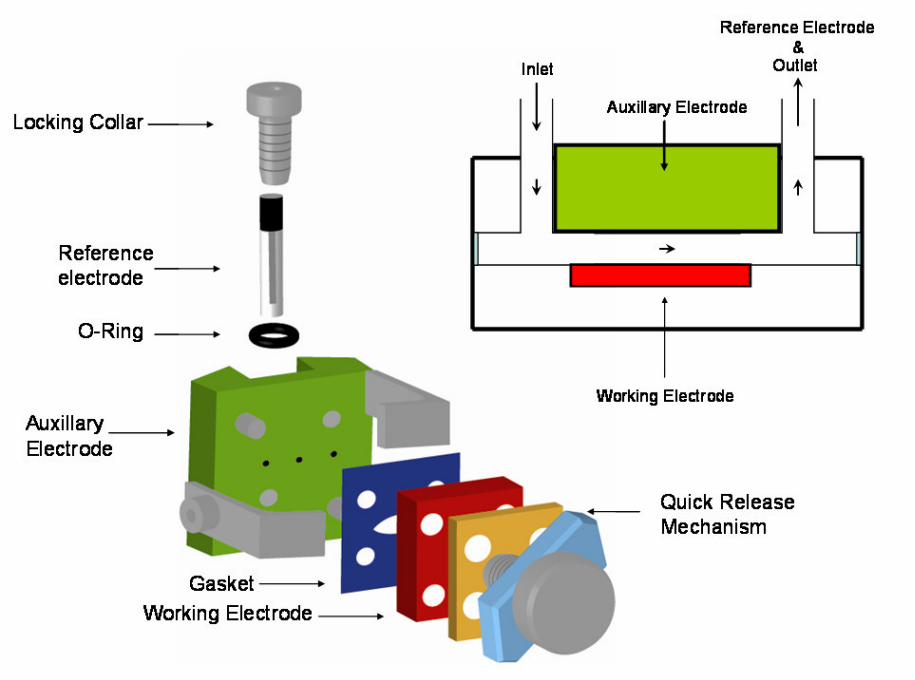

Fig 1.5: ECD BAS amperometric flow detection cell illustrating eluent flow. (Reproduced from Handbook of Electrochemistry, Edited by Zoski, C.G. [74] and Bioanalytical Systems [75]).

Using a HPLC-ECD method developed by Floyd *et al.*, [76-77] the levels of 8-oxoG and also 8-oxodG were discovered to be comparable, suggesting that both enzyme digestion, using nuclease P1 and alkaline phosphatase and acid hydrolysis using formic acid were ideal for oxidative damage analysis. The method showed a linear calibration with a correlation coefficient of 0.9993. The limit of detection of the method was 0.5 8-oxoG lesions per 10^6 unmodified bases for a sample size of 50 µg DNA. The measured background levels were in the order of 2-5 lesions per 10^6 unmodified bases, depending on the cells that were analysed. Limits of detection for a HPLC-ECD method are generally in the nM range [78].

A HPLC-ECD method was also used by Long *et al.* [79] in the determination of 8-oxoG. This method incorporates gradient elution and a C_{18} separation. The nucleoside equivalent was used as an internal standard, with ECD vs. a Pd electrode at 300 mV. The limit of detection was found to be 22 ng ml^{-1}. The linearity of the method showed a correlation coefficient of 0.998 for studies of both human urine and human plasma and was validated over four orders of magnitude from 22-66,800 ng ml^{-1} for human urine and over the range 22-3340 ng ml^{-1} for human plasma. The simultaneous detection of both G and 8-oxoG is possible with the use of both UV and ECD detection. G can be determined by UV detection, and 8-oxoG is selectively detected by ECD, by choosing a potential where G is not oxidised. G and 8-oxoG can theoretically be detected by UV detection; however, it is difficult to separate both moieties using HPLC. Also, 8-oxoG is present in very low concentrations and the higher G concentration in the background makes the determination of 8-oxoG more difficult to quantify accurately. UV detection does not have the ability to detect levels of 8-oxoG as low as those found in biological samples. By using ECD detection, 8-oxoG can be selectively detected because it has a lower oxidation potential than G [10]. This can be achieved by using a detection voltage at which only 8-oxoG is oxidised at the electrode.

1.4.2.4 ^{32}P- postlabelling

^{32}P postlabelling is widely used in the study of oxidative damage to DNA due to its sensitivity. It can be used for biological samples as it does not require isotopical pre-labelling of DNA. The main problem with ^{32}P postlabelling is the high background readings caused by the unmodified bases. This can be avoided by

the chromatographic pre-purification of modified bases by an affinity chromatography step [15, 54, 60].

This method of detection was used by Gupta *et al.* [80] involving the enrichment of the 8-oxodG lesion prior to ^{32}P-postlabeling. The sensitivity of the method was found to be <1 8-oxodG/ 10^7 bases in a sample size of 1μg, with LODs in the fmol region [81].

Coupling this method to HPLC gives it the potential to lower its LOD to 1 modified base per 10^9 unmodified bases [82]. The results obtained in the study conducted by Zeisig *et al.* using this method were reproducible, showing standard deviations not greater than 10% and also comparable with those of a HPLC-ECD method. Artifactual oxidation has been identified as a major disadvantage to ^{32}P-Postlabelling assays. Radioactive decay from the label can cause oxidation and thus and due to the high sensitivity of the method, artifactual oxidation can cause misrepresentation of the results [54].

1.4.2.5 Capillary electrophoresis (CE)

CE is a separation technique based on the electrophoretic mobility of ions. The sample mixture travels through a capillary filled with electrolyte buffer to which a potential difference has been applied [83]. CE has been applied to the detection of 8-oxoG and 8-OH-dG [84, 85]. Arnett *et al*. studied the formation of 8-oxoG and 8-OH-dG in the rat cerebral cortex using CE coupled to ECD detection. Using microdialysis, the adducts were pre-concentrated and then analysed using CE-ECD. Base stacking was used in order to increase the sensitivity of the system,

allowing for nanomolar LODs. The results obtained for this study compared well with results obtained by an LC-MS study [84].

Mei *et al*. used CE-ECD to determine the 8-OH-dG in urine samples of cancer patients. The CE-ECD method gave lower relative standard deviations when compared to a GC-MS method. The urine was pretreated and the 8-oxoG preconcentrated with solid phase extraction and reconstituted prior to analysis. The GC method used in this study was also pretreated with TMS. The CE-ECD method was not, however, compared to a HPLC-ECD method, and as GC is known to cause artifactual oxidation, and this is the likely cause of the resulting high deviation [85]. CE-ECD, because of its low artifactual oxidation and minimal pretreatment, is ideal for analysis of biological samples.

1.4.3 Introduction to available biology-based methods for the determination of oxidative damage to DNA

Biological-based methods of analysis are attractive due to their high sensitivity and specificity. Examples of methods used in the direct detection of DNA damage adducts are immunocytochemical methods, gel-electrophoresis based methods and flow cytometry. [86-89] Molecular biological methods such as gel electrophoresis, used in the nicking assay, and the comet assay, are used to detect damage to double stranded DNA. Biological methods are not as easily and accurately calibrated as chemistry based methods. This is the major limitation to all of these methods. Their major advantage over chemistry-based methods, however,

is the power of their sensitivity and specificity in their detection of oxidative damage to DNA.

1.4.3.1 Immunoanalytical methods

Immunocytochemistry is based on the use of specific antibodies for detection of analytes. Polyclonal (mixed) or monoclonal (single specific) antibodies are prepared with specificity for the analyte of interest, they are immobilised on a surface, and they can then bind the analyte of interest. The detection of the analyte can then be performed by attaching a label, which may be a fluorescent label, or a radioactive label, or the detection may involve an enzyme substrate reaction resulting in a detectable colour change, as in enzyme linked immunosorbent assays (ELISAs). Immunoaffinity chromatography involves the use of antibodies bound to a column; this can be used effectively in pre-concentration or purification steps.

Therefore antibodies specific to DNA oxidation lesions can be used to detect oxidative damage to DNA. The main limitation of immunoanalysis is due to non-specific binding of the antibodies to other similar analytes and matrix molecules [90, 91].

1.4.3.2 Electrophoretic separation

Gel electrophoresis, via the nicking assay is an effective method for the determination of DNA damage to the double helix, allowing for the determination of strand breaks. Analytes are separated depending on their relative charges and size. These properties determine the analytes' ability to move through the gel. A sample is injected into the gel. A potential is then applied across the gel, and

depending on their properties the analytes are separated, resulting in a series of bands across the gel. Many important biological molecules such as amino acids, peptides, proteins, nucleotides, and nucleic acids, possess ionisable groups. This implies that at any given pH, they can exist as electrically charged species either as cations (+) or anions (-). Depending on the nature of the net charge, the charged particles will migrate either to the cathode or to the anode [91]. Gel electrophoresis is used in DNA typing, where DNA is fragmented at particular sequence points on the genome and compared to a control sample [3]. Hence, it can be used in the detection of DNA damage also. Supercoiled DNA, open circular and linear DNA can be separated by this method. This type of damage will only give an indication to the extent of strand breakage in a sample of damaged DNA. It cannot be used to quantify lesions and cannot qualitatively determine DNA lesions.

1.4.3.3 The Comet assay

The comet assay or single cell gel electrophoresis is a variation of gel electrophoresis, except the separation is performed on single cells [89]. It is based on the unravelling or relaxation of supercoiled loops of DNA. Indirect DNA damage, which does not directly cause strand breaks, can also be detected by cellular repair enzymes that cut or "nick" DNA at the point of lesions. As well as oxidative damage, the comet assay can be used as a test for genotoxicity and for assessing the fundamental aspects of DNA damage and cellular responses to this damage. Unlike conventional gel electrophoresis, DNA does not migrate in defined fragments in the comet assay. There are relatively very few breaks per cell and so the distances between breaks are minimal, therefore, a tail of free broken ends or

relaxed loops of the supercoil, resembling a comet is seen. Some genotoxic agents induce alkali labile sites, which under the alkaline conditions of the comet assay are converted to breaks. The resulting comets obtained, post electrophoresis, are analysed using fluorescence microscopy. Fig 1.6 summarises the comet assay. The main benefits of this method are its sensitivity, as well as its speed and simplicity. It does, however, have the limitation of most biological methods, as it is not easy to accurately calibrate. Quantitative measurements are performed by arbitrarily assigning magnitude values to determine the extent of tail propagation. The quantitation therefore, is based on relating tail intensity to strand breaks [89, 92, 93].

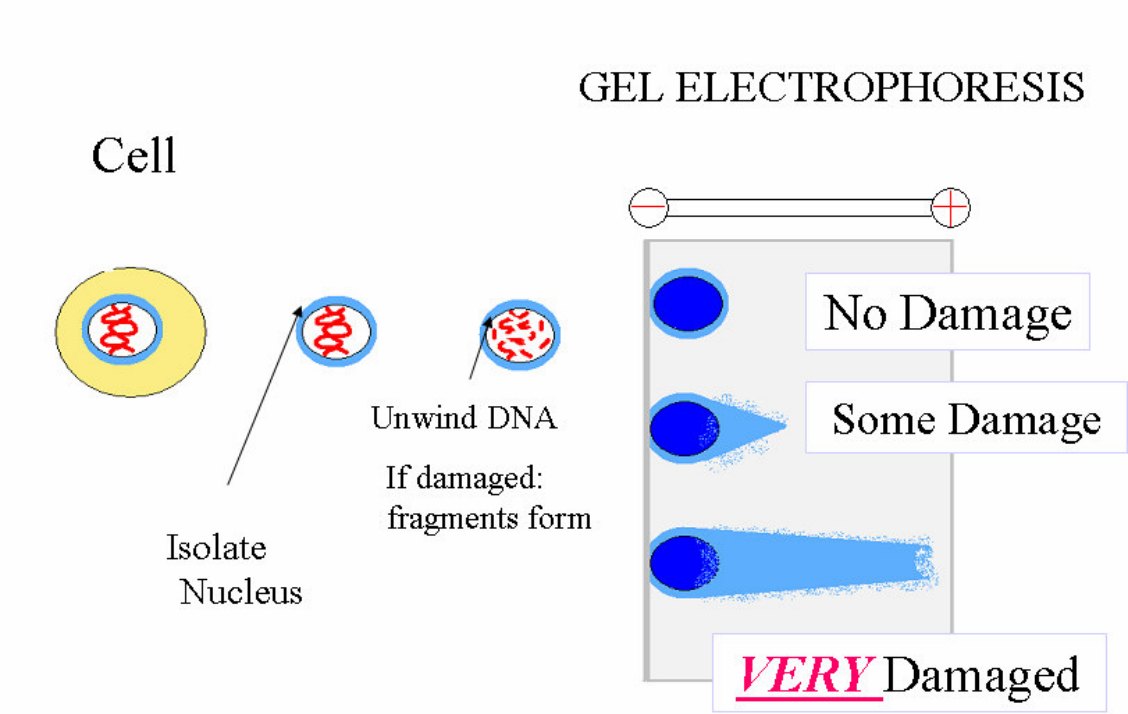

Fig 1.6: Illustration outlining the Comet assay. The nucleus of a cell is isolated, the DNA unwound by alkali treatment, and then subjected to a potential difference across a gel. The resulting comet shape is an indicator of the extent of damage caused to the cell [92, 93].

The nature of the determination of damage to DNA means that the Comet assay is not able to specifically detect 8-oxoG formation or damage to specific nucleobases. Therefore, the specificity of the method can be enhanced by the use of enzymes that are specific to particular DNA lesions. This involves a pre-treatment step in order to break the DNA at specific damaged sites, where an enzyme nicks the DNA at particular sites that have been damaged. In order to detect 8-oxoG, the enzymes formamidopyrimidine DNA glycosylase (FPG), which is used for for 8-

oxoG and Fapy-G determination; endonuclease III (Endo III), which is used for the detection of oxidised purines; and human 8-oxoG DNA glycosylase (hOGG1), specific to 8-oxoG have been used to cut the DNA at all 8-oxoG lesion sites. Unlike hOGG1, Endo III and FPG are not 8-oxoG specific as they can also nick DNA at alkylated bases. [94, 95]

1.4.3.4 Flow cytometry

Flow cytometry is a means of measuring certain physical and chemical characteristics of cells or particles as they travel in suspension one by one past a sensing point. It involves the use of a Laser beam that is projected through a stream of liquid containing cells or other analyte particles. When the focused light strikes the analytes, they give a signal, which is picked up by a detector and converted to data. As cells flow, one at a time, through the detector's region of interrogation, multiple properties of each cell can be measured at high rates, up to and over 1000 cells/second. The measured properties can then be correlated to the property of investigation [86, 96]. This method can be used to determine damage to DNA by comparing damaged cells to undamaged cells. Because of the high analysis rate of this assay, it can give a more comprehensive view of oxidative damage in a larger sample group than other biological methods, thus giving more representative values of the extent of damage caused.

1.4.4 Application of biology-based methods to the detection of oxidative damage to DNA

1.4.4.1 Immunoanalytical methods

Yin *et al.* developed an immunoaffinity chromatography-ELISA method for the determination of 8-oxodG with the use of monoclonal antibodies [88]. The limits of detection in using the two monoclonal antibodies developed for 8-oxodG were 5 and 2 picomolar, respectively. The values correlated well with those for the HPLC-ECD method to which they were compared, but the levels of 8-OH-dG shown in the results were much higher than those obtained with the HPLC-ECD method. This may have been due to some unspecific binding of 8-oxoG, G and dG and other similar damage products, *e.g.* 8-mercaptoguanosine, 8-bromoguanosine, 8-methyl guanosine, 7-methylguanosine and 6-mercaptoguanosine. An immunoaffinity purification step was implemented to minimize interference. However, the antibody used in the purification, still showed some affinity to the other interfering molecules, though the level of interference was minimised considerably.

This method has been applied to the determination of oxidative stress by Rossner *et al.* who monitored 8-OH-dG in bus drivers, who demonstrated higher levels of oxidative stress in bus drivers compared to a control group [97].

Collins *et al.* compared an ELISA method to HPLC-MS/MS determination of oxidative stress by examining 8-OH-dG. The immunoassay method results showed higher levels of damage than the HPLC-MS/MS method, which was likely due to

unspecific binding from interfering molecules. The ability of ELISA to specifically determine 8-OH-dG, therefore, was questionable [98].

1.4.4.2 Electrophoretic separation

Park *et al.* used an electrophoretic method for the determination of oxidative damage to DNA inflicted by the Fenton reaction, in order to see the effects that cysteine had on the Fenton reaction [99]. The method involved looking at the extent of relaxation of supercoiled DNA to open circular DNA. The DNA was prepared and mixed with a loading dye, and separated on a 1% agarose gel, which was then stained with ethidium bromide before the bands were measured. The use of dangerous chemicals is a limitation to this assay. Another limitation is that it is not a method of quantitation of oxidative damage, nor is it completely specific to oxidative damage to DNA.

Kim *et al.* also used electrophoresis as part of their study of 8-oxoG and its ability to induce intramolecular damage, but protect against intermolecular damage [100]. They separated supercoiled, open circular and linear DNA using a 0.8% agarose gel and ethidium bromide staining. The quantitation of each was performed by computer-assisted estimation. It was determined that 8-oxoG caused for formation of open circular from supercoiled DNA intermolecularly.

1.4.4.3 The comet assay

The comet assay is the most commonly used biology-based assay for the determination of DNA damage. In a study by Cavallo *et al.* both the comet assay and flow cytometry were used to obtain a picture of oxidative damage by looking at

both the levels of ROS and the amount of damage caused to cells [86, 92]. Measurements taken from the comet assay were: %DNA in the tail, the tail length, and the tail moment, which is the product of relative tail intensity and length that provides a parameter of DNA damage. The FPG enzyme recognises the oxidative damage lesion, 8-oxoG, and cuts the DNA at this point producing apurinic sites, which are then converted to breaks by the associated AP-endonuclease activity. FPG can; however, recognise and break strands at Fapy-G and Fapy-A points. This, therefore, is a source of over-estimation of 8-oxoG by this assay.

The tail moment was measured and given as proportional to the number of DNA strand breaks. In this study, the Comet assay was conducted with and without the use of the FPG enzyme. By conducting the study with and without the oxidative lesion specific FPG, it was investigated if damage was directly caused by $NiSO_4$, or if it caused point Fapy-mutations which were then picked up by the FPG enzyme. There were small tail moment measurements without the FPG enzyme but significant oxidative damage found, with the use of FPG. The study showed therefore, that there was a lack of direct $NiSO_4$-induced DNA damage.

Shen and Ong [101] studied oxidative damage to human sperm cells by the comet assay and a HPLC-ECD method. The benefits of the comet assay, as outlined by Shen and Ong, are its simplicity and its sensitivity. Only a small number of cells are needed and single cells can be observed. It is also less expensive than other chemistry based methods such as HPLC-ECD. The only major issue with the comet assay is that it is difficult to quantitate the extent of the damage caused to the cells.

Some means of quantitation that have been used involve measuring the degree of tail migration, and measuring the proportion of damaged cells in a mixture [92]. The tail migration extent, however, may not show reproducibility and is therefore difficult to calibrate, one of the major drawbacks of biological assays. It is however, not specific to oxidative damage, and is used to detect all kinds of DNA damage. Therefore there must be an emphasis on controlled experiments as well as reduction of contamination and interference, in order to ensure that the damage monitored in the DNA is that which it is experimentally subjected to [101].

1.4.4.4 Flow cytometry

Cavallo *et al.* [85] used a flow cytometry method for the determination of ROS levels in cells treated with nickel and H_2O_2 as a means of determining oxidative damage to DNA. The study also included a direct measurement of damage via the comet assay. Non-fluorescent dichlorofluorescin diacetate, DCF-DA is converted to DCFH by cellular esterase, this new product, when in contact with strong oxidising agents such as ROS is oxidised to dichlorofluorescin (DCF), which is fluorescent. By means of flow cytometry, DCF was determined in the cells, giving an indication to the levels of ROS present in the cells. The limit of detection of this method is in the region of picomolar concentrations [102].

1.5 THESIS OBJECTIVES

This thesis aims to examine the oxidative damage to DNA that is caused by transition metals. This study is vital in order to determine if the formation of 8-oxoG can be caused by transition metals such as Ni, Co, Cd, Zn and Mn, in a similar manner to Fe and Cu, which implicate Fenton and Fenton-like reactions, respectively. Further oxidation of 8-oxoG is indicative of its intermediate status and therefore it is of great interest to determine 8-oxoG oxidation products arising from reaction of G with these Fenton-metal reactants.

In order to conduct this study, the best available methods of analysis are to be used. As determined by ESCODD [53, 54], it is widely accepted that HPLC-ECD and HPLC-MS are the best available chemistry-based methods of analysis for determination of oxidative damage to DNA. They cause low levels of artifactual oxidation, are sensitive and are quantitative, unlike biological assays, which lack the calibration and accuracy of HPLC-ECD and HPLC-MS. The study aims to develop a fast separation for the determination of DNA bases and nucleosides for temporal resolution of G-oxidation reactions.

This temporal resolution should, therefore, allow for an insight into the mechanisms of oxidative damage to DNA, specifically G, by these transition metals. HPLC-MS, in particular, can give a vital qualitative and quantitative determination of all oxidation products. Utilising this method should therefore, allow for the determination of a suitable biomarker of oxidative DNA damage by transition metals.

1.6 CONCLUSIONS AND THESIS OUTLINE

Though there has been much research in the area of oxidative damage by ROS, the literature survey highlights many routes for future research. There has been significant research into the mechanisms of oxidative damage to DNA, with searches for potential oxidation products and elucidating the chemical structures of products formed [18, 49]. Their formation over time has yet to be determined, analyzing whether they are good biomarkers of damage or just transient intermediates. The temporal analysis of the mechanism of these reactions, therefore, presents a distinct gap in published research. Elucidating the formation of a range of oxidation products over time will give us valuable insights into the formation and the fate of each of these oxidation products, with a view to finding a suitable stable biomarker. The chronological analysis of these oxidation products can also allow the use of the knowledge gained for this mechanism in order to determine how these types of reactions may propagate *in vivo*.

The literature review that is presented in Chapter 1 illustrates that there is a need for the elucidation of the mechanism of transition metal induced oxidative damage to DNA. It has been shown that transition metals can cause damage, but the mechanism of oxidation product formation over time and the range of products that can be formed is not as thoroughly researched. The research presented in the following chapters focuses on the damage that is caused to DNA by transition metals. There has been much research into the Fenton reaction in particular, mediated by Fe. The Cu-Fenton reaction has also been investigated in some detail, though the extent to which other ingested transition metals participate in the Fenton

reaction has not been analysed in any depth. The purpose of this research therefore is to determine mechanisms underlying transition metal mediated Fenton-like reactions and their ability to damage DNA.

Ni, a carcinogenic and abundant transition metal has been identified as a potential cause of oxidative damage, and is also recognised as a carcinogen. There has been much work into determining its role in oxidative damage to DNA, as is discussed in Chapter 2, however, this research has focused on the effects of Ni-mediated oxidative damage and not the mechanisms by which this can occur. The research presented in Chapter 2, examines the Ni-mediated Fenton reaction as a potential mechanism of DNA damage by Ni in detail. The results illustrate that the Ni-Fenton reaction can cause 8-oxoG formation, though only as a transient intermediate. Therefore, other oxidation products of G were analysed in a successful investigation that yielded GH and oxGH as potential biomarkers of Ni-induced damage. As Fe, Cu and Ni all mediated oxidative damage to DNA via Fenton-chemistry, it raised the question of whether all transition metals could initiate and propagate oxidative damage via this mechanism. This type of investigation was severely hindered, however, due to the long analysis times and low sample throughput of the methodology used for the Ni analysis.

Therefore, Chapter 3 applied of the latest advances of analytical chemistry to the determination of oxidative stress. A RP C_{18} monolith HPLC column was coupled to the separation of nucleosides and nucleobases. In order to complete the thorough temporal analysis of metal analysis accurately, there was a need for a high volume of samples to be analysed. In this chapter, the separation was improved to

reduce the analysis time for each sample by 90%. The use of high flow rates to minimise the analysis time was possible with the use of monolith columns and thus allowed for higher sample throughput in analysis of DNA damage. The separation was coupled to ECD to allow for the determination of electrochemically active G and dG oxidation products 8-oxoG and 8-OH-dG.

Chapter 4 applied this faster monolith column HPLC-ECD separation to the determination of oxidative G damage by Zn, Cd, Co, Mn, and Mg, in order to determine the mechanism of damage to G by way of transition metal-Fenton reactions similar to those for Fe and Cu. Chapter 4 also presents a mass spectrometric (MS) study of oxidative damage to DNA by these transition metals, with a view to elucidating and comparing mechanism of oxidative damage to DNA by each metal and a view to determining a suitable biomarker. The study showed the formation of 8-oxoG from all metals, except Mg, though in lower concentrations than those shown for Ni. The formation of 8-oxoG was again illustrative of its intermediate nature in G oxidation, and hence, the formation of 8-oxoG oxidation products were investigated. Co and Mn were seen to form oxGH from G solution and GH from G in DNA, similar to Ni. Zn and Cd did not produce detectable levels of oxGH or GH.

The ability of some transition metals to generate similar oxidation products in similar yields highlighted that all the metals did not react in an analogous manner. This raised the question of the nature of the ROS involved in this transition metal induced damage by Fenton-like reactions. While literature suggests that $^{\cdot}OH$ is the ROS of interest, especially for Fe, the results generated in Chapter 4 indicate

that this may not be the ROS generated in all cases. Chapter 5, therefore presents a study into the nature of the ROS formed for all the investigated transition metals, in order to determine if, similar to the Fe-Fenton reaction, the ·OH is the cause of damage. The study, using radical scavenger 4-hydroxybenzoic acid (4-HBA) confirmed that ·OH was only produced from the Fe-Fenton reaction. Cu, Co, Cd and Ni all reacted similarly which indicated that a different ROS was involved here. Zn and Mn appeared to react via another mechanism of DNA damage that was undetectable using the ·OH radical scavenger, 4-HBA.

Finally, Chapter 6 discusses the conclusions drawn from this research and suggests potential future work that this research presents in order to gain further understanding of oxidative damage to DNA.

1.7 REFERENCES

1. Campbell, N.A.; Reese, J.B; Mitchell, L.G.; Biology, **5th Edition;** Benjamin Cummings Publishers, California, **1999**.
2. Watson, J.; Crick, F.H.C.; *Nature*, 171; **1953**, 737-738.
3. Matthews, C.K.; Van Holde, K.E.; Biochemistry **3rd Edition;** Benjamin Cummings publishing company California, **2000.**
4. Wisemann, H.; Halliwell, B.; *Biochemistry Journal,* 313; **1996,** 17-29.
5. Halliwell, B.; Gutteridge, J.M.C.; Free Radicals in Biology and Medicine, **2nd Edition;** Clarendon Press, New York, Oxford University Press, **1989**.
6. Vital Statistics Report, *Fourth Quarter and Yearly Summary 2006*; Central Statistics Office, Government of Ireland, Stationary Office Publishers, Dublin, Ireland **2007**.
7. UK National Statistics, *Cancer Statistics, Registrations 2004*, Series MB1 no. 35; Her Majesty's Stationary Office, **2007**.
8. United States Governmnent, Department of Health and Human Services, Report: *The burden of Chronic Diseases and their risk factors*, **2004**.
9. Moller, P.; Loft, S.; *Mutation Research*, 551; **2004**, 79-89.
10. Steenken, S.; Jovanovic, S.Y.; *Journal of the American Chemical Society*, 119; **1997**, 617-618.
11. Steenken, S.; Jovanovic, S.Y.; *Journal of the American Chemical Society*, 122; **2000**, 2373-2374.
12. Kasai, H.; *Free Radical Biology and Medicine,* 33; **2002**, 450-456.
13. Wallace, S.S.; *Free Radical Biology and Medicine*, 33; **2002**, 1-14.

14. Steenken, S.; *Chemistry Reviews*, 89; **1989**, 503-520.

15. White, B.; PhD Thesis, Dublin City University, **2005**.

16. Bose, R.M.; Moghaddas, S.; Mazzer, P.A.; Dudores, L.P.; Joudah, L.; Stroup, D.; *Nucleic Acids Research,* 27; **1999**, 2219-2226.

17. McNaught, A.D.; Wilkinson, A.; *IUPAC Compendium of Chemical Terminology*, **2nd Edition; 1997.**

18. Cadet, J.; Delatour, T.; Douki, T.; Gasparutto, D.; Pouget. J.P.; Ravanant, J.L.; Sauviago, S.; *Mutation Research*, 424; **1999,** 9-21.

19. Crespo Hernandes, C.E.; Arce, R.; *Journal of Photochemistry and Photobiology B: Biology*, 73; **2004**, 167-175.

20. Martinez, G.R.; Lourieru, A.P.M.; Marques, S.A.; Miyamoto, S.; Yamaguchi, L.F.; Onuki, J.; Almeida, E.A.; Garcia, C.C.M.; Barbosa, L.F.; Medeiros, M.H.G.; Di Mascio, P.; *Mutation Research*, 544; **2003**, 115-127.

21. Burrows, C.J.; Muller, J.G.; Kornyushyna, O.; Luo, W.; Duarte, V.; Leipold, M.D.; David, S.S.; *Environmental Health Perspectives*, 110; **2002**, 713-717.

22. Raoul, S.; Cadet, J.; *Journal of the American Chemical Society*, 118; **1996**, 1892-1898.

23. Schimanski A., Freisinger E., Erxleben A., Lippert B., *Inorganica Chimica Acta*, 283; **1998,** 223-232.

24. Ravanat, J.L.; Doukt, T.; Cadet, J.; *Journal of Photochemistry and Photobiology*, *B: Biology*, 63; **2001**, 88-102.

25. White, B.; Tarun, M.C.; Gathergood, N.; Rusling, J.F.; Smyth, M.R.; *Molecular Biosystems,* 1; **2005**, 373-381.

26. Henderson, P.T.; Delaney, J.C.; Muller, J.G.; Neely, W.L.; Tannenbaum, S.R.; Burrows, C.J.; Essigmann, J.M.; *Biochemistry*, 42; **2003**, 9257-9262.

27. Dizdaroglu, M.; Jarunga, P.; Birincioglu, M.; Rodriques, H,; *Free Radical Biology and Medicine*, 32; **2002**, 1102-1105.

28. DeBoer, J.; Hoejmaker J.H.J.; *Carcinogenesis,* 21; **2000**, 453-460.

29. Hazra, T.K.; Das, A.; Das, S.; Choudnuri, S.; Kow, Y.W.; Roy, R.; *DNA Repair*, 6; **2007**, 470-480.

30. Zelko, I.N.; Mariani, T.J.; Folz, R.J.; *Free Radical Biology and Medicine*, 33; **2002**, 337-349.

31. Henle, E.S.; Linn, S.; Journal of Biological Chemistry, 272; **1997**, 19095-19098.

32. Guemouri, L.; Artur, Y.; Herbeth, B.; Jeandel, C.; Cuny, G.; Siest, G.; *Clinical Chemistry*, 37; **1991**, 1932-1937.

33. Bolzan, A.D.; Bianchi, M.S.; Bianchi, N.O.; *Clinical Biochemistry*, 30; **1997**, 449-454.

34. Duarte, T.L.; Jones, G.D.D.; *Free Radical Biology and Medicine*, 43; **2007**, 1165-1175.

35. Halliwell, B.; *Mutation Research*, 475; **2001**, 29-35.

36. May, J.M.; *FASEB Journal*, 13; **1999**, 995-1006.

37. Zingg, J.M.; *Molecular Aspects of Medicine*, 28; **2007**, 397-399.

38. Traber, M.G.; Atkinson, J.; *Free Radical Biology and Medicine*, 43; **2007,** 4-15.

39. Ramoutar, R.R; Brumaghim, J.L.; *Journal of Inorganic Biochemistry*, 101; **2007,** 1028-1035.

40. Fang, Y.Z.; Yang, S.; Wu, G.; *Nutrition*, 18; **2002,** 872-879.

41. Sies, H.; Stahl, W.; Sundquist, A.R.; *Annals of the New York Academy of Sciences*, 669, **1992**, 7-20.

42. Beckmann, K.B.; Ames, B.L.; *Physiological Reviews*, 78; **1998**, 547-581.

43. Zana, M.; Janka, Z.; Kálmán, J.; *Neurobiology of Aging*, 28; **2007**, 648-676.

44. Irie, M.; Miyata, M.; Kasai, H.; *Journal of Psychiatric Research*, 39; **2005**, 553-560.

45. Granot, E.; Kohen, R.; *Clinical Nutrition*, 23; **2004**, 3-11.

46. Dhalla, N.S.; Sethi, R.; Takeda, N.; Nagano, M.; *Pathophysiology*, 5; **1998,** 11.

47. Keyer, K.; Strohmeier Gort, A.; Imlay, J.A.; *Journal of Bacteriology*, 117; **1995**, 6782-6790.

48. Bianco, N.R.; Chaplin, L.J.; Montano, M.M.; *Biochemical Journal,* 385; **2005**, 279-287.

49. Ravanat, J.-L.; Martinez, G.R.; Medeiros, M.H.G.; Di Mascio, P.; Cadet, J.; *Archives of Biochemistry and Biophysics*, 423; **2004**, 23–30.

50. Breen, A.P.; Murphy J.A.; *Free Radical Biology and Medicine,* 18; **1995** 1033-1077.

51. Walling, C.; *Accounts of Chemical Research*, 8; **1975,** 125-131.

52. Kasai, H.; *Mutation Research*, 387; **1997,** 147-163.

53. Collins, A.; *Carcinogenesis*, 23; **2002**, 2129-2133.

54. Cadet, J.; *Free Radical Research*, 29; **1998**, 541-550.

55. Helbock, H. J.; Beckman, K.B.; Shigenaga, M.K.; Walter, P.B.; Woodall, A.A.; Yeo, H.C.; Ames B.N.; *Proceedings of the National Academy of Sciences of the United States of America*, 95; **1998**, 288-293.

56. Collins, A.; *Free Radical Biology and Medicine,* 34; **2003**, 1089-1099.

57. Harris, D.C.; *Quantitative Chemical Analysis*, **6th edition**, WH Freeman & Co, USA, **2003**.

58. Williams, D.H.; Fleming, I.; *Spectroscopic Methods of Analysis*, **5th Edition**, Mc Graw Hill Publishing Company, **1995.**

59. Dizdaroglu, M.; *Analytical Biochemistry*, 114; **1985**, 593-603.

60. Cadet, J.; Weinfeld, M.; *Analytical Chemistry*, 65; **1993**, 675-682.

61. Ravanat, J.L.; Turesky, R.J.; Gremaud, E.; Trudel, L.J.; Stadler, R.H.; *Chemical Research in Toxicology*, 8; **1995**, 1039-1045.

62. Singh, R.; McEwan, M.; Lamb, J.H.; Santella, R.M.; Farmer, P.B.; *Rapid Communications in Mass Spectrometry*, 17; **2003**, 126-134.

63. Rodriguez, H.; Jurado, J.; Laval, J.; Dizdaroglu, M.; *Nucleic Acids Research*; 28; **2000**, e75 (i-vii).

64. Cadet, J.; Douki, T.; Ravanat, J.L.; *Environmental Health Perspectives*, 105; **1997**, 1034-1039.

65. Douki, T.; Delatour, F.; Blanchini, F.; Cadet, J.; *Carcinogenesis*, 17; **1996,** 347-353.

66. Jenner, A.; England, T.G.; Aruoma, O.I.; Halliwell, B.; *Biochemical Journal*, 331; **1998**, 365-369.

67. White, B.; Smyth, M.R.; Stuart, J.D.; Rusling, J.F.; *Journal of the American Chemical Society*, 125; **2003**, 6604-6605.

68. Collins, A.R.; Cadet, J.; Moller, L.; Poulsen, H.E.; Vina, J.; *Archives of Biochemistry and Biophysics*, 423; **2004,** 57-65.

69. Moller, H.; Hoffer, T.; *Carcinogenesis*, 18; **1997**, 2415-2419.

70. Snyder, L.; Glajch, J.; *Practical HPLC: Method Development*, J. Wiley Publishers, New York, **1988**.

71. Dizdaroglu, M.; Jaruga, P.; Birincioglu, M.; Rodriques, H.; *Free Radical Biology and Medicine*, 32; **2002**, 1102-1105.

72. Ravanat, J.L.; Douki, T.; Duez, P.; Gremaud, E.; Herbert, K.; Hofer, T.; Lasserre,L.; Saint-Pierre, C.; Favier, A.; Cadet, J.; *Carcinogenesis*, 23; **2002**, 1911-1918.

73. Understanding API: Electrospray – and API, Bruker- HP Esquire-LC Operations Manual, **Version 3.1**.

74. Zoski, C.G. (Editor); *Handbook of Electrochemistry*, Elsevier, Oxford, UK, **2007**.

75. Bioanalytical Systems LC-ECD and ECD Accessories, Electrode Polishing and Care Manual, **2001**. (www.bioanalytical.com/mans/)

76. Floyd, R.A.; Watson, J.A.; Wang, P.K.; Altmiller, D.H.; Rickard, R.C.; *Free Radical Research Communications*, 1; **1986**, 163-172.

77. Ravanant J.-L, Gremaud E., Markovic J., Turesky R.J., *Analytical Biochemistry*, 260; **1998**, 30-37.

78. Herbert, K.E.; Fletcher, S.; Chauhan, D.; Ladapo, A.; Nirwan, J.; Munson, S.; Mistry, P.; *European Journal of Nutrition*, 45; **2006,** 97-104.

79. Long, L.; McCabe, D.R.; Dolan, M.E.; *Journal of Chromatography B*, 731; **1999,** 241-249.

80. Gupta, R.C.; Arif, J.M.; *Chemical Research in Toxicology*, 14; **2001,** 951-957.

81. Nagy, E.; Johansson, C.; Zeisig, M, Moller, L.; *Journal of Chromatography B*; 827; **2005**, 94-103.

82. Zeisig M., Hofer T., Cadet J., Moller L., *Carcinogenesis*, 20, **1999**, 1241-1245.

83. Marina, M.L.; Rios, A.; Valcarel, M.; *Analysis and Detection by Capillary Electrophoresis*, Elsevier Science, Boston & Amsterdam, **2005**.

84. Arnett, S.D.; Osbourn, D.M.; Moore, K.D.; Vandaveer, S.S.; Lunte, C.E.; *Journal of Chromatography B*, 827; **2005**, 16-25.

85. Mei, S.; Yao, O.; Wu, C.; Xu, G.; *Journal of Chromatography B*, 827; **2005**, 83-87.

86. Cavallo, D.; Ursini, C.L.; Setini, A.; Chianese, C.; Piegari, P.; Perniconi, B.; Iavacoli, S.; *Toxicology In Vitro*, 17; **2003**, 603-607.

87. Lloyd, D.; Philips, D.; *Mutation Research*, 424; **1999**, 23-36.

88. Yin, B.; Whyatt, R.M.; Perera, F.P.; Randall, M.C.; Cooper, T.B.; Santella, R.M.; *Free Radical Biology and Medicine*, 18, **1995**, 1023-1032.

89. Collins, A.R.; Dobson, V.L.; Dusinska, M.; Kennedy, G.; Stetina, R.; *Mutation Research*, 375; **1997**, 183-193.

90. Beesley, J.A.; *Immunocytochemistry; A Practical Approach*, Oxford University Press, Oxford, UK, **1993**.

91. Holme, D.J.; Peck, H.; *Analytical Biochemistry*, **2nd Edition**, Longman Scientific and Technology Publishers, Essex, UK, **1993**.

92. Rojas, E.; Lopez, M.C.; Valverde, M.*; Journal of Chromatography B, Biomedical Sciences and Applications*, 722; **1999**, 225-254.

93. Colleu-Durel, S.; Guitton, N.; Nourgalieva, K.; Legue, F.; Levegul, J.; Danic, B.; Chenal, C.; *European Journal of Cancer*, 40; **2004**, 445-451.

94. Smith, C.C.; O'Donovan, M.; Martin, E.; *Toxicology*, 226; **2006**, 36.

95. Collins, A.; Gedik, C.M.; *FASEB Journal*, 19; **2005**, 882-84.

96. Sharpio, H.M.; *Practical Flow Cytometry*, **2nd Edition**, Alan R. Liss Inc. Publishers, New York, USA, **1988**.

97. Rossnet Jr, P.; Svecova, V.; Mikova, A.; Lnenickova, Z.; Solansky, I.; Sram, R.J.; *Mutation Research: Fundamental and Molecular Mechanisms of Mutagenesis*, 642; **2008**, 14-20.

98. Cooke, M.S.; Singh, R.; Hall, G.K.; Mistry, V.; Duarte, T.L.; Farmer, P.B.; Evans, M.; *Free Radical Biology and Medicine*, 41, **2006**, 1829-1836.

99. Park, S.; Imlay, J.A.; *Journal of Bacteriology*, 6, **2003**, 1942-19.

100. Kim, J.E.; Choi, S.; Yoo, J.A.; Chung, M.H.; *FEBS letters*, 556; **2004,** 104-110.

101. Shen, H.-M.; Ong, C.-N.; *Free Radical Biology and Medicine*, 28; **2000**, 529-536.

102. Cathcart, R.; Schweirs, E.; Ames, B.N.; *Analytical Biochemistry*, 134; **1983**, 111-116.

2 NICKEL(II)-CATALYSED OXIDATIVE DAMAGE TO GUANINE AND DNA BEYOND 8-OXOGUANINE

2.1 INTRODUCTION

2.1.1 Transition metals – an introduction

The transition metal series is referred to as the d-block as for the most part they have partly filled d-orbitals, with some also having partly filled s orbitals also. Transition metals have the ability to vary oxidation states, as illustrated in Table 2.1, and are oxidised and reduced easily. Some oxidation states are more common than others, *e.g.*, iron can have oxidation states from (II) to (VI), but the +2 and +3 states are the most common.

Oxidation States of Transition Metals							
Sc			**+3**				
Ti	+1	**+2**	**+3**	**+4**			
V	+1	**+2**	**+3**	**+4**	**+5**		
Cr	+1	**+2**	**+3**	+4	+5	**+6**	
Mn	+1	**+2**	**+3**	**+4**	+5	**+6**	**+7**
Fe	+1	**+2**	**+3**	+4	+5	+6	
Co	+1	**+2**	**+3**	+4	+5		
Ni	+1	**+2**	+3	+4			
Cu	**+1**	**+2**	+3				
Zn/ Cd		**+2**					

Table 2.1: Possible oxidation states for the first row of transition metals [1, 2].

Oxidation states higher than +3 generally do not exist in aqueous solution [1-3]. The varying oxidation state is due to the availability of d-orbitals around the metal nucleus. These available orbitals can accept extra electrons, or can stabilise the loss of electrons [1, 4]. They are largely more electropositive than the ligands that they interact with and therefore are usually oxidised. These properties separate them from the main group elements [4].

Transition metals are an essential part of our diet. Zn, Fe and Mg are essential elements in the everyday diet in relatively large amounts. They are generally quite abundant in the environment and are very important in nature, with many of the first row in particular being important trace elements in biological reactions. These include, but are not limited to, oxygen vitamin B12 which is a Co compound, as well as many enzymes relying on Zn and Cu [4]. Fe is important in oxygen transport, and is found in the haemoglobin of red blood cells, as well as in various enzymes and in myoglobin [5]. Fe deficiency results in anaemia. Excess Fe, or Fe overload can also occur and can result in immunological disturbances. Fe overload can occur acutely or chronically, and can be inherited [5]. Zn is needed for a healthy immune system and reproductive system, in males especially. Cu is required in trace amounts for healthy skin, blood, nerves and joints; Mn for bones and enzyme regulations and Cr(III) for blood sugar regulation [6-8].

2.1.2 The Fenton reaction

The Fe-catalysed production of the ·OH from H_2O_2 was first discovered in 1894 by H.J.H. Fenton (Scheme 2.1) [9]. It is speculated that this reaction may involve an oxo-iron species intermediate.

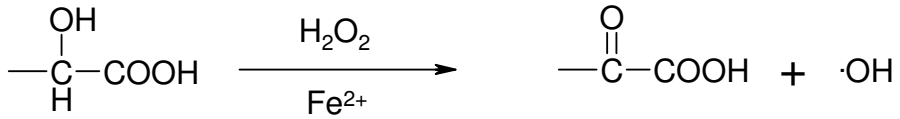

Scheme 2.1: The Fenton Reaction as proposed by H.J.H. Fenton in 1894 [9].

The Fenton reaction holds for most transition metal oxidation pairs, *e.g.* Fe(II)/Fe(III), Ni(II)/Ni(III) and Cu(I)/Cu(II), with each of these oxidation pairs capable of catalysing the Fenton reaction. The metal is oxidised from the 'n' oxidation state to the 'n+1' oxidation state, while the peroxide group is reduced causing the production of a hydroxyl radical. The metal may then reduced back to its lower oxidation state, 'n'. This can be achieved by cellular reducing agents [10, 11].

The Fenton reaction can occur *in vivo*, by reaction of cellular H_2O_2 with transition metals. Cellular H_2O_2 is primarily produced by the enzymatic dismutase of $O_2^{\cdot-}$ in the mitochondria of cells by SOD [12] and it can also come from exogenous sources such as cigarette smoke and pollutants.

The second order rate constant for the formation of the ·OH via the Fe(II)-mediated Fenton reaction is 76 l mol^{-1} s^{-1}, and for the Cu(II)-mediated reaction is

4.7×10^3 mol^{-1} s^{-1}. This indicates that there may be between 46 to 458 $^{\cdot}OH$ formed per second in a cell, indicating that even the lower rate of reaction is biologically significant [5].

In order for the Fenton reaction to occur *in vivo*, both H_2O_2 and the transition metal must be labile and also in close proximity. The transition metal involved must be in a sufficiently reduced oxidation state. Biological reducing agents can enhance the reaction by generating or re-generating reduced states of transition metals making them available for the Fenton reaction [13]. The regeneration of the reduced state ensure that even at trace levels such as those encountered *in vivo*, the supply of transition metal is not exhausted. Examples of reducing agents *in vivo* include ascorbate, glutathione [14] and nicotinamide adenine dinucleotide, NADH [11]. The oxidised 8-oxoG cation radical is also implicated in the reduction of the transition metal back to a Fenton-active state [15]. This damage via the Fenton reaction can be mediated *in vivo* by labile transition metals, such as Fe, Cu and Ni [14].

2.1.3 Nickel and oxidative damage to DNA

Ni is an abundant transition metal in the environment. It is a trace element, present in some chocolate, nuts, oatmeal, beans and pulses, with daily dietary intake varying from approximately 100 to 900 μg/day [16-18]. Ni has been found in its highest concentrations in the lungs, kidneys and in some hormone-producing tissues [19-20]. Some Ni compounds are known carcinogens, *e.g.* nickel subsulfide and nickel carbonyl have been reported to cause lung and nasal cancer and have been

labelled as Group A and Group B2 carcinogens respectively. Metallic Ni can also cause skin irritations and dermatitis and is a Group C carcinogen [21-22].

In a study of the effect of carcinogenic Ni compounds, Kawanishi *et al.* looked at the effects of $NiSO_4$ induced oxidative damage to DNA. The formation of 8-OH-dG was monitored over time with samples taken at lengthy intervals (2, 4, 16 and 24 hours). Ni was found to induce damage to DNA [23]. Ni subsulfide and Ni oxides have been determined to contribute to oxidative damage directly by reaction with H_2O_2, and indirectly by involvement in inflammation and phagocyte activation. Even at small doses, Ni from $NiSO_4$ could inflict oxidative damage as well as impair the cellular antioxidant repair system. A burst of ROS and an increase in the oxidative damage induced by $NiSO_4$ was observed on addition of H_2O_2, implying the involvement of the Fenton reaction [24].

The Ni(II) Fenton reaction is involved in oxidative stress and apoptosis (programmed cell death) as a means of preventing cancer [25]. Co-administration of H_2O_2 with Ni containing compounds induced an increased formation of ROS, which could induce oxidative damage to DNA as well as lipid peroxidation and protein modification [25].

Due to its ability to vary oxidation states, Ni in certain complexes with natural ligands can also participate in redox reactions at physiological pH and may well be able, therefore, to generate strong oxidising species in its reaction with H_2O_2 [26]. Available Ni *in vivo* should, therefore, be able to cause oxidative damage to DNA by the production of noxious $^{\cdot}OH$ and other types of ROS by this reaction. The formation of 8-oxoG from reactions involving DNA and Ni has been

reported before, though in relatively low levels. Damage to DNA by different Ni compounds and the enhancement of Ni oxidation by biological ligands resulted in 8-oxoG formation [14, 27-31]. It has also been noted that there is an association between Ni concentration and the amount of oxidative lesions in urine [34]. The formation of oxidative lesions in DNA bases found in urine over time has not been monitored extensively with min. by min. sampling. Such min. by min. sampling would allow for a more detailed insight into the mechanisms of Ni(II) -mediated damage to DNA bases. Because of its carcinogenic properties and its redox abilities, Ni was chosen for this research.

2.2 SCOPE OF THE RESEARCH

This research is focused on the elucidation of the mechanism of *in vitro* oxidation of G; both free in solution and in the DNA backbone, by a Ni(II)-mediated reaction. The methods used in this study were HPLC-UV-ECD for the determination of 8-oxoG and G and HPLC-MS/MS for the determination of 8-oxoG and structural determination of its further oxidation products. It is important to gain an understanding of the range of oxidation products formed from this type of DNA oxidation in order to determine the specific mechanism of the Ni(II)-mediated oxidation of DNA in order to compare this with Fe and Cu-induced damage. By comparing different transition metals and the mechanisms involved in their induction of oxidative stress *in vitro*, it may provide necessary information about the chemistry behind this biological phenomenon that can occur *in vivo*.

2.3 EXPERIMENTAL

2.3.1 Materials

All chemicals, including the DNA bases guanine (G0381, ≥99%), adenine (A8626, ≥99%), thymine (T0376, ≥99%), cytosine (C3506, ≥99%), and uracil (U0750, ≥99%), 7,8-dihydro-8-oxoguanine (R288608), calf thymus DNA sodium salt (D1501, Type I, fibres) [2,000 av. base pairs, 41.2% G/C] and nickel sulphate hexahydrate (22,767-6, ACS reagent, 99%), were purchased from Sigma-Aldrich (Tallaght, Dublin, Ireland). Ethanol, methanol and HPLC-MS grade methanol were purchased from Labscan Ltd. (Dublin, Ireland). Deionised water was purified using a MilliQ system to a specific resistance of greater than 18 MΩ-cm. All HPLC buffers and mobile phases were filtered through a 47 mm, 0.45 μm polyvinylidene fluoride (PVDF) micropore filter prior to use. Fresh solutions of all standards were prepared weekly.

2.3.2 Incubation of G, 8-oxoG and DNA with Ni(II) and H_2O_2

For HPLC-UV-ECD, a 10 mM solution of G, prepared in 0.1 M NaOH, was incubated at 37 ^{o}C with 1.5 mM $NiSO_4.6H_2O$ and 0.5 M solution of H_2O_2. A 2.4 mM 8-oxoG standard, also prepared in 0.1 M NaOH, and a 2 mg ml^{-1} standard of DNA in 50 mM ammonium acetate buffer pH 5.5 were analysed similarly.

Incubations were carried out from 0-30 min, with duplicate sampling of 100 μl at 1 min. intervals. The reaction was quenched in 1 ml of cold ethanol (cooled to –18 ^{o}C). The solution was then dried under nitrogen and refrigerated until analysis by

HPLC. G and 8-oxoG samples were reconstituted in 100 µL 0.1 M NaOH followed by dilution with 900 µL 50 mM ammonium acetate/ 85 mM acetic acid buffer, pH 5.5. DNA was hydrolysed with formic acid to release DNA bases and then reconstituted with 50 mM ammonium acetate/85 mM acetic acid buffer, pH 5.5 prior to analysis. For mass spectrometric analysis, samples were prepared in 10 mM NaOH and reconstituted in 100 µl 10 mM NaOH and 900 µl 50 mM ammonium acetate, pH 5.5. All samples were filtered through a 4.5 µm micropore filter prior to injection.

2.3.3 HPLC-UV-ECD analysis of 8-oxoG formation

Unless otherwise stated; Samples were separated by RP HPLC using a Varian ProStar HPLC system with Varian ProStar 230 Solvent Delivery Module and a Varian ProStar 310 UV-VIS Detector. The eluent composition was 50 mM ammonium acetate/ 85 mM acetic acid, pH 4.6:methanol (90:10) through a Restek RP Ultra C_{18} 5 µm 4.6 x 250 mm column, equipped with Ultra C_{18} 4 x 10 mm guard column. The separation was carried out at 1.0 ml/min. isocratic elution and the run time for the separation was 6 min. G and uracil were detected using UV detection at 254 nm and any 8-oxoG formed was detected by electrochemical detection (ECD), using a BAS CC-4 electrochemical cell comprising of glassy carbon working electrode, stainless steel auxiliary electrode and Ag/AgCl reference electrode at a detection potential +550 mV. ECD chromatograms were generated using a Shimadzu integrator. UN-SCAN-IT digitising software, version 5.0 (Silk Scientific

Corporation) was used to digitise integrator chromatograms, which were then imported into SigmaPlot 8.0 (SPSS Inc.) or MS Office Excel (Microsoft Corporation).

2.3.4 HPLC-MS/MS analysis of further oxidation products

Incubated samples were analysed by HPLC-MS-MS using an Agilent 1100 HPLC System with diode array detection coupled to a Bruker Daltonics Esquire 3000 LC-MS with ESI. Reconstituted samples were separated by HPLC using gradient elution through the Supelco Supelcosil LC-18 RP column 5 μm 2.1 mm x 250 mm. Eluent A consisted of 10 mM ammonium acetate buffer, pH 5.5. Eluent B was 50/50 methanol/water. A flow rate of 0.2 ml/min. was used with a linear gradient of 0-10% B from 0-22 min, 10-0% B from 22-25 min. DNA bases and oxidation products were also detected by UV detection at 210, 254 and 280 nm. Mass spectrometric analysis was carried out at an ionisation temperature of 300 ^{o}C and at an ionisation potential of +15 V unless otherwise stated.

2.3.5 Controlled experiments

Controlled incubations were performed, with both G and 8-oxoG. Each of the oxidation reagents was replaced with deionised water, first singly, to determine whether one of the reagents could generate oxidative damage alone, and then both reagents were replaced to measure how much, if any, artifactual oxidation was caused by the reaction conditions themselves.

Atomic absorption spectroscopy was carried out using a Spectra AA 50 Varian graphite furnace atomic absorption spectrometer.

2.4 RESULTS AND DISCUSSION

2.4.1 Determination of 8-oxoG formation over time

In a study of Fe-Fenton chemistry [32], a major erratic change in concentration of 8-oxoG over time was observed, with highest concentrations at just under 5 min, 14 min. and 20 min. A similar experiment was conducted in this study using Ni, the results of which compared with the Fe-Fenton results. Ni gave a similar erratic formation of 8-oxoG with the sharp increases noted at 6 min., 16 min. and 20 min. in this study, suggesting a similar reaction process.

8-oxoG is subject to further oxidation by the same ROS, due to its lower oxidation potential in comparison to G. The 8-oxoG moiety is highlighted as an intermediate in the G oxidation scheme, due to its ease of further oxidation. This is illustrated by the oscillating 8-oxoG concentration over the incubation periods monitored.

A HPLC-ECD chromatogram illustrating the peak for 8-oxoG, is shown below in Fig. 2.1. Calibration curves for G with UV detection gave a correlation coefficient value of 0.9997 and a calibration of 8-oxoG, detected by ECD had correlation of 0.9889. Both of these calibration curves were linear. The LOD of the ECD was 0.1 μM.

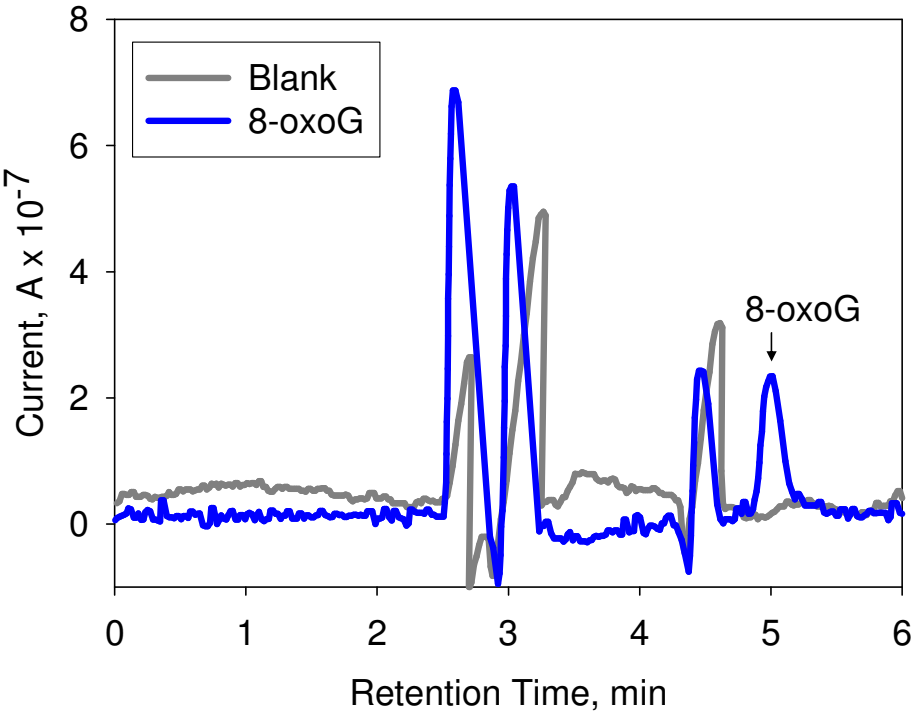

Fig. 2.1: HPLC-ECD chromatogram illustrating 8-oxoG peak. Separation carried out at 1.0 ml min^{-1} using 50 mM ammonium acetate/ 85 mM acetic acid, pH 4.6:methanol (90:10) eluent on Restek 4.6 x 250 mm RP Ultra C_{18} 5 µm column and ECD was set at +550 mV vs. Ag/AgCl. Data was processed using a Shimadzu Integrator.

2.4.1.1 Controlled experiments

A number of control experiments were undertaken on G, to ensure that all results were due to Ni/H_2O_2 induced oxidative damage to DNA, and not due to artifactual oxidation from the methodology involved or from residual contaminants such as iron in any of the reactants. ECD was applied in order to determine the concentration of 8-oxoG production.

A residual concentration of 8-oxoG was generated by the addition of H_2O_2 alone (the same amount of 8-oxoG as was measured in untreated DNA, 0.06 ± 0.02 μM). However, there was no increase in the concentration of 8-oxoG present as the incubation time with H_2O_2 increased and the concentration of 8-oxoG did not fluctuate with increasing incubation time. Neither was there any consumption of free G as the incubation time increased, nor any fluctuation in its concentration.

Significant concentrations of 8-oxoG were not detected in any of the remaining controls, indicating that the oxidative damage caused was by the Ni(II)-H_2O_2 reaction. There was no 8-oxoG detected when G was dried under nitrogen with no incubation performed. G concentration was monitored with UV detection and both G and 8-oxoG concentrations remained constant during all these controlled incubations.

As a further control, graphite furnace atomic absorption spectroscopy (GF-AAS) studies carried out on nickel sulphate samples indicated that there was less than 0.0001% Fe in these samples. This means for the 1.5 mM Ni(II) used in the experiments there was less than 0.0000075 mM (7.5 nM) of Fe present. As illustrated in the control experiments, concentration of Fe was not responsible for the oxidative damage observed below.

2.4.1.2 G incubations

The incubation of G with Ni(II) and H_2O_2 showed an oscillatory concentration of 8-oxoG over the 30 min. incubation period. In the Ni-H_2O_2 mix, the highest oscillations were found to occur for 8-oxoG at 6, 16 and 21 min, as seen in Fig. 2.1. Samples were taken in duplicate at one min. intervals; however, they

were not taken simultaneously, but rather approximately 10 s apart. Therefore, the reaction would have progressed within these 10 s. The first sample was taken after approximately 15 s and so there was some 8-oxoG formed after the first sample was taken. The resulting plots show large error bars, further indicating the progression of the reaction in between samples, especially in the formation of 8-oxoG where large error bars were seen on the higher peaks. The error bars shown illustrate the standard deviation of duplicate samples injected in triplicate in Figs. 2.2-2.4. It should be noted that the first point on the graph is after 15 s. These large differences between runs illustrate the complexity of the reactions involved in this system.

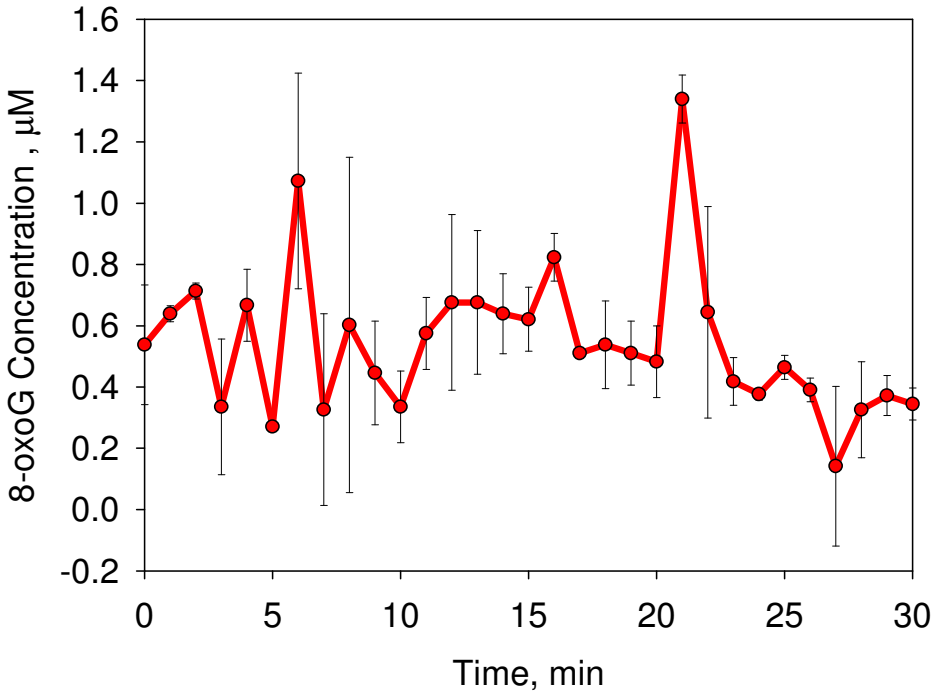

Fig. 2.2: Effect of 1.5 mM $NiSO_4.6H_2O$ and 50 mM H_2O_2 Fenton reagents on 8-oxoG concentration as a function of time, after incubation with free G at 37 ^oC. The mean of each of the duplicate samples is taken. Separation and detection carried out as described in Fig. 2.1 (N=6).

2.4.1.3 Varying the concentration of Ni

The effect of varying the concentration of Ni(II) on the reaction of G and H_2O_2 was also investigated. Ni(II) was prepared in 3 mM and 4.5 mM concentrations in order to determine if the concentration of Ni(II) has an effect on the progression of the reaction. The concentration of H_2O_2 was still in excess at 50 mM, and the concentration of the G remained the same as in the previous experiments. The results show, as illustrated below in Figs. 2.3 and 2.4 that at the higher concentrations, there is also an irregular 8-oxoG formation pattern from G.

Varying the Ni concentration did not affect the nature of the reaction involved. There was still a sporadic formation of 8-oxoG over the incubation period. For the 3 mM $NiSO_4$ incubation there was clearly a high concentration peak at approximately 7 min. and again at 11 min. The highest concentration oscillation for the 4.5 mM Ni-incubation was at 9 min. and there was a definite oscillatory pattern observed over the entire incubation period. The concentration of 8-oxoG formed from the 3 mM Ni incubation was from approximately 2 to 5.5 μM and was higher than that formed using 1.5 mM, which was from approximately 0.2 to 1.4 μM. The 4.5 mM Nickel incubation proved again to produce higher concentrations of 8-oxoG, up to approximately 7 μM.

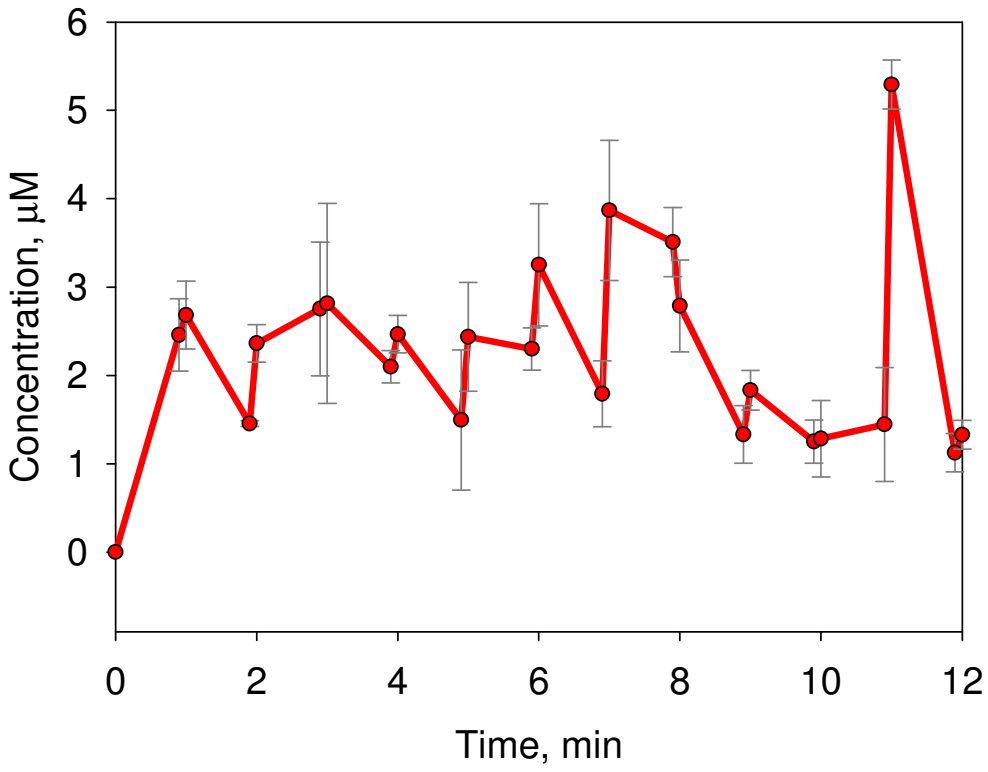

Fig. 2.3: Effect of 3 mM $NiSO_4.6H_2O$ and 50 mM H_2O_2 Fenton reagents on 8-oxoG concentration as a function of time, after incubation with free G 37 ^oC. Separation carried out using 50 mM ammonium acetate/ 85 mM acetic acid, pH 4.6:ACN (98.8:1.2) on Phenomenex 4.6 x 100 mm RP Onyx C_{18} column eluent and ECD at +600 mV vs. Ag/AgCl. The mean of each of the duplicate samples was taken. (N=3)

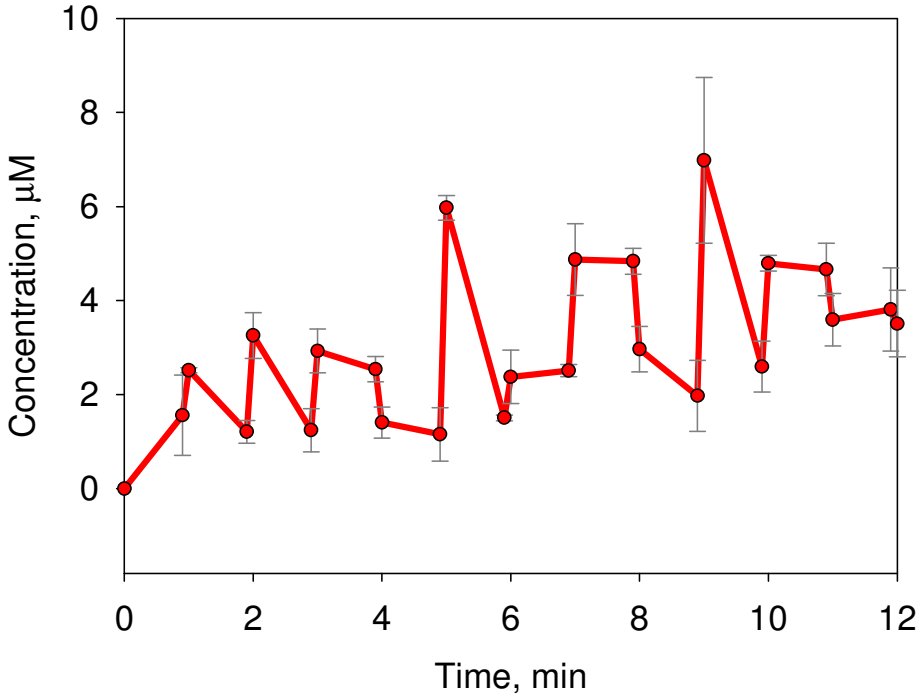

Fig 2.4: Effect of 4.5 mM $NiSO_4.6H_2O$ and 50 mM H_2O_2 Fenton reagents on 8-oxoG concentration as a function of time, after incubation of free G at 37 ^oC. Separation and detection was as per Fig 2.3. The mean of each of the duplicate samples was taken. (N=3)

2.4.1.4 8-oxoG Incubations

The incubation of 8-oxoG showed a similar erratic pattern to that observed from free G. The concentration of 8-oxoG was initially very high, but decreased sharply almost immediately, and illustrated that the reaction proceeded extremely rapidly (Fig. 2.4). The initial concentration was calculated to be 192 µM (based on initial concentration of 2.4 mM diluted by the addition of the oxidising reagents, and a 1/10 dilution upon reconstitution). However, the 0 min. concentration

observed in Fig. 2.5 (1.4 µM) corresponds to samples taken immediately upon the addition of the reagents, which was about 15 s after the reaction had begun, indicating how rapidly the initial 8-oxoG oxidation proceeded. A large oscillation was noted at 6 min. 8-oxoG oxidation by the Ni-H_2O_2 reaction was monitored over a total time of 12 min.

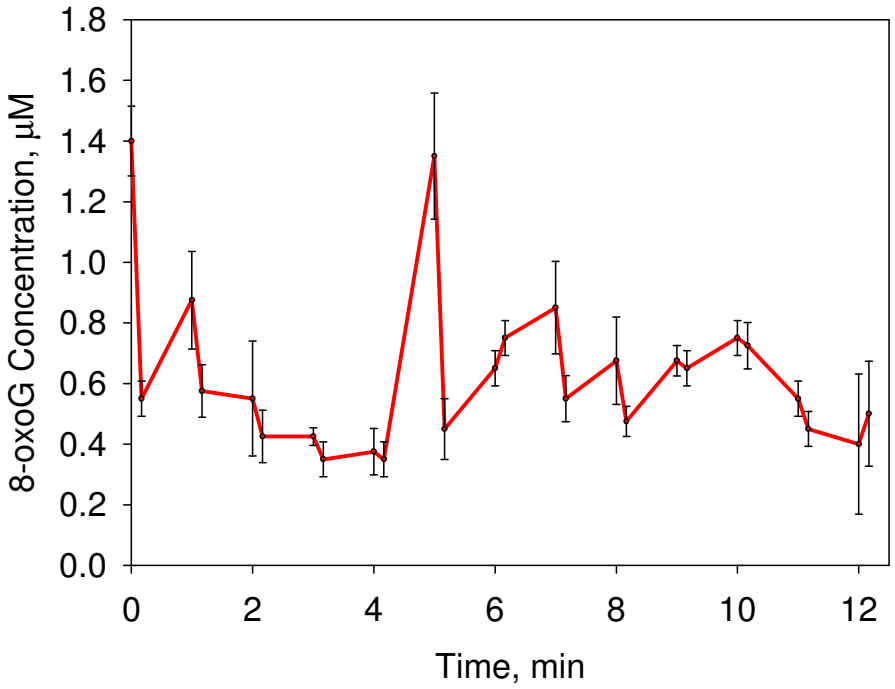

Fig. 2.5: Effect of 1.5 mM $NiSO_4.6H_2O$ and 50 mM H_2O_2 Fenton reagents on 8-oxoG concentration monitored over a 12 min. incubation with 8-oxoG at 37°C. (N=3) Separation and detection as per Fig 2.1.

2.4.1.5 DNA incubations

Ni(II)-mediated oxidative damage to G in DNA was then investigated by incubating calf thymus DNA with $NiSO_4$ and H_2O_2. The incubations were

performed over a 30 min. time period and at pH 5.5, with samples taken at 1 min. intervals. Single samples were taken at each min. and analysed in triplicate by HPLC-UV-ECD. The concentration of G in DNA and the concentration of 8-oxoG formed were monitored at each min. of the incubation period. The results observed showed chaotic patterns for 8-oxoG as was seen previously in the reaction of free G with the Ni(II) and H_2O_2 reagents. The fluctuating pattern of 8-oxoG formation is illustrated in Fig. 2.6.

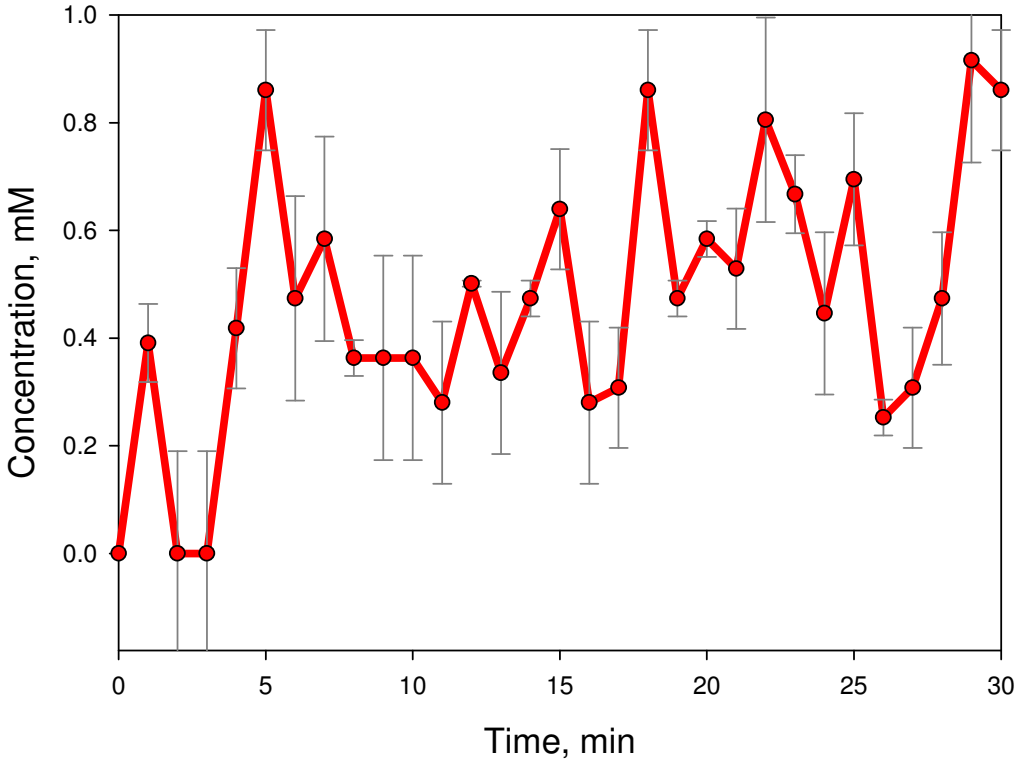

Fig. 2.6: Effect of 1.5 mM $NiSO_4.6H_2O$ and 50 mM H_2O_2 Fenton reagents on 8-oxoG concentration as a function of time, after incubation of DNA at 37 ^oC. (N=6) Separation and detection was as per Fig 2.1.

The concentration of 8-oxoG was seen to fluctuate over the incubation period. The concentration at the initial sampling was below the LOD of the ECD detector. The concentration then proceeded to increase slightly, 1 min. into the incubation, but decreased again for the next two min. The concentration then increased dramatically and the erratic, almost oscillatory pattern continued but the concentration of 8-oxoG did not fall below 0.2 μM, which was the workable LOD of the ECD system used. The highest concentrations of 8-oxoG observed were at 5 min, 18 min. and 29 min, where the concentration of 8-oxoG exceeded approximately 0.8 μM.

The concentration of 8-oxoG formed from these Ni experiments; however, were significantly lower than the concentrations noted for the previous iron experiments, probably as Ni is a much weaker oxidant. There is a possibility that nickel binds to the G molecule to enhance its oxidative abilities, thus causing G to enhance its own oxidation. Ni's oxidation powers are known to be enhanced when it binds to certain biomolecules, such as peptides [14, 27-31].

When this formation of 8oxoG was noted as a result of G oxidation at pH 11, the experiment was then carried forward to DNA at pH 5.5. The experiments on G alone were performed at pH 11 due to solubility issues. This limited the biological significance of the study, but was deemed necessary to conduct a preliminary study to ensure that the method was applicable to the detection of both G and 8-oxoG, and to ensure that 8-oxoG was actually being formed from the Ni(II)-catalysed oxidation of G.

On incubation of DNA with the reagents at physiological pH, 8-oxoG formation was monitored over a 30 min. incubation period, and again a chaotic pattern was observed. The 8-oxoG concentrations from G in DNA are approximately 2/3 of that from free G, as the concentration of G was less than that studied in free G solutions. There may also have been some protection given by the DNA backbone, and the other DNA bases could have reacted with the oxidising agents in solution, though in this study there was no investigation into oxidation products of the other DNA bases. This may be an interesting area of future study. The highest concentration of 8-oxoG concentration from Ni(II) mediated oxidative damage were found to occur at 5, 18, 22 and 29 min. The maximum 8-oxoG concentration recorded was 0.91 μM. A mass balance ratio of [8-oxoG]/{[G]+[8-oxoG]} against reaction time is shown in Fig. 2.7.

If 8-oxoG was the only product, this ratio should increase with 8-oxoG formation and plateau if 8-oxoG production ceases. The fact that the ratio did not result in a linear increase in 8-oxoG concentration, and instead oscillations were seen even here, further confirms the suggestion that the many reactions involved here were occurring simultaneously and 8-oxoG was being formed and consumed and regenerated. It also implies that 8-oxoG was not a final product of the reaction, and was just an intermediate. This evidence prompted investigation of further oxidation products.

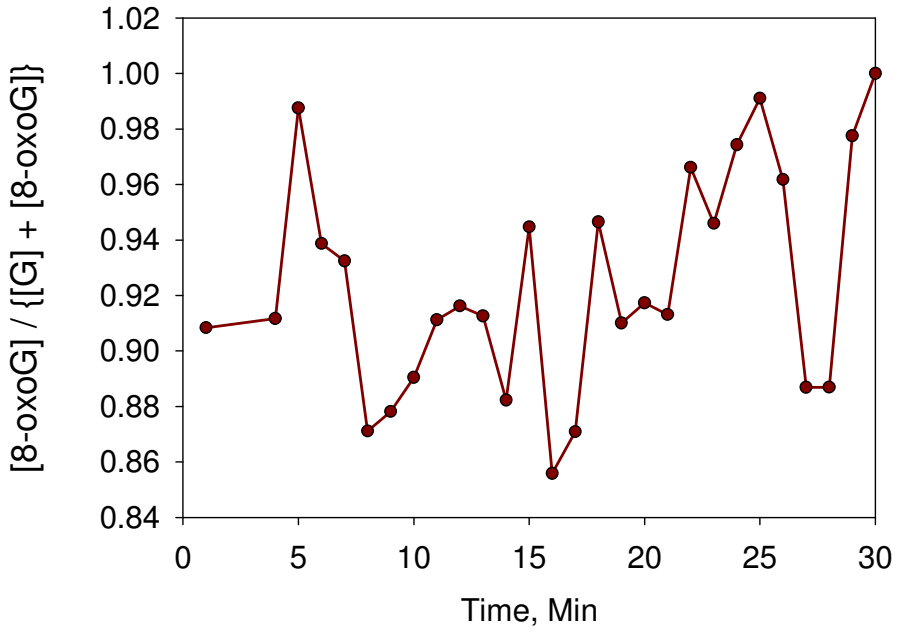

Fig. 2.7: The concentration of 8-oxoG as a ratio [8-oxoG]/{[G]+[8-oxoG]} over a 120 min. incubation period on incubation of DNA with 1.5mM $NiSO_4$ and 50mM H_2O_2 at 37°C. The concentrations displayed are in mM for both 8-oxoG and for G. Data as per Fig 2.5. Separation and detection as per Fig 2.1.

2.4.2 Mass spectrometric analysis of further oxidation products

The mass spectrometric analysis of the reaction of G, 8-oxoG and DNA with the reagents $NiSO_4$ and H_2O_2 gave a valuable insight into the mechanism of oxidation to G and 8-oxoG when free in solution and also when in the DNA backbone. It was evident that 8-oxoG was further reacting as an intermediate in the

overall process, and therefore further investigation was necessary to determine any further oxidation products of 8-oxoG. Previously identified 8-oxoG oxidation products from the literature, as well as a short summary of G oxidation from various mechanisms are illustrated in Scheme 2.2. The final products of Ni-Fenton reaction induced oxidation to G were determined by investigating the presence of these known 8-oxoG oxidation products by HPLC-MS.

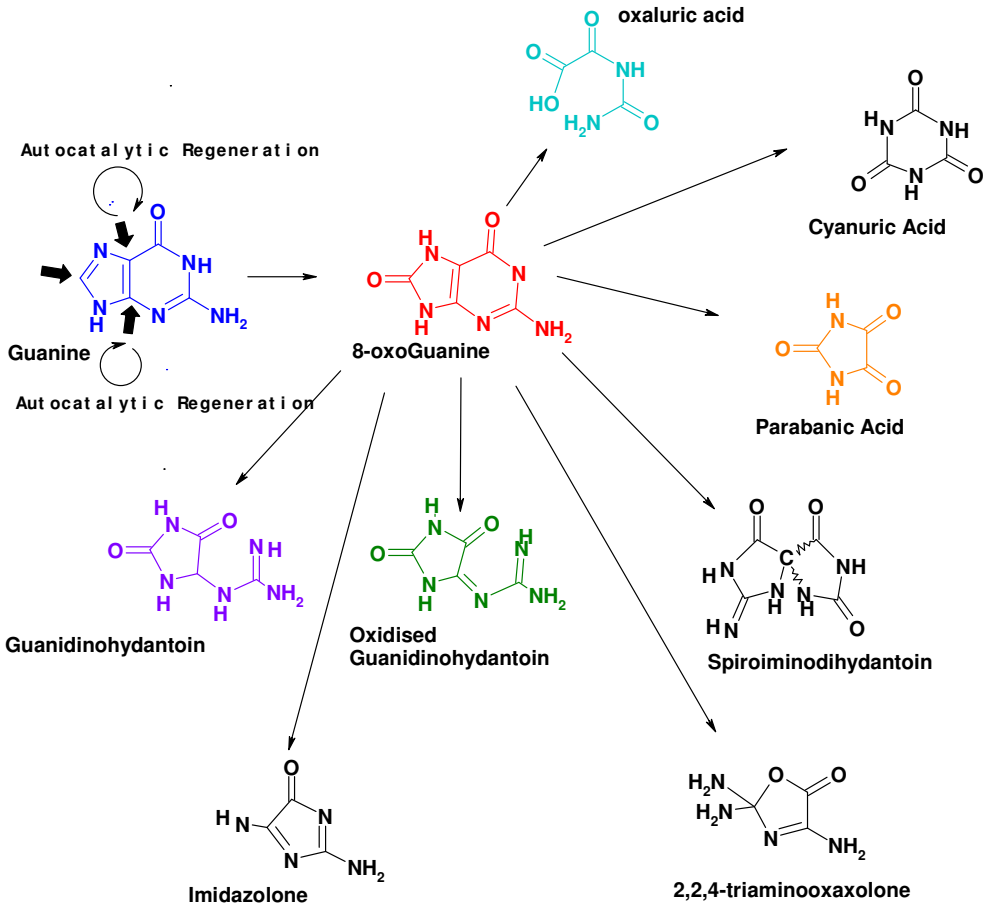

Scheme 2.2: Summary of G oxidation and further oxidation products of 8-oxoG [31, 34-37].

2.4.2.1 G analysis

The presence of suspected oxidative damage products guanidinohydantoin (GH), oxidised guanidinohydantoin (oxGH), spiroimidodihydantoin (Sp) and other similar products were investigated by analysing *m/z* values 156, 157, 158 and 159 [37-40]. The retention time of the peak at *m/z* 156, corresponding to protonated adduct [oxGH + H^+] was just over 6 min, illustrated in Fig. 2.8. A peak of *m/z* 157 was also detected. The structure of oxGH is illustrated in Scheme 2.3, below. This peak was not observed at a higher skim voltage of +30 V, indicating that the soft ionisation technique possibly allowed for double protonation of the oxGH moiety. There was no *m/z* 158 peak found in the sample. The peak at *m/z* 159 eluted with the solvent front, suggesting that it was not retained on the column, or was a component of the mobile phase. There was no peak at *m/z* 168, which would have corresponded to 8-oxoG observed in any of the G incubation samples.

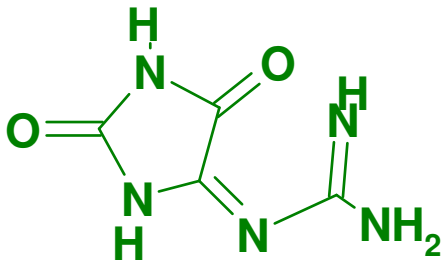

Scheme 2.3: Oxidised Guanidinohydantoin, (oxGH) [31].

The formation of oxGH, as well as GH (157 g mol^{-1}) and Sp (193 g mol^{-1}) involves the oxidation of 8-oxoG to 5-hydroxy-8-oxoG and then subsequent formation of these oxidation products. 5-hydroxy-8-oxoG is a highly reactive

intermediate and depending on the pH of the solution will form GH, oxGH, or Sp [38]. In this case, at pH 11, oxGH was formed, as would be expected.

The peak observed at *m/z* 152 corresponded to the [G + H^+] adduct. A negative ionisation potential skim voltage was then applied, in order to confirm results obtained from the mass spectrometric analysis obtained using the previous positive ionisation potentials. The extracted ion chromatograms obtained, post HPLC separation, showed the occurrence of a peak retained at less than 6 min, which corresponded to *m/z* 154, the corresponding negative ion of the *m/z* 156 product. The negative ionisation potential scan produced a deprotonated internal standard uracil at *m/z* 111, and a deprotonated G at *m/z* 150.

2.4.2.2 8-oxoG analysis

8-oxoG was analysed in positive scan mode at an ionisation skim voltage of +15V. A peak at *m/z* 168 was observed, corresponding to the [8-oxoG + H^+] adduct, as would be expected in the sample. There were no quantifiable peaks at *m/z* 158 or *m/z* 184, which, if present, would imply that 8-oxoG was fully oxidised to GH and Sp respectively. The peak that emerged at *m/z* 156 was detected; this would suggest the formation of oxGH. This is indicative that this product did, in fact, come from the further oxidation of 8-oxoG, and further illustrates the intermediate role of 8-oxoG in G oxidation.

2.4.2.3 MS/MS analysis of product of m/z 156, detected in both G and 8-oxoG

A tandem mass spectrometric scan (MS/MS) was performed on Product 1 (*m/z* 156), at retention time 6.2 min. in order to identify this product, and confirm

the presence of oxGH. The MS/MS spectrum of the *m/z* 156 peak, illustrating fragmentation is shown in Fig. 2.7. The base peak of the spectrum was *m/z* 113, and other peaks observed were *m/z* 114 and 139.6. The peak at *m/z* 86.1 seen below in Fig. 2.8 was due to background or matrix effects, and was not a fragment ion of the product compound.

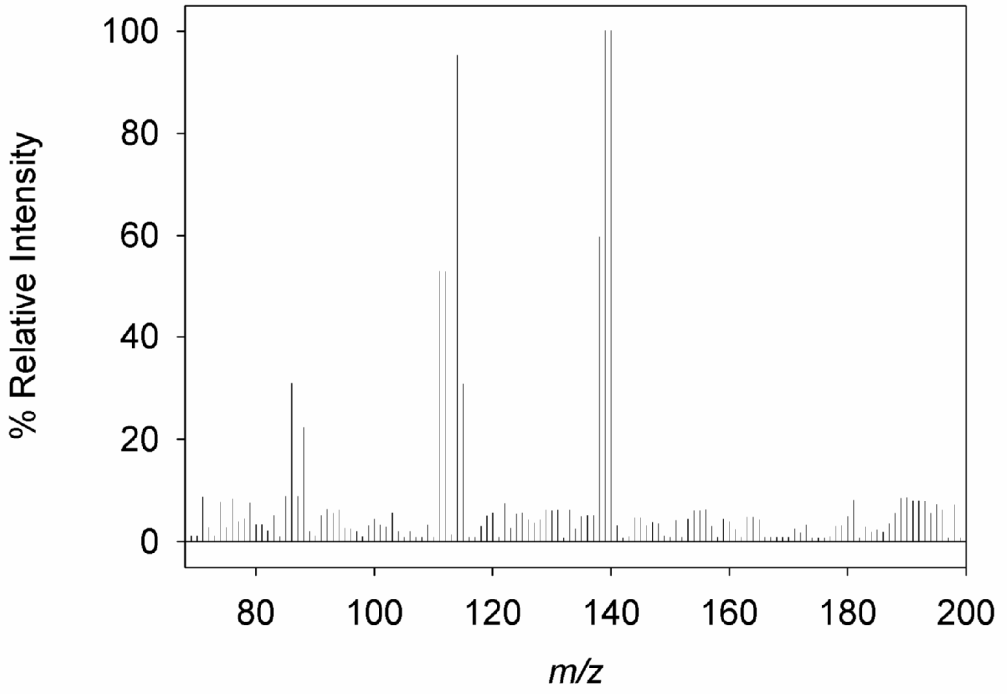

Fig. 2.8: MS/MS spectrum of peak found at *m/z* 156, illustrating fragment ions at *m/z* 113.3 and *m/z* 139.6. The MS/MS spectrum was measured after incubation of guanine with Fenton reagents $NiSO_4.6H_2O$ and H_2O_2 at 37^{o}C. The ionisation potential used was +15 V.

There were two fragment peaks observed, at *m/z* 113.1 and 139.6. Structures for these fragmentation ions are proposed in Scheme 2.4, and are consistent with the

fragmentation observed in the mass spectrum obtained for oxGH, strongly corroborating the proposal that this product was indeed oxGH.

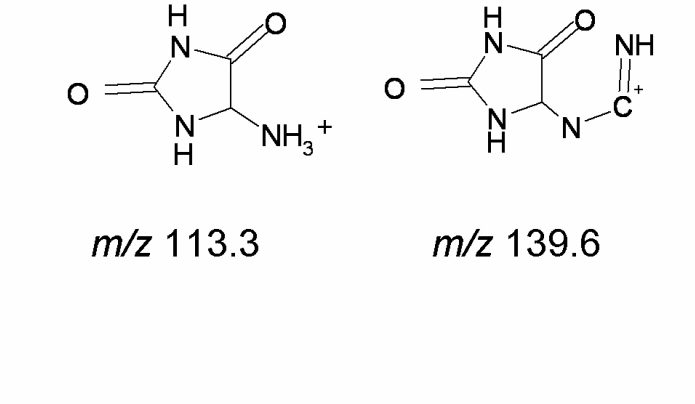

Scheme 2.4: Structure of fragment ions of oxGH seen in mass spectrum obtained from MS/MS scan of peak at *m/z* 156.

A G oxidation product, *m/z* 156, was observed over the 120 min. incubation period with the Ni(II) mediated reagents. The product concentration was seen to increase linearly, proportional to incubation time up to 60 min, after which the concentration appeared to reach a plateau, indicating that the reaction may be complete at this point, or had slowed down considerably (Fig. 2.9). As the previous incubations were only up to 12 min. for 8-oxoG and 30 min. for G and DNA, the reaction after this point could not be compared to the results obtained in the HPLC-ECD assay. Further investigation of the formation of oxGH was carried out by incubation of G for 96 hr. Samples were analysed using both mass spectrometry and HPLC-ECD up to this extended time. The formation of the *m/z* 156 product was noted after 96 hr. incubation with the reagents. It should also be noted that a small

concentration of 8-oxoG was also detected (*m/z* 168), indicating that even after 96 hr., the reaction was still continuing at this point.

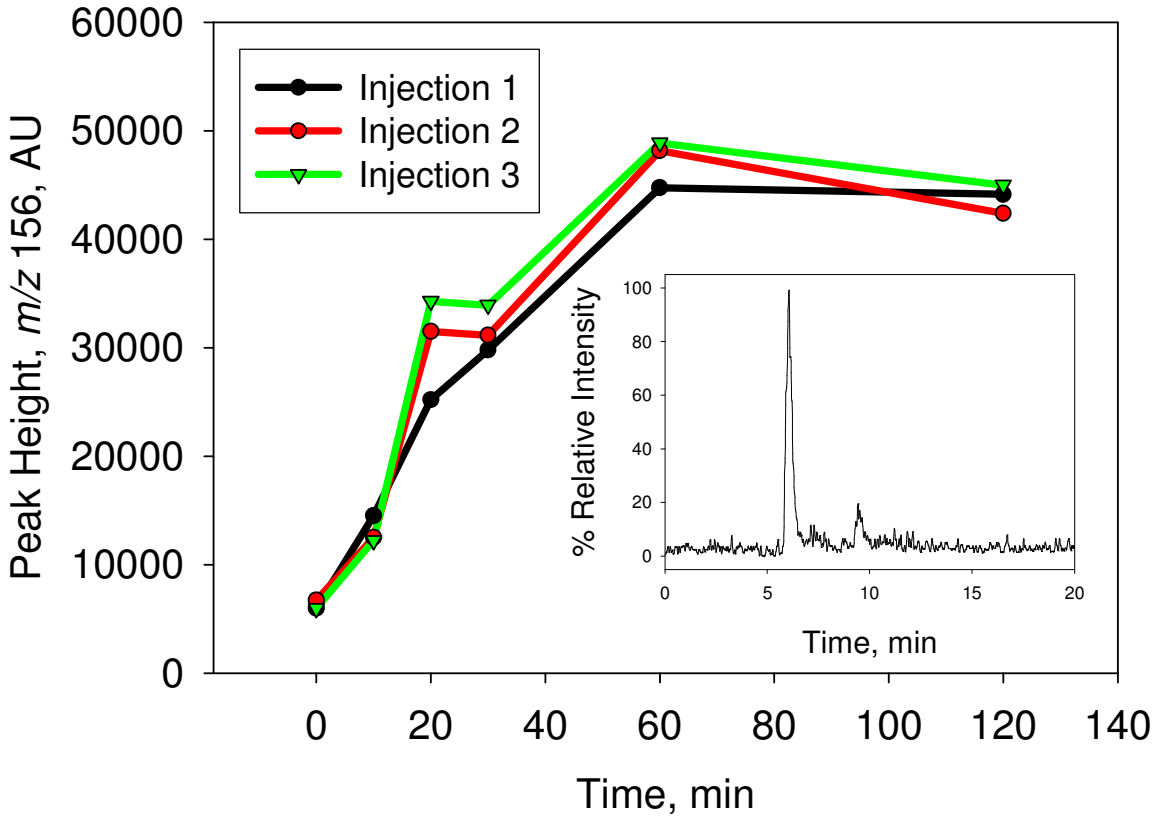

Fig. 2.9: Formation of product at *m/z* 156 from G in 10 mM NaOH over 120 min. on incubation with 1.5 mM $NiSO_4$ and 50 mM H_2O_2 Fenton reagents in stirred solution at 37 ^oC (N=3). Inset shows extracted ion chromatogram for *m/z* 156. Sample analysed by HPLC-MS as described in Section 2.3.4.

Controlled experiments showed no formation of a peak at *m/z* 156, indicating that it was indeed a product of oxidative damage via the Ni (II)-mediated reaction.

2.4.2.4 DNA analysis

A similar experiment was undertaken for the analysis of G oxidation products formed from the DNA backbone by mass spectrometry. There was no peak at *m/z* 156 observed in this experiment, which indicated that the product at *m/z* 156 was not formed from G in the DNA backbone. Similarly this experiment was carried out over an incubation period of 120 min. The G peak was observed at *m/z* 152, as was expected. A peak at *m/z* 158 was detected. Other peaks observed in the DNA sample were at *m/z* 168 corresponding to 8-oxoG. A negative ion mode analysis was also carried out on the DNA samples. This scan showed peaks of *m/z* 150 and *m/z* 166 corresponding to G and 8-oxoG, respectively.

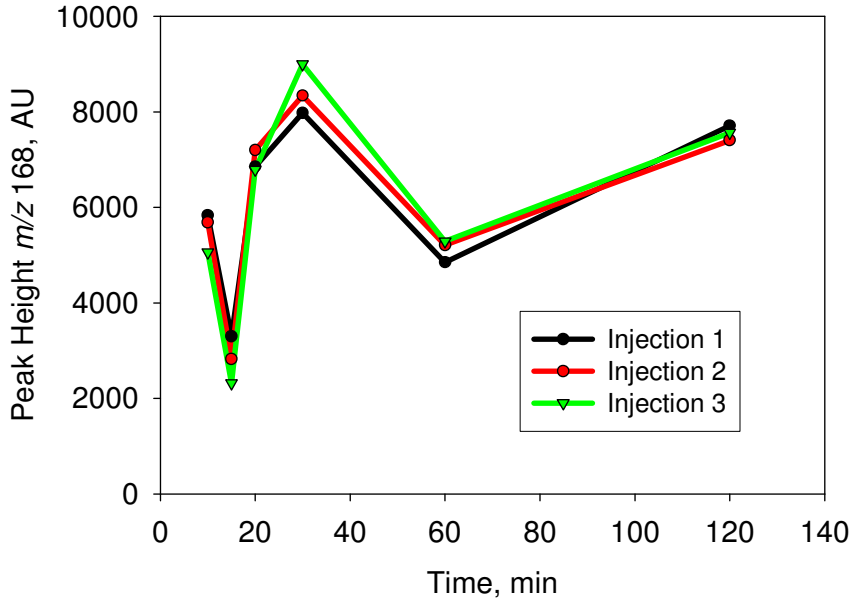

Fig. 2.10: Formation of 8-oxoG (*m/z* 168) from G in DNA on incubation over 120 min. with 1.5 mM Ni(II) and 50 mM H_2O_2 Fenton reagents at 37^{o}C. The electrospray ionisation skim voltage used for the analysis was +15 V. (N=3)

As the peak at *m/z* 168, corresponding to 8-oxoG, was formed from DNA incubations with Ni(II) and H_2O_2 Fenton reagents, the formation of this compound was monitored. It can be seen in Fig. 2.10 that there was a erratic, oscillatory-type pattern of 8-oxoG formation observed. This was seen on repeat analysis. The concentration of 8-oxoG decreased to a minimum at 15 min, followed by a sharp increase to its peak concentration at 20 min

The formation of the product at *m/z* 158 was then monitored, over the 120 min. incubation period, and is illustrated in Fig. 2.11. The formation of this product was detected in positive ion mode (*m/z* 158) 20 min. into the incubation, was not detected in negative ion mode. There was no oxGH formation from DNA at this lower pH. This would indicate that, therefore, the main final product of DNA oxidation in physiological conditions mediated by Ni(II) was most likely GH, illustrated in Scheme 2.5. The concentration of the *m/z* 158 peak, GH, proportional to the intensity of the peak, increased with increasing incubation time. This final oxidation product did not form in a variable pattern similar to 8-oxoG and this indicated that it was not an intermediate, and therefore a potential biomarker of oxidative damage to DNA.

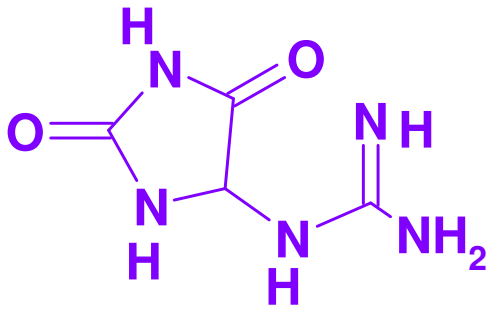

Scheme. 2.5: Guanidinohydantoin (GH) [37].

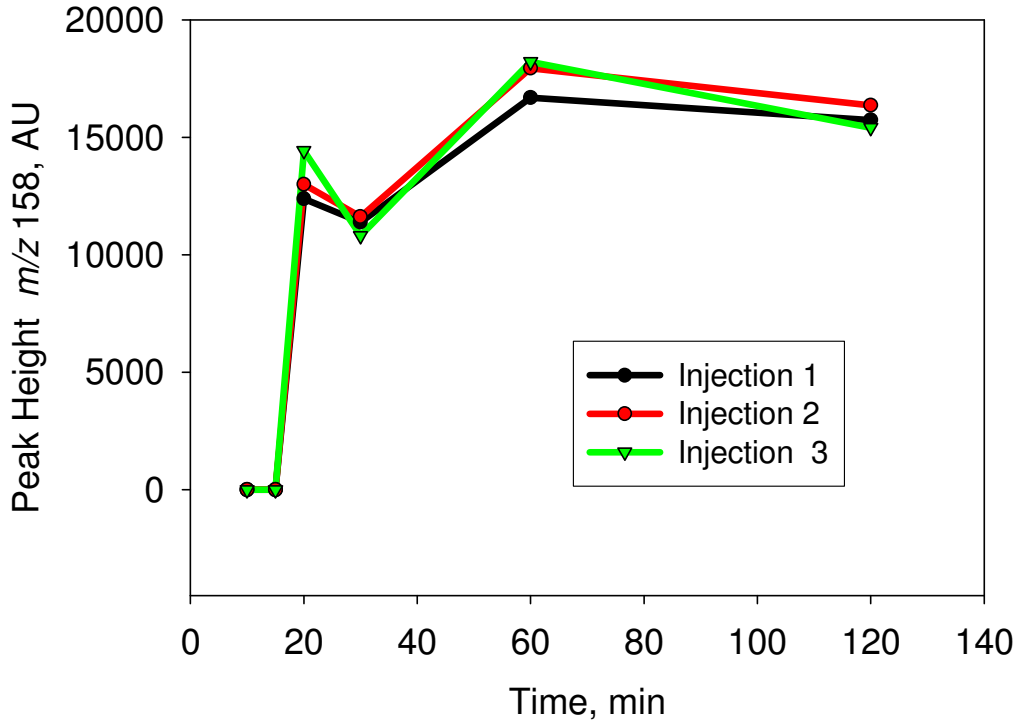

Fig. 2.11: Formation of product at *m/z* 158 from G in DNA, over 120 min. incubation period with 1.5 mM $NiSO_4$ and 50 mM H_2O_2 Fenton reagents at 37 ^oC. The ionization potential was +15 V.

The results described in this study support the idea that 8-oxoG is not a suitable biomarker for the accurate detection of these diseases due to its instability and almost oscillatory formation. The erratic pattern of 8-oxoG formation, showed a complex mechanism which involved the degradation of G resulting in the formation of 8-oxoG, and subsequent further oxidation of 8-oxoG.

This result, as was seen with the Fe-mediated Fenton reaction, illustrates a complicated mechanism which may involve numerous processes and reactions resulting in oscillatory reaction switching similar to that seen in s uch reactions as the Belusov Zhabotinsky reaction [33, 34]. The next step in this research is to elucidate this fluctuant mechanism in order to determine the exact mechanism behind this complicated nature of 8-oxoG concentration.

A simplified summary of a potential mechanism of G and 8-oxoG oxidation is illustrated in Fig 2.12. In part 1, the G is oxidised at the C8 position and the species formed is further oxidised to 8-oxoG.

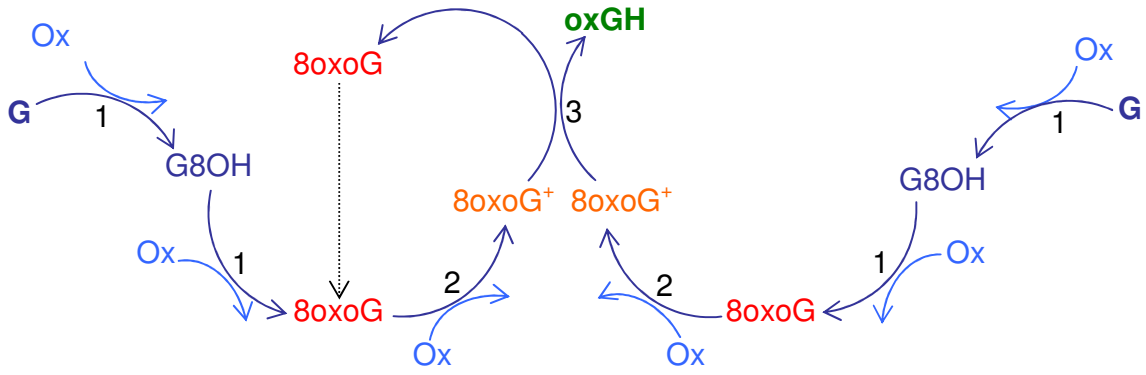

Fig. 2.12: Summary diagram illustrating a potential simplified mechanism of oxidation of Guanine. Part 1 shows oxidation of Guanine to 8-oxoG in a two step oxidation process. Part 2 shows the further oxidation of the 8-oxoG molecule to form an oxidised, highly reactive 8-oxoG+ moiety. Part 3 shows the reaction of two 8-oxoG+ to form a further oxidation product, oxGH, as well as reforming an 8-oxoG molecule, which can feed back into the reaction at the start of Part 2.

The 8-oxoG is then quickly further oxidised to form another intermediate compound, which has been named 8-oxoG+. It is the reaction of two of these highly reactive intermediates which can go on to form the further oxidation products GH, oxGH or Sp, depending on pH, as well as reforming 8-oxoG. 5-hydroxy8-oxoguanine may be an intermediate in the formation of the final oxidation products. The reformation of 8-oxoG will feed back into Scheme 2, causing the fluctuation of 8-oxoG concentration over the course of the reaction. It is for this reason that a very complicated pattern of 8-oxoG formation was observed.

2.5 CONCLUSION

The results that have been obtained in this study give some enlightenment into the mechanism of oxidative damage by Ni(II) and H_2O_2, that to our knowledge, have previously gone unreported. This work has shown that the Ni, a known carcinogen mediated oxidation of G in DNA by a Fenton-like mechanism, resulting in oscillatory pattern of 8-oxoG concentration. This result is indicative of a complex reaction mechanism, involving formation and further oxidation of 8-oxoG. It also confirms that 8-oxoG has an intermediate role in G oxidation and, therefore, is not a suitable biomarker for the determination of oxidative damage to DNA.

A determination of potential biomarkers of oxidative damage to G by Ni was then conducted. It was found, by HPLC-MS/MS analysis, that the major product of G oxidation was ox-GH at pH 11 and GH at pH 5.5. The formation of these products was of a steady increase over time, implying that they are more suitable for use as a biomarker unlike their precursor, 8-oxoG.

These results are an important stepping stone in fully elucidating the mechanisms of oxidative damage to DNA by Ni(II). There appears to be a complex, multifaceted reaction mechanism, incorporating numerous reactants, intermediates and a variety of possible products. Further work should involve analysis of other transition metals to investigate whether they behave in a similar fashion. To enable this, however, analysis methodologies should be improved to allow greater throughput of samples.

2.6 REFERENCES

1. Cotton, F.A.; Wilkinson, G.; *Basic Inorganic Chemistry*, **3rd Edition**, J. Wiley Publishers, New York, USA, **1995**.
2. Cotton, F.A.; Wilkinson, G.; Murrillo, C.A.; *Advanced Inorganic Chemistry*, **6th Edition**, J. Wiley Publishers, New York, USA, **1999**.
3. Purdue University College of Science, General Chemistry Website, http://chemed.chem.purdue.edu, Purdue University, West Lafayette, In, USA.
4. Winter, M.; *d-Block Chemistry*, Oxford Chemistry Primers, Oxford, UK, **1994**.
5. Halliwell, B.; Gutteridge J. M. C.; *Free Radicals in Biology and Medicine*, 2nd edition, Clarendon Press; New York, Oxford University Press, **1989**.
6. The Arthritis Centre of Riverside website, Information on Optimal Nutrition; www.thearthritiscentre.com/nutrition.htm, The arthritis Centre of Riverside, CA, USA.
7. Hendler, S.S.; *Doctors Vitamin and Mineral Encyclopaedia*, Fireside, New York, USA, **1990**.
8. Somer, E.; *Essential Guide to Vitamins and Minerals*, **2nd Edition**, Harper Collins, New York, USA, **1995**.
9. Walling, C.; *Accounts of Chemical Research*, 8; **1975**, 135
10. Henle, E..S.; Luo, Y.; Gassmann, W.; Linn, S.; *Journal of Biological Chemistry*, 271; **1996**, 21177-21186.

11. Henle, E.S., Linn, S.; *Journal of Biological Chemistry*, 272, **1997**, 19095-19098.

12. Landis, G.; Tower, J.; *Mechanisms of Ageing and Development*, 126; **2005,** 365-379.

13. Oikawa, S.; Kawanishi, S.; *Biochimica et Biophysica Acta*, 1399; **1998,** 19-30.

14. Lloyd, D.; Philips, D.; *Mutation Research*, 424; **1999**, 23-36

15. White, B.; PhD Thesis, *Dublin City University*, **2005**.

16. Christensen, J. M.; Kristiansen, J.; Nielsen, N. H.; Menne, T.; Byrialsen, K.; *Toxicology Letters;* 108; **1999**, 185-189.

17. Nielson, F.H. Journal of *Trace Elements in Experimental Medicine,* 13; **2000**, 113-129.

18. Mertz, W. *Proceedings of the Nutrition Society;* **33**: 307; 1974.

19. Flyvholm, M.-A.; Nielsen, G. D.; Andersen, A.; *European Food Research and Technology;* 179; **1984**, 427 – 431.

20. Ysart, G.; Miller, P.; Croasdale, M.; Crews, H.; Robb, P.; Baxter, M.; De L'Argy, C.; Harrison, N. *Food Additives Contaminants;* 17; **2000**, 775 – 786.

21.

a. U.S. Environmental Protection Agency. Nickel Compounds, Hazard Summary. National Center for Environmental Assessment, Office of Research and Development, Washington, DC, **2000**.

b. U.S. Environmental Protection Agency. *Health Assessment Document for Nickel*. EPA/600/8-83/012F. National Center for Environmental Assessment, Office of Research and Development, Washington, DC. **1986**

c. U.S. Environmental Protection Agency. *Integrated Risk Information System (IRIS) on Nickel, Soluble Salts*. National Center for Environmental Assessment, Office of Research and Development, Washington, DC., **1999.**

22. Tuteja, N.; Singh, M. B.; Misra, M. K.; Bhalla, P. L.; Tuteja, R. Molecular Mechanisms of DNA damage and repair: Progress in Plants. *Critical Reviews Biochemistry Molecular Biology;* 36; **2001,** 337-397.

23. Kawanishi, S.; Inoue, S.; Oikawa, S.; Yamashita, N.; Toyokuni, S.; Kawanishi, M.; Nishino, K.; *Free Radical Biology Medicine;* 31; **2001**, 108-116.

24. Cavallo, D.; Ursini, C.L.; Setini, A.; Chianese, C.; Piegari, P.; Perniconi, B.; Iavacoli, S.; *Toxicology In Vitro*, 17; **2003**, 603-607.

25. Leonard, S.S.; Harris, G.K.; Xianglin, S.; *Free Radical Biology and Medicine,* 37; **2004**, 1921-1942.

26. Kasprzak, F.; Sunderman Jr., W.; Salinokow, K.; *Mutation Research,* 533; **2003**, 67-97.

27. Wozniak, K.; Blasiak, J.; *Mutation Research: Genetic Toxicology*; 514: **2002**, 233-243.

28. Kasprzak, K. S.; Diwan, B. A.; Rice, J. M.; Misra, M.; Riggs, C. W.; Olinski, R.; Dizdaroglu, M.; *Chemical Research Toxicology,* 5; **1992**, 809-815.

29. Merzenich, H.; Hartwig, A.; Ahrens, W.; Beyersmann, D.; Schlepegrell, R.; Scholze, M.; Timm, J.; Jockel, K. H.; *Cancer Epidemiology Biomarker and Prevention*, 10: **2001**, 515-522.

30. Datta, A. K.; Misra, M.; North, S. L.; Kasprzak, K. S.; *Carcinogenesis*; 13; **1992**; 283-287.

31. Dally, H.; Hartwig, A.; *Carcinogenesis*; 18; **1997**, 1021-1026.

32. White, B.; Smyth, M. R.; Stuart, J. D.; Rusling, J. F.; *Journal of the American Chemical Society;* 125; **2003**, 6604-6605.

33. Noyes, R. M.*; Journal of Physical Chemistry*; 94; **1990**, 4404-4412.

34. Scott, S. J. Oscillations, Waves and Chaos in Chemical Kinetics, *Oxford University Press*, **1994**.

35. Burrows, C. J.; Muller, J. G.; Kornyushyna, O.; Luo, W.; Duarte, V.; Leipold, M. D.; David, S. S.; *Environmental Health Perspectives*; 110; **2002**, 713-717.

36. Raoul, S.; Cadet, *Journal of the American Chemical Society;* 118; **1996**, 1892-1898.

37. Schimanski, A.; Freisinger, E.; Erxleben, A.; Lippert, B. *Inorganica Chimica Acta;* 283; **1998**, 223-232.

38. White, B.; Tarun, M. C.; Gathergood, N.; Rusling, J. F.; Smyth, M. R.; *Molecular Biosystems*; 1; **2005**, 373-381.

3 ANALYTICAL METHODOLOGY FOR THE DETERMINATION OF OXIDATIVE DAMAGE TO DNA BY HPLC-UV-ECD.

3.1 INTRODUCTION

In the interest of fully and accurately elucidating and comparing the mechanisms of oxidative damage to both DNA bases and nucleosides it is essential to have a method that is precise, accurate and fast, with minimal artifactual oxidation [1].

One recognised method of determination of products of oxidative stress is HPLC coupled to electrochemical detection (HPLC-ECD) [2-4]. ECD allows for a selective determination of oxidation products 8-oxoG and 8-OH-dG, in the presence of their unmodified precursors that is not possible with simple UV detection of oxidation products [5]. The separation of DNA bases and nucleosides using the same isocratic method is uncommon. Nucleoside separations are usually carried out using gradient elution; the use of gradient elution is not necessary for the separation of DNA bases [6].

Chromatographers aim to develop reproducible, efficient, fast separations for an array of analytes. There are two main types of HPLC based on hydrophobic interactions; these are reversed phase (RP) and normal phase (NP) HPLC. In NP-HPLC, the column packing is more hydrophilic than the mobile phase, and is usually comprised of silica type packing. It is used for the separation of polar analytes, retaining the hydrophilic molecules longer. In RP-HPLC, the stationary phase is more hydrophobic than the mobile phase, and is used for the separation based on hydrophobicity, with more hydrophilic or polar analytes eluting first. This is the more commonly used type of HPLC [7-9].

The main advantages of this method include its versatility. Optimum separation conditions can be achieved for the efficient separation of similar compounds, by manipulating various aspects of the separation, such as the mobile phase composition, the flow rate, or the temperature. The system can also easily be coupled to many types of online detectors including, but not limited to, UV spectrophotometers, fluorescence detectors, electrochemical detectors and mass spectrometers [7]. The versatility of HPLC therefore means that it can be applied to a wide variety of analytes and applications. However, with every aspect of chemical analysis becoming more miniaturised and analyses requiring greater temporal resolution and in real time, it is vital that the methods of analysis that are currently in practise can keep up with moving trends [10]. Faster separations are desirable but without impact on separation quality, *i.e.* without affecting separation efficiency or peak resolution [11].

Packed silica particle columns are most commonly used in chromatographic analysis. They have the ability to be used for a wide variety of separations, both normal and reversed phase, with polar or organic modifying groups [7, 8, 12]. However, they are not particularly amenable when reducing analysis times. At higher flow rates, especially, increased column back pressure can cause the particle bed to shift and thus generate irregular pore sizes or column voids. This is especially problematic in larger particle size packing. Therefore, reducing the particle size can enhance the separation efficiency and may reduce the analysis time. The smaller packing, due its high efficiency and good resolution, means that shorter column lengths can be used. These columns generate much higher pressures

and in some cases, there has been specialised Ultra High Pressure Liquid Chromatography (UHPLC) systems developed to withstand the intense pressures created using these columns. Monolith columns can present an alternative to UHPLC as they also are capable of highly efficient separations, but with a greatly reduced back pressure [13-15].

Monolith columns, since their discovery have been at the height of recent discussion in separation science, as they exhibit superior or at least comparable separation ability over regular particle packed columns [16-17]. There are various types of monolith columns, including silica, which can have organic modifiers, and also organic polymer columns [11] and a number of methods of preparation of monolith preparation, including the sol-gel process [18]. In HPLC, they show low back pressure with high flow rates not previously viable for use in HPLC with no compromise in efficiency or resolution, allowing for well resolved and efficient separations, even with complex large biomolecules [13, 19]. Applications of monolith columns are not limited to just HPLC. They have been applied to solid-phase extraction, preconcentration, [14] capillary electrochromatography, capillary-HPLC-MS [13] and even on a large plant scale for purification [14, 20]. Monoliths do, however, suffer from some drawbacks including sensitivity to high pH values, high solvent consumption and poor reproducibility between columns [21].

The van Deemter equation, or plate height equation [7], is used as a tool of measuring column performance. A van Deemter plot of plate height, H against linear velocity is shown in Fig. 3.9. The plate height is proportional to the variance over distance travelled, and can also be calculated as shown below as a relationship

between the column length and the number of plates. A smaller plate height indicates a narrower bandwidth, and is an indicator of a better separation performance. The Van Deemter equation, shown in Eqn. 3.1

$$H = A + B/\nu + C\nu, \qquad \textbf{Eqn. 3.1}$$

is comprised of three terms. The *A* term, independent of flow rate, describes Eddy diffusion, the multiple paths taken by a solute when passing through a column. The nature of the column internal structure's inhomogeneity means that an analyte plug will spread out to an extent that is determined by the number of different paths taken by solute molecules. Vervoort *et al.* have determined that the homogeneity of a column's structure has a great impact on the *A* term, where a more homogenous structure will lower the *A* term significantly, giving a much lower H value, and thus an improved column performance. [22] The B term is inversely proportional to the flow rate, therefore, the B term is reduced at high flow rate, especially significant with monolith columns. It is a measure of the band broadening by longitudinal diffusion within a column. At high flow rates, the plug is pushed through the column and the band of analyte does not diffuse as much as at lower flow rates. In monolith columns, the permeability of the stationary phase at lower flow rates can cause the analyte band to diffuse more than would be the case in a packed column of lower permeability. However, the higher permeability also allows for the use of these higher flow rates, and so monoliths are ideal for use with lower back pressure at high flow rates [23]. The C term of the van Deemter equation is the mass transfer coefficient. As the solute passes through the column it will have various interactions with the mobile phase and the stationary phase. The term is dependent on the flow

rate, proportionally, indicating that at a higher flow rate, the plate height value is increased. This value, therefore, is important in monolithic separations, to ensure that an optimal flow rate is used in the separation. The C term is very dependent on the effective diffusion coefficient, and with a high molecular diffusivity the C term will be reduced [24-25].

For the A, there was a very significant decrease in peak height, shown in the van Deemter plot in Fig 3.9, illustrating that with increasing flow rate the chromatography improved for this peak. Each of the other peaks showed an increase in plate height value, though this was not significant enough to suggest that the separation had been compromised, and so it is suggested that there was a comparable separation across the range of flow rates. Plate height, H was calculated as follows as described in Eqn. 3.2

$$H = \frac{L}{N} \qquad \textbf{Eqn. 3.2}$$

where L is column length and N is the number of theoretical plates as calculated by Eqn. 3.3.

$$N = \frac{5.55 t_r^2}{w_{1/2}^2} \qquad \textbf{Eqn. 3.3}$$

where t_r is the retention time and $w_{1/2}$ is the peak width at half height. The adjusted peak height, generally used for the Knox plot, takes into account the size of particles in the column [26]. Peak height without any adjustment was used for the monolith column.

3.2 SCOPE OF THE RESEARCH

This study incorporated the use of a commercially available endcapped silica C_{18} RP Phenomenex Onyx monolith for the separation of both DNA bases and nucleosides on the same fast, simple and isocratic HPLC method, coupled to ECD for the determination of oxidative damage. This investigation compared the performance of the monolith against the performance of a regular particle packed column by examining the efficiency, resolution, peak asymmetry and reduction in retention time for each of the two separations. The high speed, isocratic monolith separation, which allows for the simultaneous determination of DNA bases and nucleosides, was then coupled with ECD for the specific and sensitive detection of oxidation products. The method was modified to reduce the flow rate by splitting the flow to the ECD detection, in order to reduce noise and pressure in the ECD detection. This separation resulted in a significant increase in temporal resolution and therefore has the potential to facilitate elucidation of DNA damage mechanisms with fast analysis and reduced artifactual oxidation and degradation of products.

3.3 EXPERIMENTAL

3.3.1 Materials

Deionised water used was purified using a MilliQ system to a specific resistance of greater than 18.2 MΩ-cm. All chemicals including the DNA bases and

nucleosides guanine (G0381, ≥99%), adenine (A8626, ≥99%), thymine (T0376, ≥99%), cytosine (C3506, ≥99%), and uracil (U0750, ≥99%), 7,8-dihydro-8-oxoguanine (R288608), 2'-deoxycytidine, 2'-deoxyguanosine, 2'-deoxyadenosine and 2'-deoxyuridine, ammonium acetate, and glacial acetic acid were purchased from Sigma-Aldrich (Tallaght, Dublin, Ireland). Ethanol, methanol and HPLC-MS grade methanol were purchased from Labscan Ltd. (Dublin, Ireland).

3.3.2 Chromatographic conditions

All HPLC buffers and mobile phases were filtered through a 47 mm, 0.45 μm polyvinylidene fluoride (PVDF) micropore filter (Pall, Michigan, USA) prior to use. Fresh solutions of all standards were prepared weekly, with the exception of 8-oxoG, which was prepared on day of use. HPLC analysis was performed using a Varian ProStar HPLC system with Varian ProStar 230 Solvent Delivery Module and Varian ProStar 310 UV-VIS Detector. The HPLC system was operated using Varian ProStar 6 chromatography system.

For packed column analysis, this system was coupled with a Restek RP Ultra C_{18} 5 μm 4.6 x 250 mm column, (Restek Ireland, Belfast, UK) equipped with Trident XG-XF 10mm guard cartridge fitting and 4 mm x 2 μm cap frits and ultra C_{18} 4 x 10 mm guard column with a 50 mM ammonium acetate buffer, pH 4.6/ACN (97:3) mobile phase. For monolith separations, the HPLC system was coupled to a Phenomenex Onyx RP-18 monolith column of dimensions 4.6 mm x 100 mm (Phenomenex UK, Cheshire, UK). The column temperature was ambient and the UV detector was set to 254 nm.

3.3.3 Electrochemical detection

Electrochemical cyclic voltammogram and electrolysis studies of G and dG were carried out using a CH Instruments 800B or 1000 potentiostat with accompanying software (CH Instruments, Austin, Texas, USA). Square wave voltammetry was carried out using a BAS instruments electrochemical analyser 100B. (BASi, Warwickshire, UK)

Standards were prepared immediately before each experiment to ensure no artifactual oxidation occurred. The effect of pH was measured by diluting G in phosphate buffer, pH 2.15, 6.8 and 12.33 and performing a CV scan. G and 8-oxoG standards were prepared in each of the buffers at a concentration of 10 mM. Solubility issues were encountered for G encountered at pH 2.15 and pH 6.8, however, G dissolved readily in the high pH solution. A 10 mM dG standard was prepared in deionised water and was subsequently diluted by a factor of 10, to 1 mM, in the appropriate buffer for the study. There were no solubility issues encountered with dG.

For the effect of light on the experiment, two 0.5 mM G stock standards were prepared from the 1 mM working standard at pH 6.8 in phosphate buffer by preparing a ½ dilution (3 ml Stock Standard + 3 ml buffer) . One of these standards was exposed to daylight for one day, and the other was not exposed to any light.

The effect of aerobic conditions vs. anaerobic conditions was analysed by purging samples of G with N_2 for a period of 25 min. prior to analysis and compared with G that was not purged.

HPLC-ECD was performed using a BAS CC-4 electrochemical cell comprising of glassy carbon working electrode, stainless steel auxiliary electrode and Ag/AgCl reference electrode at a detection potential of +600 mV (Bioanalytical Systems Ltd. Warwickshire, UK.) ECD chromatograms were generated using the amperometric i-t curve function of a CH Instruments 800B potentiostat. UN-SCAN-IT digitising software (Silk Scientific Corporation) was used where applicable to digitise print chromatograms, followed by analysis by Microsoft Excel or Sigma Plot Version 8.0.

3.4 RESULTS AND DISCUSSION

3.4.1 Study of the electrochemistry of guanine

3.4.1.1 The effect of pH

The effect of pH on peak potential of G was examined by comparing the peak oxidation potential for three solutions of G at varying pHs in phosphate buffers, pH 2.15, pH 6.8 and pH 12.33. There were some solubility issues encountered at the lower two pH solutions, which is inline with previous issues that have been encountered with G for HPLC analysis [27-28]. Samples were diluted to lower concentrations but even at these lower concentrations, G precipitated out of solution.

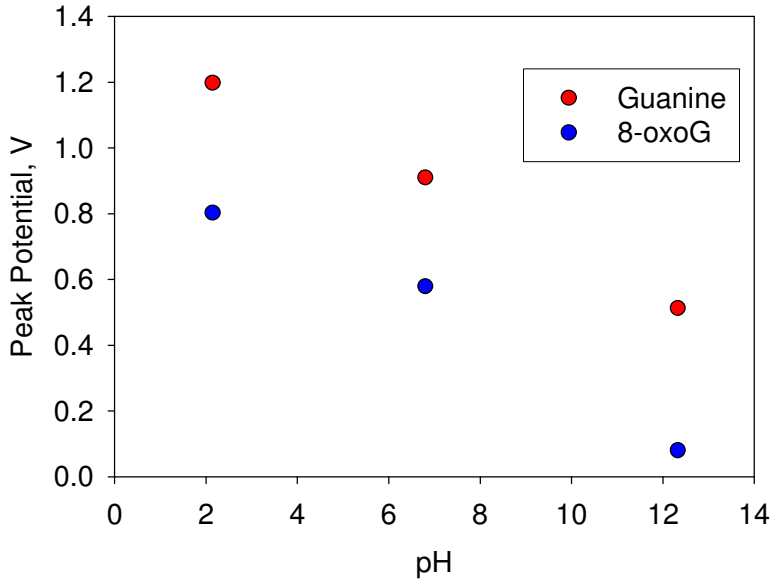

Fig 3.1: A study of the dependence of peak oxidation potential (+) for both Guanine and 8-oxoG on pH of solution using phosphate buffers at pH 2.15, pH 6.8 and pH 12.33 vs. Ag/AgCl.

The pH of the solution of G had a great impact on the oxidation potential of the solution, most likely due to the protonation and deprotonation of the G moiety, changing the difficulty to oxidise the substance depending on the pH. A significant decrease in oxidation potential noted with increasing pH (Fig 3.1). Both trends were linear with R^2 values for G and 8-oxoG were 0.998 and 0.973, respectively, both showing good correlation between points. The lines had similar slopes indicating that both substances' oxidation potential had a very similar dependence on pH, *i.e.*, both decreased with increasing pH. G was much easier to oxidise at a higher pH, most likely due to the free protons available for a $1e^-$, $1H^+$ oxidation. The difference in oxidation potential with varying pH is extremely important when selecting electrochemical detection conditions, including detection potential, when considering the mobile phase that is to be used in the HPLC method.

3.4.1.2 The effect of light

In both the dark and light exposed scans, Fig 3.2 and 3.3 respectively, there was a large oxidation peak at just over 0.8 V, corresponding to oxidation of G. The blank control, phosphate buffer, pH 6.8, showed a small oxidation peak, at a different peak potential to the 8-oxoG, indicative that there was no background interference at the same peak potential as 8-oxoG in the matrix.

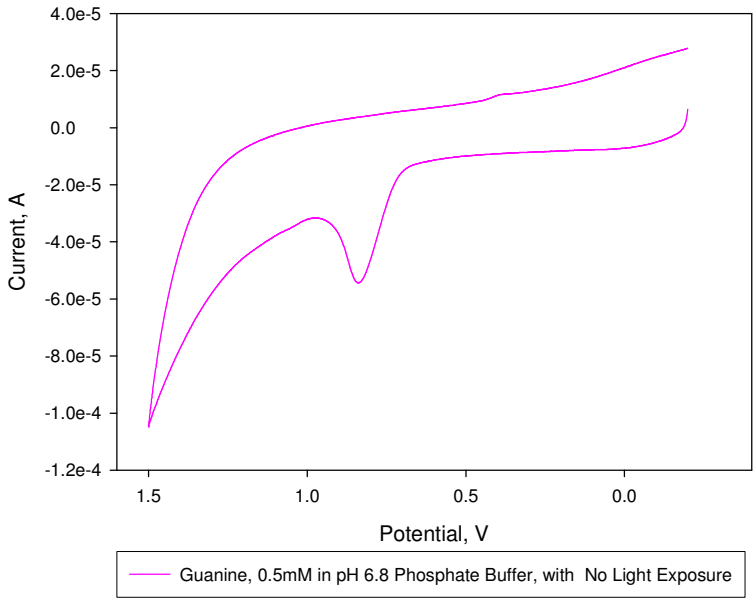

Fig. 3.2: CV of 0.5 mM G in pH 6.8 phosphate buffer, after being kept shielded from daylight for one day. Blank sample shown in Fig. 3.3. Scan rate 0.5 V s^{-1} vs. Ag/AgCl.

In the daylight exposed sample, there was a second oxidation peak, occurring at a potential of just over 0.4 V and this had a coupled reduction peak. The reduction peak did not correspond to G, as is evident from the dark exposed sample, where there was no product formation. This is assumed to correspond to 8-oxoG. There was no 8-oxoG detected at a slower scan rate of 0.1 V/s in either sample. This may have been due to the ease of further oxidation of the 8-oxoG as the potential was increased during the scan. The higher scan rate used, 0.5 V/s, however, showed the oxidation and reduction peaks corresponding to the formation of 8-oxoG (Fig 3.3). It is well known that UV radiation can cause the oxidation of G to form 8-oxoG [29]. The G solution was also left for a further two days in the

dark and daylight conditions. On subsequent scans, there was no detected 8-oxoG in either sample.

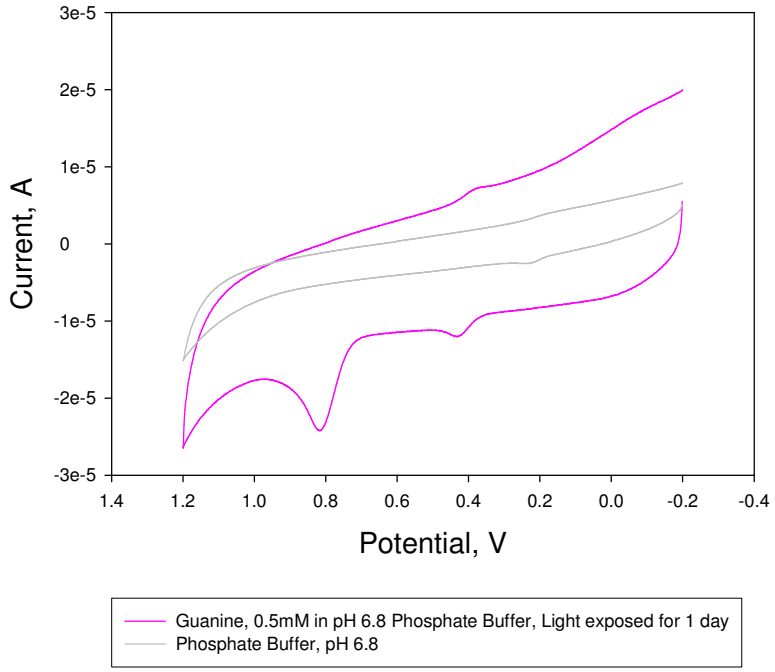

Fig. 3.3: CV of 0.5 mM Guanine in pH 6.8 phosphate buffer, after being exposed to daylight for one day. Scan rate 0.5 Vs^{-1} vs. Ag/AgCl.

3.4.1.3 Aerobic vs. anaerobic conditions

There was no significant difference observed between the anaerobic, purged sample and the aerobic sample left open to the atmosphere.

3.4.1.4 Square wave voltammetry

Square Wave Voltammetry was applied to a solution of G in phosphate buffer, pH 8.0 in order to determine the formation of 8-oxoG over time by electrochemical oxidation of the G.

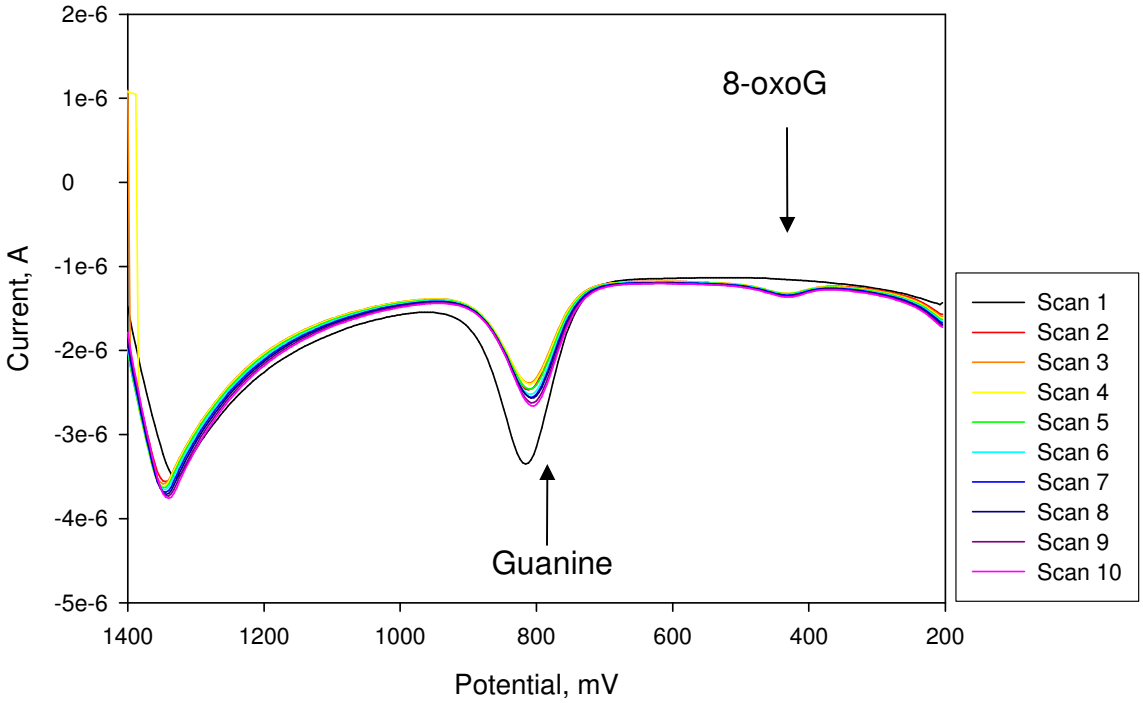

Fig 3.4: Square Wave Voltammetric Scans of a solution of Guanine, illustrating the formation of 8-oxoG peak in phosphate buffer, pH 6.8 vs. Ag/AgCl.

The results, in Fig. 3.4, show that on repeated one directional oxidising SWV sweeps, the G peak, in the region of 800 mV was seen to decrease, and there was a formation of a peak at approximately 400 mV, corresponding to the suspected formation of 8-oxoG. In this study, the potential was repeatedly swept from 1400 to 200 mV and the current monitored for 10 scans. The repeated scans caused the electrochemical oxidation of G. In the initial scan there was no 8-oxoG formation seen; however, this peak was visible in each of the subsequent scans. G was seen to

decrease in magnitude after the first scan, upon oxidation to 8-oxoG. On subsequent scans, there was a slight increase in magnitude of G oxidation peaks, though the levels of 8-oxoG formed in the process were comparable with each scan. The data clearly illustrated the formation of 8-oxoG as a result of the oxidation of G. The solution was stirred constantly, therefore, it was assumed that with each scan there is fresh G oxidised. There was no oscillatory or erratic formation of 8-oxoG observed for this reason. Ideally, in order to observe oscillations, G should be immobilised and oxidised on the surface of the electrode. This has been performed for Fe(II)-induced oxidative damage to DNA, and the expected oscillations were observed. [30]

3.4.2 HPLC comparison of RP-packed and monolith columns

3.4.2.1 HPLC-UV

A UV spectrum for each of the five analyte bases was obtained in a 50 mM ammonium acetate/85 mM acetic acid buffer, pH 4.6: methanol (90:10). The spectra showed optimal absorbance at 275 nm in a deionised water matrix. This was not the case, however, when the mobile phase at pH 4.5 was used as a sample matrix. The optimal absorbance was determined to be 254 nm (Fig. 3.5).

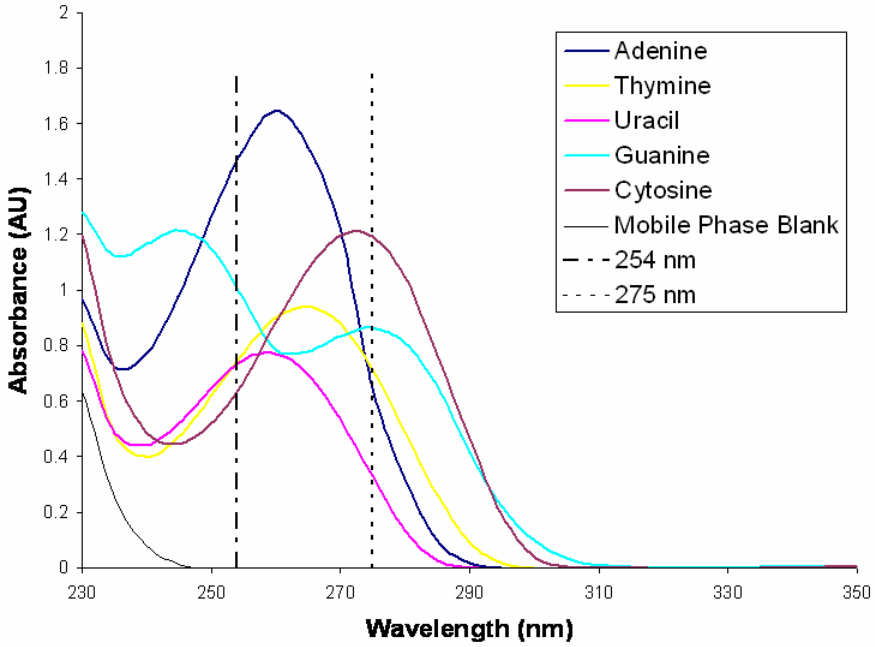

Fig 3.5: UV spectra for each of the DNA bases adenine, thymine, uracil, guanine, and cytosine in a matrix of composition 50 mM ammonium acetate/85 mM acetic acid buffer, pH 4.6/methanol (90:10).

The separation described below was based on a Restek C_{18} packed column method that had been previously used for HPLC-UV-ECD analysis of DNA bases and their oxidative damage products, as described in Chapter 2. The method was adjusted to separate both DNA bases and nucleosides and their oxidative damage products simultaneously [22,23]. The techniques and parameters were modified for use on a Phenomenex Onyx monolith RP-18 column, and the flow rate adjusted to allow for higher sample throughput, and hence a more comprehensive study, while still being able to perform sensitive electrochemical detection. The chromatography

of the packed column and the monolith column were compared for their performance.

Using a packed Restek C_{18} RP column, 50 mM ammonium acetate buffer/85 mM acetic acid, pH 4.6:methanol (90:10) was optimal for the separation of G, C, A, T, dG, dC and dA. Separation using 5%, 10% or 15% ACN or 5% methanol caused co-elution of the earlier eluting compounds, and therefore each of these mobile phase compositions were deemed inadequate. This separation, illustrated in Fig 3.6, was optimised to complete baseline separation for all peaks, with the exception of 2'-deoxyuridine and thymine. This co-elution was also observed on the monolith column, and so was left out of further separations, as 2'-deoxyuridine is only present in RNA, and not in DNA. Therefore its co-elution with thymine did not present a problem in this study of oxidative damage. It should be noted that the separation time using flow rate1.0 mL min^{-1} was of almost 40 min. in duration.

The separation of DNA bases and nucleosides was then optimised using a Phenomenex Onyx monolith RP-18 end capped column. 2'-deoxyuridine was not used in this separation, due to the previous co-elution issues that were faced. Using the same conditions as those used with the packed column, 1 mM G, U, C, A, T, dU, dG, dC and dA mixed standard was injected into a 1.0 mL min^{-1} eluent stream of 50 mM ammonium acetate buffer, pH 4.6/ACN (97:3), the result was a co-elution of the G and dC peaks.

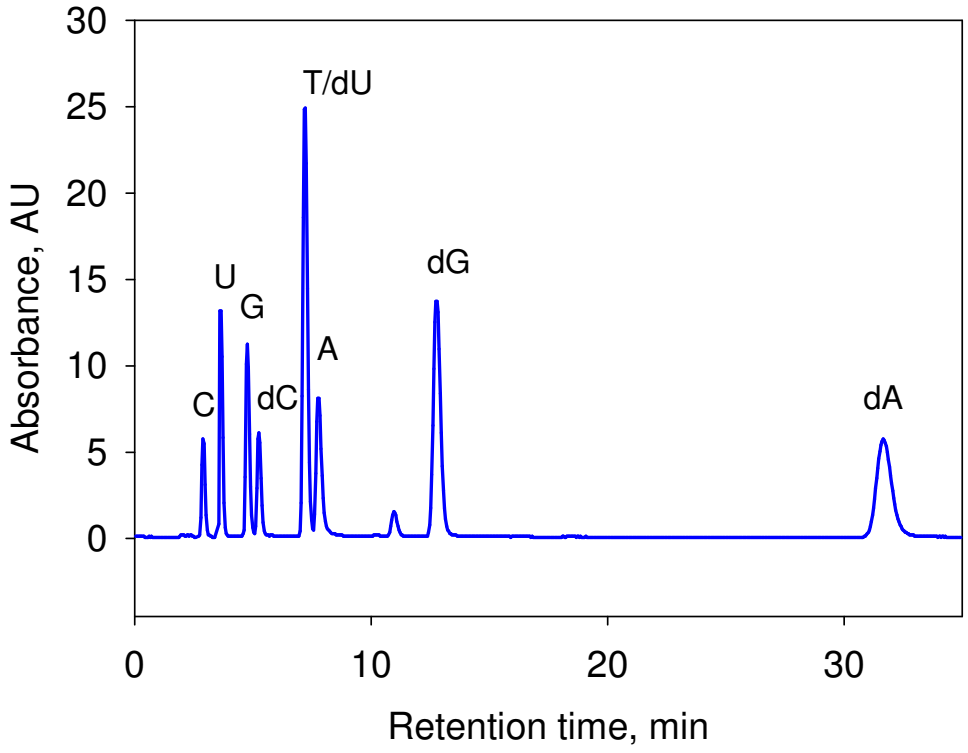

Fig 3.6: HPLC separation of DNA nucleosides and bases with UV detection at 254 nm using a Restek C_{18} 5 µm packed column with mobile phase of 50 mM ammonium acetate buffer/85 mM acetic acid, pH 4.6:ACN (97:3) at a flow rate of 1 mL min^{-1}, detection at 254 nm. Elution order: cytosine, uracil, guanine, 2'-deoxycytidine, thymine and 2'-deoxyuridine, adenine, 2'-deoxyguanosine, 2'-deoxyadenosine.

The organic content of the mobile phase was adjusted step-wise to a lower ACN content, in order to improve the separation. 1.2% ACN showed optimal resolution between the G and dC peaks.

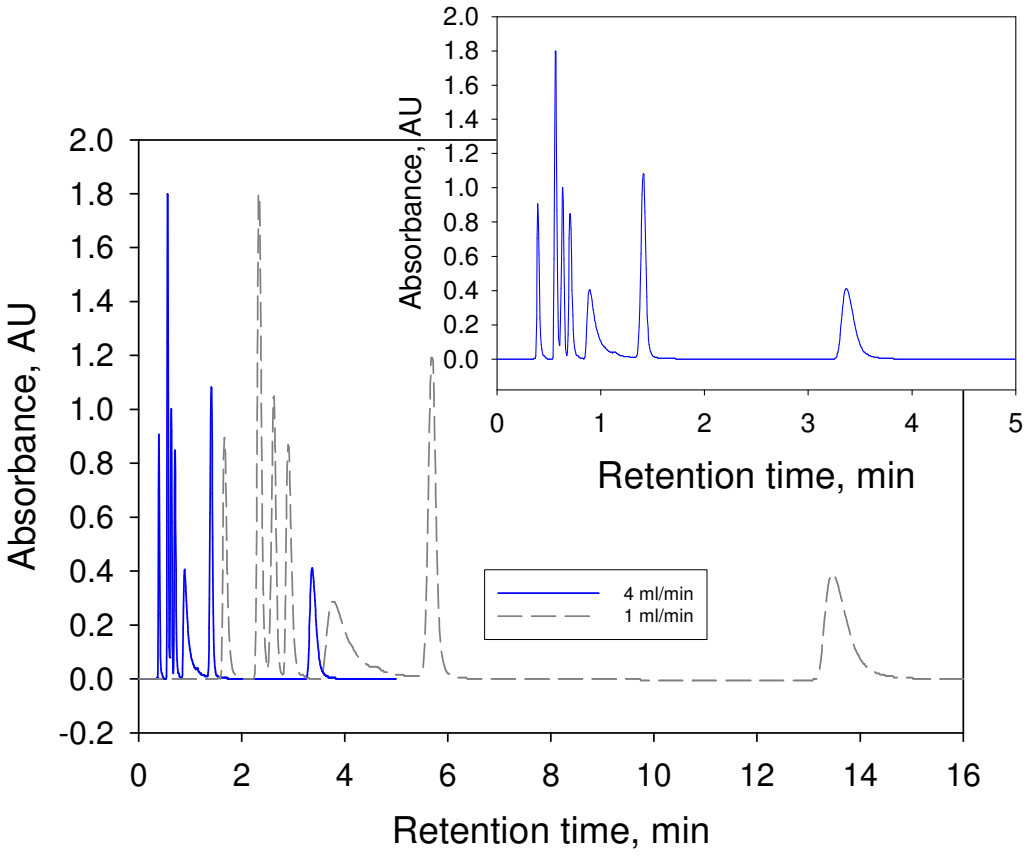

Fig 3.7: HPLC separation of DNA nucleosides and bases with UV detection at 254 nm using a Phenomenex Onyx monolith RP-18 column with mobile phase of 50 mM ammonium acetate/85 mM acetic acid buffer, pH 4.6/ACN (99.8:1.2) at a flow rate of 1 mL min^{-1} (dashed line) and at a flow rate of 4 mL min^{-1} (solid line). Elution order: cytosine, guanine, 2'-deoxycytidine, thymine, adenine, 2'-deoxyguanosine, 2'-deoxyadenosine. Inset: Separation obtained at flow rate of 4 mL min^{-1}.

The flow rate was then increased in 0.5 mL min^{-1} increments from 1.0 mL min^{-1} to 4.0 mL min^{-1}. This separation is shown in Fig. 3.7. The quality of the separation was analysed at each of these flow rates. It was evident that the

performance of a monolith column was at its best at the higher flow rates, with no significant loss in efficiency and comparable or better asymmetry, as discussed below. The benefit of increasing the flow rate was especially noticeable for the A peak. It should be noted that due to co-elution, that uridine could not be used as an internal standard for any future studies; nonetheless the separation was adequate for the separation of the DNA bases and nucleosides, as the nucleoside uridine is only present in RNA. For internal standard purposes; however, U, (the DNA base equivalent) was completely baseline resolved, eluting between C and G on both the packed column and the monolith column (data not shown) and therefore could be used if an internal DNA standard was needed.

Figure 3.8 (a) illustrates a significant decrease in asymmetry for A with increasing flow rate. The van Deemter and Knox plots (figs. 3.9 and 3.10, respectively) show a decrease in plate height with increasing linear velocity for A. The Knox plot also illustrated a comparison between the Restek packed column at 1.0 ml min^{-1} and the Phenomenex monolith at both 1.0 ml min^{-1} and 4.0 ml min^{-1}. There was a higher level of asymmetry in the monolith at 1.0 ml min^{-1} in comparison to the packed column, though in most cases, at 4.0 ml min^{-1} this tailing was reduced to a level comparable to that of the packed column, indicating the improvement of the separation with increased flow.

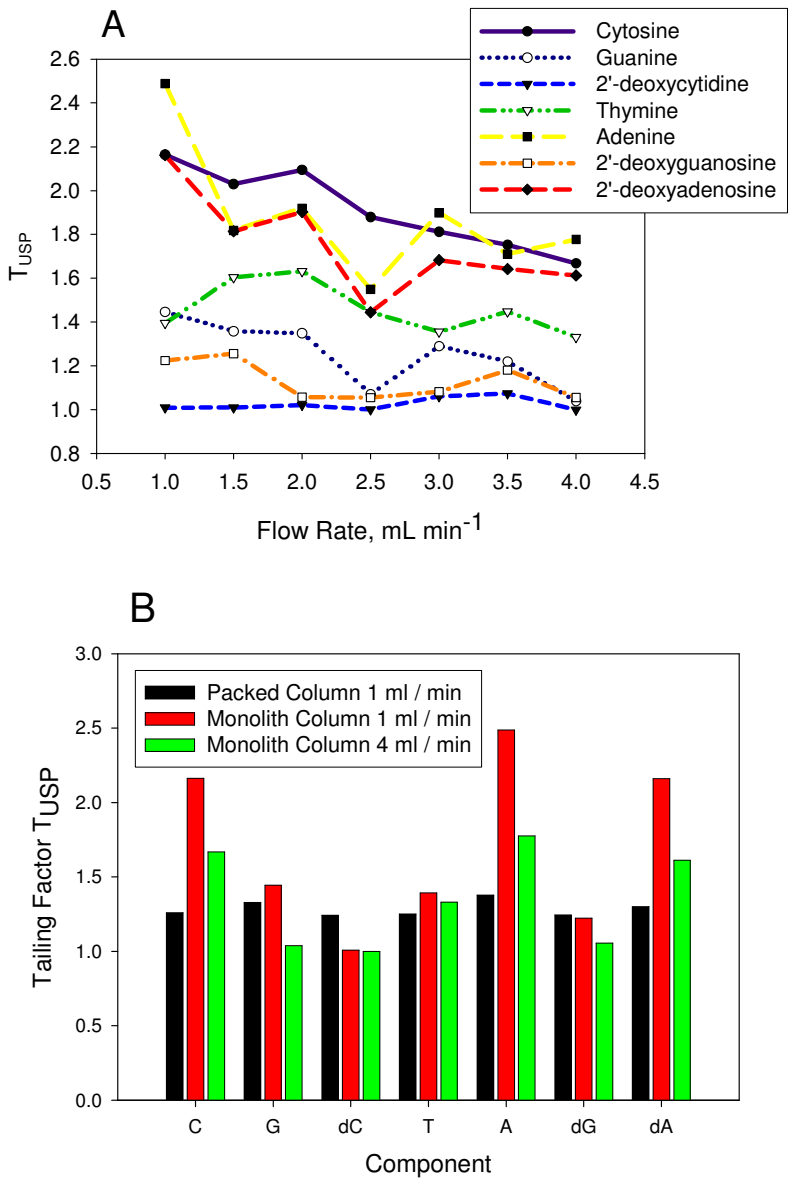

Fig 3.8: a.Effect of increasing flow rate on peak asymmetry (USP Tailing, T_{USP}) for each of the separation components, cytosine, guanine, 2'-deoxycytidine, thymine, adenine, 2'-deoxyguanosine, 2'-deoxyadenosine on a Phenomenex 4.6 mm x 100 mm Onyx RP-18 Monolith.

b. Comparison of tailing factor between packed (Restek 5 µm 4.6 x 250 mm RP Ultra C18) and monolith (Phenomenex 4.6 mm x 100 mm Onyx RP-18 monolith) columns for each component.

In general, peak asymmetry decreased or was comparable with increasing flow rate for all peaks, but most especially for adenine and 2'-deoxyadenosine. This was illustrative that the tailing of the peaks improved with an increasing flow rate on the monolith column. The peak widths themselves for the monolithic column were greatly reduced by increasing the flow rate through the monolithic column.

At the higher flow rate, the level of asymmetry was reduced for most peaks until they were comparable with those of the packed column. The separation time, even at 1.0 ml min^{-1} using the monolith with 1.2% ACN mobile phase was just 14 min. and this was reduced to less than 4 min. Therefore, overall, there was a 90% decrease in runtime from 40 min. on a packed column to 4 min. on a monolithic column with no significant loss in resolution (Table 3.2).

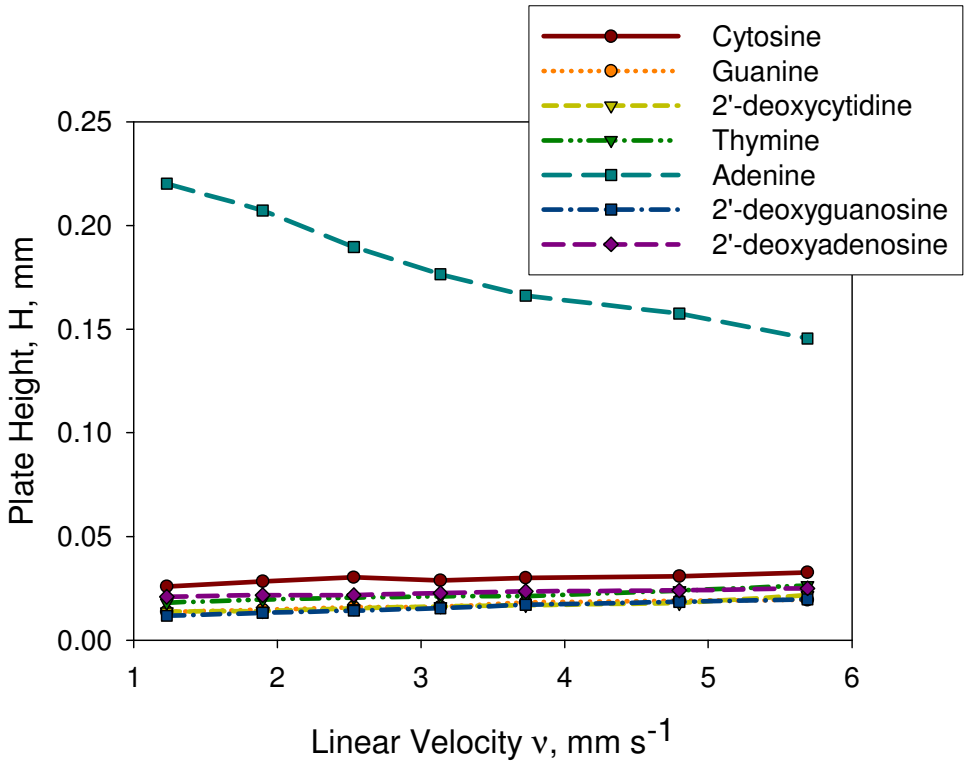

Fig 3.9: Van Deemter Plot of Plate Height, H for each of the separation components, cytosine, guanine, 2'-deoxycytidine, thymine, adenine, 2'-deoxyguanosine, 2'-deoxyadenosine on the monolith column (Phenomenex 4.6 mm x 100 mm Onyx RP-18 monolith) against eluent linear velocity.

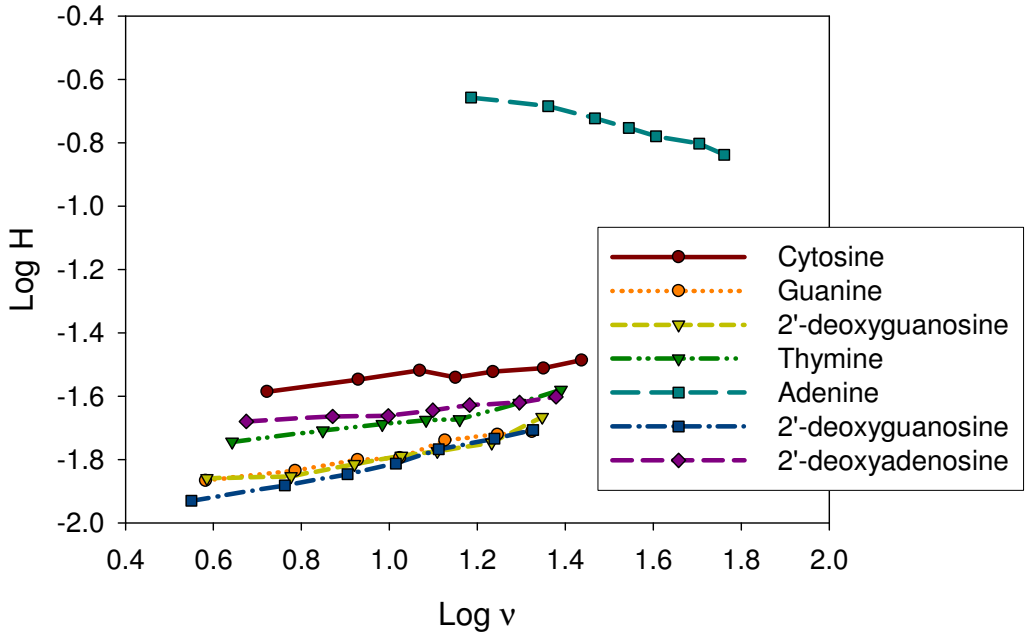

Fig. 3.10: Knox Plot of log of reduced peak height for each of the separation components, cytosine, guanine, 2'-deoxycytidine, thymine, adenine, 2'-deoxyguanosine, 2'-deoxyadenosine on the monolith column (Phenomenex Onyx RP-18 monolith 4.6 mm x 100 mm) against the log of the linear velocity.

The separation efficiencies were reduced slightly for the early eluting compounds with increasing flow using the monolithic column. However, this reduction was primarily due to the decreased retention time for these components, as the number of theoretical plates is proportional to the retention time. The separation efficiency for A was reduced on transfer of the separation to the monolithic column. This may be due to increased silanol activity often observed with monoliths. A significant reduction in number of theoretical plates is noted for

some components (Table 3.1), though it is accepted that the calculated efficiency values can decrease with increase in flow rate [31].

The pressure in the packed column, at 1.0 mL min^{-1} was approximately 203 x 10^6 Pa (approx 3000 psi), whereas in the monolith column, it was just 2.53 x 10^6 Pa (367 psi). As the flow rate, and hence back pressure increased, peak shapes were improved or not changed significantly, as was evident from the improvement in asymmetry with flow rate in Fig. 3.8. The asymmetry, measured as tailing, was reduced slightly or comparable for each of the components with increasing flow velocity. There were no significant changes in asymmetry that would indicate a compromise in separation quality. There was also noticeable reduction in tailing for Ade which was be the most problematic peak, where tailing is concerned.

The efficiencies of each component of the DNA and nucleoside mixture were comparable over the entire range of flow rates. There was not a dramatic increase to illustrate the significant reductions in overall runtime, as the retention times were reduced along with the peak width at half height. Some components, especially the early eluting compounds did show a decrease in efficiency, most likely due to extra column effects, though this change was not significant enough to alter the integrity of the separation.

Efficiency values were not fully able to illustrate the effectiveness of increasing the flow rate in this study. The efficiencies of each of the DNA and nucleoside mixture are illustrated in Table 3.1, and were comparable over the entire range of flow rates. There was no dramatic increase, as the retention times are reduced along with the peak width at half height.

Efficiency									
	Flow rates (ml min. $^{-1}$)	Restek (1.0)	1.0	1.5	2.0	2.5	3.0	3.5	4.0
1	Cytosine	4946	3853	3525	3299	3473	3330	3245	3060
2	Guanine	9744	7336	6831	6322	6232	5487	5252	5146
3	deoxyCytidine	9012	7233	7128	6527	6136	5944	5583	4629
4	Thymine	10322	5550	5108	4876	4738	4711	4181	3799
5	Adenine	8502	454	483	528	567	602	635	687
6	deoxyGuanosine	10875	8512	7615	7020	6495	5858	5424	5093
7	deoxyAdenosine	12901	4780	4611	4590	4410	4247	4170	3999

Table 3.1: The calculated efficiencies of each of the separation components, C, G, dC, T, A, dG, and dA illustrating the effect of flow rate on number of theoretical plates.

Resolution									
	Flow rates (ml min. $^{-1}$)	Restek (1.0)	1.0	1.5	2.0	2.5	3.0	3.5	4.0
1	Cytosine	10.5	6.1	5.8	5.5	5.6	5.3	5.3	5.6
2	Guanine	2.4	2.5	2.3	2.2	2.2	2.1	2.0	2.0
3	deoxyCytidine	7.7	2.0	2.0	2.1	2.1	2.2	2.1	1.8
4	Thymine	1.9	2.0	1.9	1.9	1.9	1.9	1.8	2.0
5	Adenine	12.1	4.0	4.0	4.1	4.2	4.2	4.3	4.8
6	deoxyGuanosine	23.6	15.1	14.7	14.5	14.1	13.7	13.5	13.4
7	deoxyAdenosine	10.5	6.1	5.8	5.5	5.6	5.3	5.3	5.6

Table 3.2: The calculated resolution values for the separation components, C, G, dC, T, A, dG and dA, illustrating the effect of flow rate on resolution.

The resolution was calculated as shown in Eqn. 3.4 below.

$$R = \frac{\Delta t_r}{w_{av}} \qquad \textbf{Eqn. 3.4}$$

Resolution remained comparable for each of the components as the flow rate increases. Baseline resolution (>1.7 for all peaks) was maintained between all adjacent components of the DNA nucleoside and bases, indicative therefore, that even with the dramatic run-time reduction and resulting closely eluting peaks, the separation was not compromised. Comparing the packed Restek column at 1.0 mL min^{-1} to the optimum monolithic flow rate of 4.0 mL min^{-1}, the resolution values were significantly higher for the Restek column. However, this was due to a dramatic decrease in the elution time when using the monolithic column, and did not represent a diminishment in the overall separation quality.

3.4.3 HPLC coupled to electrochemical detection

The peak detection potential was obtained from Hydrodynamic Voltammograms (HDV), for each of 8-oxoG and 8-OH-dG, over a potential range of 400 to 800 mV vs. Ag/AgCl. The results as displayed in Fig. 3.11 show that both samples were similarly oxidised, and could be detected adequately by electrochemical detection at approximately 650 to 700 mV in the LC mobile phase conditions used. At approximately 650 mV, greater than 90% of the 8-oxoG was fully oxidised and at 700 mV, greater than 90% of the 8-OHdG was fully oxidised. In order to ensure specific detection of 8-oxoG, G oxidation analysis was carried out at +600 mV to ensure that there was no G oxidation occurring, and thus affecting the result. For simultaneous 8-oxoG and 8-OH-dG analysis, 650 mV was

used, in order to oxidise both 8-oxoG and 8-OH-dG, with minimal interference from G.

Fig 3.12 illustrates the difference in peak oxidation potential between G and dG. The peak oxidation potential for G was 0.905 V whereas dG had a peak potential of 1.104 V. This effect was also evident in Fig. 3.11 for 8-oxoG and 8-oxodG; illustrating the effect of the attached sugar in the nucleoside on the electrochemistry of the moiety.

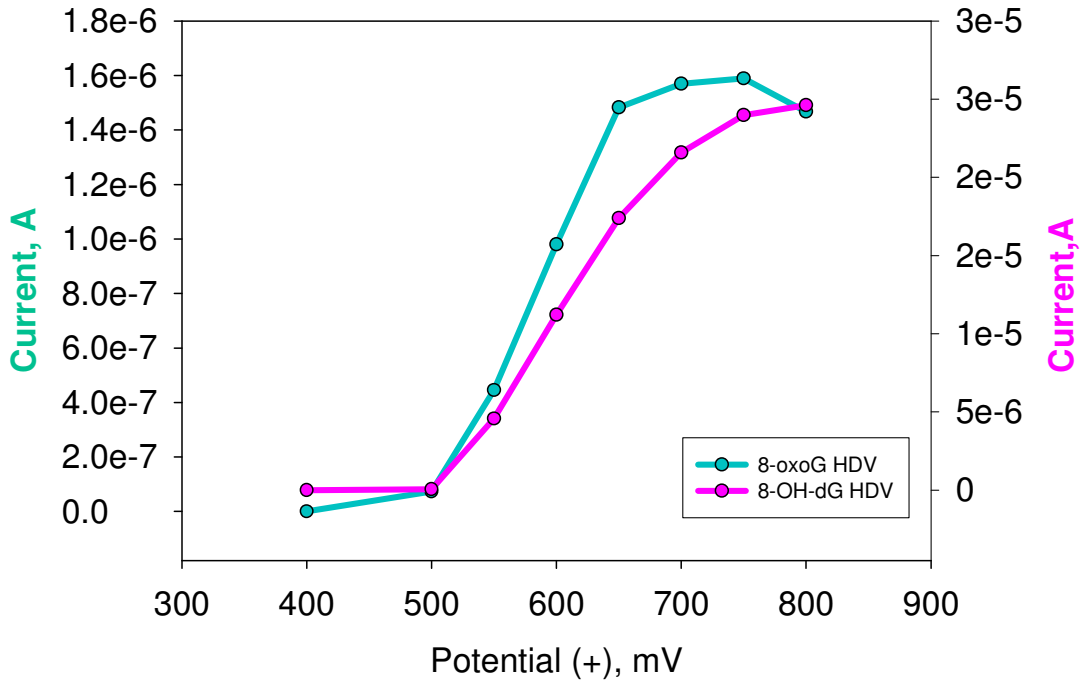

Fig 3.11: Hydrodynamic voltammograms for 8-oxoG and 8-OH-dG in 50mM ammonium acetate/85 mM acetic acid buffer, pH 4.6/ACN (97:3) vs Ag/AgCl in order to determine the peak oxidation potential for both substances.

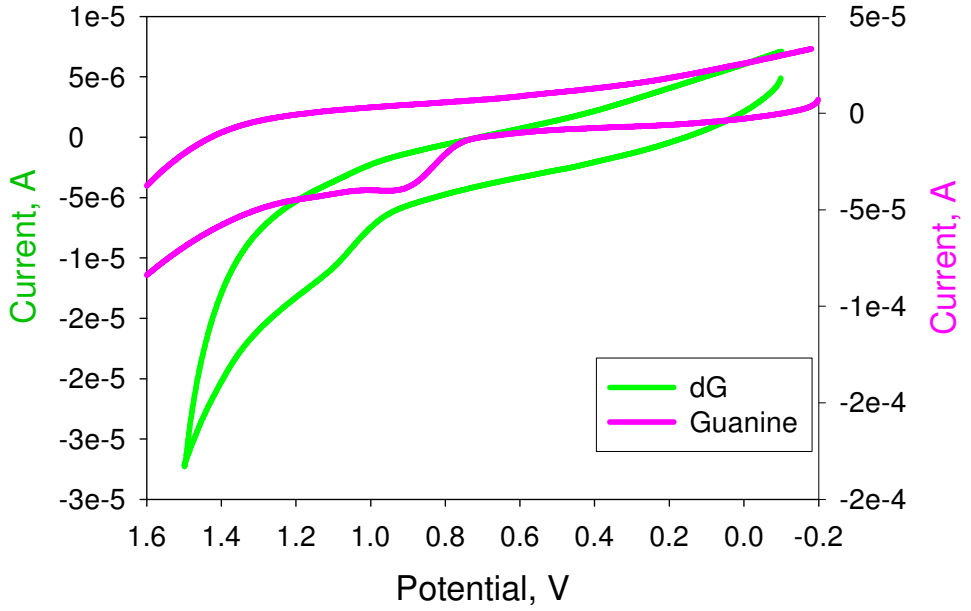

Fig 3.12: Comparison of CVs of G and dG, in phosphate buffer pH 6.8 vs. Ag/AgCl, to illustrate the difference that attachment of a sugar on the dG moiety makes to the electrochemistry.

A major issue in applying a high-speed monolith separation to the analysis of oxidative damage to DNA is the effect of the high flow on the electrochemical detection. Use of inline flow cell electrochemical detection (ECD) is ideal for low flow rate separations, but at 4.0 mL min^{-1}, baseline noise as well as high pressure in the lines and leaks became a problem. In order to use such high flow streams, a splitting of the eluent stream was necessary. Flow-splitting apparatus can be expensive; however, in this study the flow splitting was accomplished using a simple t-piece coupled with PEEK tubing, the inlet was 0.254 mm ID, as was the waste outlet, and the outlet to the ECD detector was 0.178 mm ID (Fig. 3.13). The high pressure in the lines caused by the high flow rate meant that there was a

constant flow through the smaller diameter tubing and the stream did not just go to the larger diameter waste line.

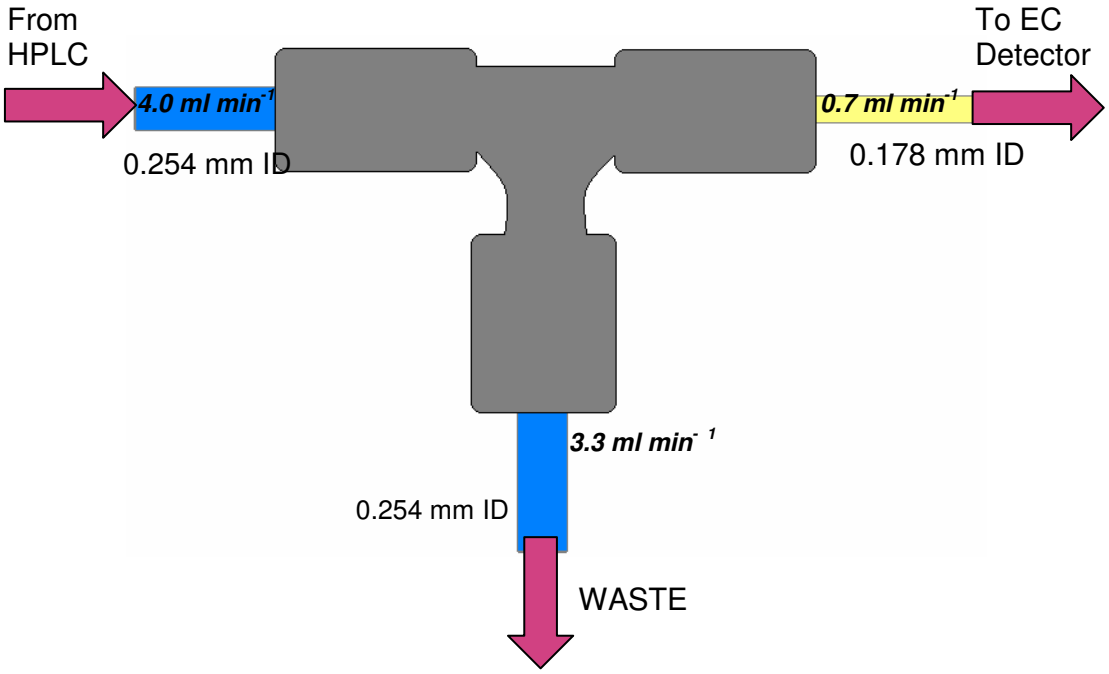

Fig. 3.13: Illustration of the T-piece flow splitting device used to minimise high flow to the electrochemical detection system.

The high pressure in the line created by the fast flowing eluate caused enough pressure to drive the split in the flow so that 3.3 mL min^{-1} was sent to waste and 0.7 mL min^{-1} was sent to the ECD detector cell.

The level of noise on the ECD detector was of approximately 1 x 10^{-10} Amps, while the G damage product 8-oxoG was still easily quantified. The selective detection of 8-oxoG and 8-OH-dG was carried out at +600 mV and 700 mV, respectively and was linear with good correlation coefficients of 0.99 or

greater recorded for concentrations in both the micromolar and millimolar ranges. The simultaneous separation of 8-oxoG and 8-OH dG was carried out at 650 mV and is shown in Fig. 3.14. The limit of detection, as with most HPLC-ECD methods, was in the nanomolar range, at approximately 50 nM [6, 27]. This was comparable to the LOD obtained with the traditional HPLC-UV-ECD which utilised the Restek C_{18} column.

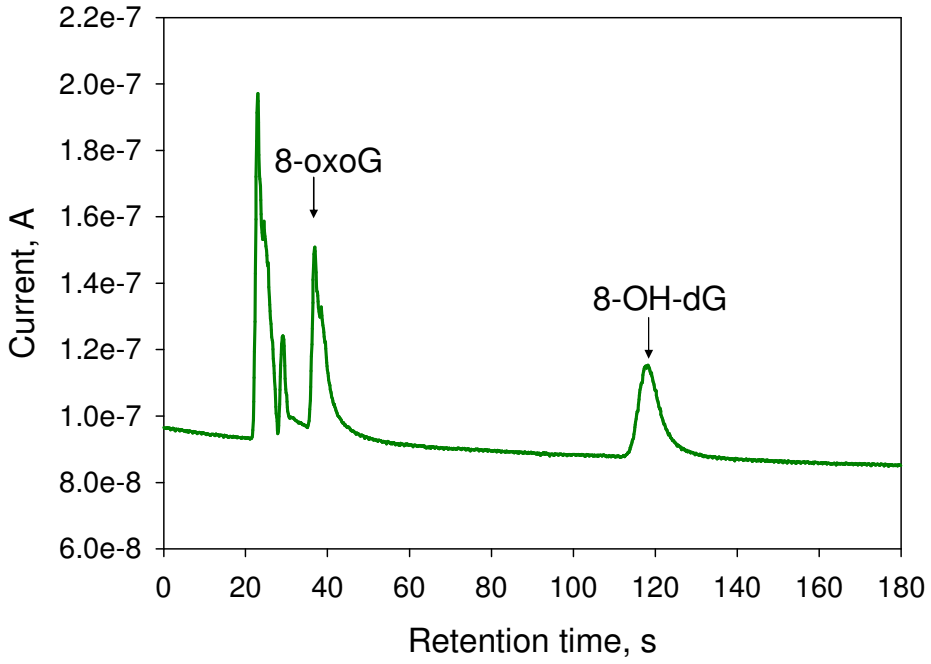

Fig 3.14: HPLC separation of DNA nucleosides and bases with ECD at +600 mV using a Phenomenex Onyx monolith RP-18 column with mobile phase of 85 mM ammonium acetate, 50 mM acetic acid buffer, pH 4.6:ACN (98.8:1.2) at a flow rate of 0.7 mL min^{-1} (Split peak is product of digitisation).

3.5 CONCLUSION

The separation of both nucleosides and DNA bases is important for the analysis of DNA damage by a range of oxidants, chemical reactions and other stresses. The detection of DNA oxidation products should be carried out in a timely manner, with minimal stresses that could result in the artifactual oxidation of these intermediate species. HPLC-ECD is one of the most widely used methods for the determination of G oxidation, and does not cause artifactual oxidation of the products. Chapter 2 involved the use of a previously developed HPLC-ECD method, which allowed for the selective detection of G oxidation product 8-oxoG. In order to conduct a thorough investigation of the temporal mechanism of oxidative damage to G, a large amount of samples were generated in the study. The long analysis time meant that there was a very low sample throughput and the analyses were time consuming.

The use of monolith columns in the RP separation of DNA bases and nucleosides and ECD of G and dG oxidation products, 8-oxoG and 8-OH-dG, respectively was investigated in this study. To our knowledge, it is the first time that ECD has been coupled to monoliths at high flow rates greater than 2.0 ml min^{-1}. The use of monolith columns minimises back pressure, while allowing for fast and efficient separations of sample components. This reduced the analysis time of all DNA bases and nucleosides by 90%, to just 4 min. The subsequent analysis of their oxidation products by electrochemical detection was achieved by splitting the flow by using PEEK tubing coupled to a t-piece in order to reduce the flow to the

ECD detector. This was applied to minimise noise and inflicted stress on the ECD component. The fast analysis time that has been achieved ensures minimal degradation of samples between injections, and hence allows for a more accurate as well as a more in-depth, comprehensive study of oxidative damage to DNA, with the potential for assisting in elucidation of the important mechanisms of oxidative stress. It allows for an in depth analysis of all transition metals.

3.6 REFERENCES

1. Kasai, H.; *Mutation Research,* 387; **1997**, 143-163.
2. Collins, A.R.; Cadet, J.; Moller, L.; Poulsen, H.E.; Vina, J.; *Archives of Biochemistry and Biophysics,* 423; **2004**, 57-65.
3. Floyd, R.A.; Watson, J.A.; Wang, P.K.; Altmiller, D.H.; Rickard, R.C.; *Free Radical Research Communications.,* 1; **1986**, 163-172.
4. Ravanant, J.L.; Gremaud, E.; Markovic J.; Turesky, R.J.; *Analytical Biochemistry*, 260; **1998**, 30-37.
5. Hensley, K.; Williamson, K.S.; Maidt, M.L.; Gabbita, S.P.; Grammas, P.; Floyd, R.A.; *Journal of High Resolution Chromatography*, 22; **1999**, 429-437.
6. Helbock, H.J.; Beckman, K.B.; Shigenaga, M.K.; Walter, P.B.; Woodall, A.A.; Yeo H.C.; Ames, B.N.; *Proceedings of the National Academy of Science of the United States of America*, 95; **1998**, 288-293.
7. Harris, D.C.; *Quantitative Chemical Analysis*, **6th edition**, WH Freeman & Co, USA, **2003.**
8. Szepesi, G.; *RP HPLC*, VCH Publishers, New York, **1992**.
9. Snyder, L.R.; Kirkland, J.J.; Glajch, J.L.; Practical *HPLC Method Development*, **1st Edition**, J. Wiley Publishers, New York, USA, **1988**.
10. Waggoner, P.S.; Craighead, H.G.; *Lab on a Chip*, 7; **2007**, 1238-1255.
11. Svec, F.; *Journal of Separation Science*, 27; **2004**, 747-766.
12. Fallon, A.; Booth, R.F.G.; Bell, L.D.; *Applications of HPLC in Biochemistry*, Elsevier, New York, **1987**.

13. Oberacher H.; Huber, C.G.; *Trends in Analytical Chemistry,* 21; **2002**, 166-174.

14. Svec, F.; *Journal of Chromatography B*, 841; **2006**, 52-64.

15. Fu, H.; Huang, X.; Jin W.; Zou, H.; *Current Opinion in Biotechnology,* 14; **2003**, 96-100.

16. Gerber, F.; Knimmen, M.; Potgeter, H.; Roth, A.; Sitfin C.; Spoendlim, C.; *Journal of Chromatography A*, 1036; **2004**, 127-133.

17. Novakova, L.; Matysova, L.; Solichova, D.; Koupparis, M.A.; Souch, P.; *Journal of Chromatography B*, 813; **2004**, 191-197.

18. Kato, M.; Sakai-Kato, K.; and Toyo'oka, T.; *Journal of Separation Science,* 28; **2005**, 1893-1908.

19. Wu, N.; Dempsey, J.; Yehl, P.M.; Dovletoglou, A.; Ellison D.; Wyvratt, J.; *Analytica Chimica Acta*, 523; **2004**, 149-156.

20. Podgornik, A.; Jancar, J.; Merhar, M.; Kozamernik, S.; Glover, D.; Cucek, K.; Barut, M.; Strancar, A.; *Journal Biochemical and Biophysical Methods*, 60; **2003**, 179-189.

21. Guillarme, D.; Nguyen, D.T.T.; Rudaz, S.; Veuthey, J.L.; *Journal of Chromatography A,* 1149; **2007**, 20-29.

22. Vervoort, N.; Gzil, P.; Baron, G.V.; Desmet, G.; *Journal of Chromatography A* 1030; **2004**, 177-186.

23. Kobayashi, H.; Tokuda, D.; Ichimaru, J.; Ikegami, T.; Miyabe, K.; Tanaka, N.; *Journal of Chromatography A* 1109; **2006**, 2-9.

24. Siouffi, A.M.; *Journal of Chromatography A*.; 1126; **2006**, 86-94.

25. Gritti, F.; Cavazzini, A.; Marchetti, N.;Guiochon, G.; *Journal of Chromatography A* , 1157; **2007**, 289-303.

26. Thomas, D.P.; Foley, J.P.; *Journal of Chromatography A.*, 1060; **2004,** 195-203.

27. Kelly, M. C.; Whitaker, G.; White, B.; Smyth, M.R., *Free Radical Biology and Medicine*; 42; **2007**, 1680-1689.

28. Herbert, K.E.; Evans, M.D.; Finnegan, M.T.V.; Farooq, S.; Mistry, N.; Podmore, I.D.; Farmer, P.; and Lunec J.; *Free Radical Biology and Medicine*, 20; **1996**, 467-473.

29. Cadet, J.; Berger, M.; Douki, T.; Morin, B.; Raoul, S.; Ravanat, J.L.; Spinelli, S.; *Biological Chemistry*, 378; **1997**, 1275–1286.

30. Dennany, L.; Forster, R. J.; White, B.; Smyth, M.; Rusling, J. F., *Journal of the American Chemical Society*, 126; **2004**, 8835-8841.

31. Guichon, G.; *Journal of Chromatography A*, 1168; **2007**, 101-168.

4 THE ROLE OF TRANSITION METALS Co, Mn, Zn AND Cd IN OXIDATIVE DAMAGE TO DNA

4.1 INTRODUCTION

Various environmental factors influence the level of oxidative stress a body is subjected to, with human DNA undergoing thousands of oxidative stresses per day. [1, 3-6] Oxidative damage to DNA has been implicated as a factor in the initiation and propagation of cancer, neurodegeneration, and heart disease as it causes strand breaks, base modifications and base mutations [2]. Understanding the mechanisms by which this damage occurs in the body is therefore paramount to fully understanding the role it plays in these diseases [7-9].

Most of the research to date has been centred around guanine (G) and 2'-deoxyguanosine (dG), and their primary oxidation products, 7,8-dihydroxy-8-oxoguanine (8-oxoG) and 8-hydroxy-2'-deoxyguanosine (8-OH-dG), respectively, as they are considered to have the potential to lead to the determination of the degree of oxidative damage to DNA. 8-oxoG and 8-OH-dG are now recognised as intermediates, as they are also susceptible to oxidative damage. This has been illustrated in Chapter 2, through analysis of 8-oxoG oxidation products, *i.e.* oxidised guanidinohydantoin (oxGH) and guanidinodihydantoin (GH). Investigating the spectrum of potential further oxidation products increases the potential to elucidate these oxidative stress mechanisms [10].

The main causes of oxidative damage are irradiation, chemical reactions and oxidation by ROS [8]. One of the most investigated ROS is the hydroxyl radical (·OH) [11, 12] which can be produced by the Fenton reaction [13, 14]. ·OH, is highly reactive and will react with all biological molecules, while it reacts preferentially with the π-bonds of DNA bases, but can also interact with the sugar

units by hydrogen abstraction [15]. ·Generally the Fenton reaction is associated with Fe catalysed production of ·OH, but other transition metals have been implicated in Fenton, or Fenton-like production of ·OH or other ROS [16].

Cd is a toxic transition metal that is classified as a category 1 human carcinogen. It is generally ingested by inhaling tobacco smoke, with smokers exposed to much higher levels of Cd than non-smokers. Food is the major source of Cd for non-smokers, from contaminated high fibre and shellfish diet, especially in industrial areas [17]. Jarup *et al.* also suggest that a low iron diet can result in higher levels of Cd in the body. Industrially, Cd is used in the manufacture of Ni/Cd batteries, and Jarup *et al.* have suggested that Cd emissions have increased dramatically as Cd products are not usually recycled [18].

Cd accumulates in the kidneys, thus causing kidney damage and is associated with renal diseases. Other diseases with which Cd exposure, is associated even at low levels, include bone diseases such as osteomalacia and osteoporosis, [19] as well as atherosclerosis [20].

The biological half life of Cd is reported as over 10 years and up to 30 years in man, with varying levels of approximately 10 to 20 μg g^{-1} in the body [21, 22]. Accumulation over time leads to chronic higher than normal exposure levels of Cd, thus increasing chances of Cd toxicity.

In areas of high Cd contamination, there is the potential for accumulation in crops such as carrots, corn, onions, tomatoes, potatoes, soy beans, wheat and lettuce, with highest concentrations in peanuts and spinach [23, 24].

Cd is unable to participate in redox reactions at physiological pH according to Hossain *et al.* [25]. The metal is, however, able to bind to biomolecules such as proteins, enzymes and DNA and can form complexes with smaller biomolecules such as nucleic acids and nucleobases. It is thought that this direct binding is the cause of the damage caused to DNA by non-redox reactive heavy metals [25].

Co is an abundant environmental contaminant. It is used in the production of alloys, as well in diamond polishing and as a drying agent in household paints and is also a pigment and a widely used catalyst. It is a toxic metal with both the ions and the metal itself having genotoxic properties [26].

Co, as well as both Cd and Zn, have been shown to accumulate in marine organisms over time, indicating that there is a potential for a build up of the metal with chronic exposure [27].

Zn is known to complex with biomolecules. Zn chloride can form a complex with A in a distorted tetrahedral conformation, the N7 of A acting as a ligator along with three chlorides [28]. Zn has a higher stability constant than Cu, Ni and Co in ternary nucleobase complexes. Zn can bind to the G moiety at the O6, N3 and C2. There are some non-Watson-Crick and Hoogs interactions, such as hydrogen bonding, π-π stacking interactions, as well as other hydrophobic interactions that determine the structure of the complexes. The N7 of G is also the primary binding Zn binding site, with Zn having a higher binding ability than Co, Ni, Mn and Mg, but a lower ability than Cd and Cu [29].

Mn is an essential metal with dietary intake of approximately 3 mg in a day, with sources including high carbohydrate cereals, pulses, vegetables and fruits [30-32]. General guidelines for a "no observed adverse effect level" (NOAEL) for Mn consumption suggest no more than 11 mg day^{-1} [32]. Mn can accumulate in the brain and it has been shown that at extreme levels, Mn can cause manganism, a neurological disorder with symptoms similar to Parkinson's disease [33, 34].

Mn is an important essential metal with functions as part of certain enzymes, including the antioxidant superoxide dismutase enzyme, Mn-SOD [35]. It has also been associated with Fenton-like formation of ROS, such as $^{\cdot}OH$, due to its ability to vary oxidation states [36, 37].

Dietary sources of Mg, are green vegetables, nuts, seeds, beans and lean meats. Dietary intakes recorded in a study by Ford *et al*. showed that there was a dietary intake of 230-330 mg/day in men and 200-240 mg/day in women in the United States of America. They found a general failure to meet the recommended daily allowances for dietary Mg, which are approximately 400 mg/day for men, 300 mg/day for women [39,40]. Mg supplementation has been used to treat ailments such as hypertension, heart failure, nervous and muscular system diseases and atherosclerosis; [39] Mg deficiency has also been linked with diabetes mellitus [40].

Mg complexes with DNA and nearby water molecules are noted to bind to the phosphate groups of the DNA helix and can increase the melting temperature for DNA [41]. Its interaction with DNA shifts the DNA UV spectrum and may interact with the amino or the hydroxyl groups on the DNA moiety and form a Mg

nucleate complex [42]. Complexation with Mg plays a role in the stabilisation of nucleic acids. Mg was found to coordinate with the O6 and N7 sites of G in an inner-sphere co-ordination. Mg can participate in both inner and outer sphere coordination simultaneously with DNA and water molecules [43].

4.2 SCOPE OF THE RESEARCH

This research focused on the elucidation of the mechanism of *in vitro* oxidation of G; both free in solution and in the DNA backbone, by a transition metal-mediated reaction. The transition metals investigated were Co, Mn, Zn and Cd. The methods used in this study were HPLC-UV-ECD using a Phenomenex Onyx RP-18 monolith column as developed in Chapter 3 for the determination of 8-oxoG and G and HPLC-MS/MS for the determination of 8-oxoG and structural determination of its further oxidation products.

It is known that Fe, Cu and Ni can damage DNA and cause the formation of oxidation products. It is therefore important to determine if this damage is characteristic to these metals, or if other metals can mediate similar reactions. Therefore a study encompassing the transition metals Co, Mn, Zn and Cd was undertaken, in order to determine if they too can cause oxidative damage to DNA in a Fenton-like mechanism. Mg, an alkali earth metal was also investigated to determine if this damage was transition metal-specific. This study gave a direct comparison between each of the metals with a view to comparing their individual mechanisms of damage to DNA.

4.3 EXPERIMENTAL

4.3.1 Materials

G (G0381, ≥99%), 7,8-dihydro-8-oxoG (R288608), calf thymus DNA sodium salt (D1501, Type I, fibres) [2,000 av. base pairs, 41.2% G/C] , cadmium sulphate hexahydrate (481882, 99.999%), cobalt(II) sulfate heptahydrate (C6768, 99%) were purchased from Sigma-Aldrich (Tallaght, Dublin, Ireland). Magnesium sulfate heptahydrate and LC-MS grade methanol were purchased from Riedel-de Haen (99.5-100.5%, <0.001%Fe), and zinc sulfate heptahydrate from Fluka (96500 95-103%, </= 0.0005% Fe). Ethanol and ACN were purchased from Labscan Ltd. (Dublin, Ireland). Deionised water was purified using a MilliQ system to a specific resistance of greater than 18 MΩ-cm. All HPLC buffers and mobile phases were filtered through a 47mm, 0.45 μm polyvinylidene fluoride (PVDF) micropore filter prior to use. Fresh solutions of all standards were prepared weekly.

4.3.2 Incubation of G, 8-oxoG and DNA with metal salt and H_2O_2

For HPLC-UV-ECD, a 10 mM solution of G, prepared in 0.1 M NaOH, was incubated at 37 ^oC with 1.5 mM of the metal salt of interest and 50 mM solution of hydrogen peroxide (H_2O_2), as described in Chapter 2. For HPLC-MS analysis a 10 mM solution of G in 10 mM NaOH or a 2 mg mL^{-1} solution was incubated at 37 ^oC in stirred solution with 1.5 mM of the metal salt of interest and 50 mM H_2O_2 solution, as described in Chapter 2. Samples were quenched in ethanol and dried under N_2 flow.

4.3.3 Acid hydrolysis of DNA for nucleobase analysis

After incubation, DNA samples were hydrolysed prior to HPLC-MS analysis. The oxidised DNA sample had 600 µl of 88% (v/v) formic acid added, and was evacuated and sealed in a 1 ml Pierce hydrolysis tube. The sample was heated to 140 ^{o}C for 30 min. in vacuum. The solvent was then evaporated to dryness under N_2 flow. The dried hydrolysis sample was stored at 4 ^{o}C until analysis, when it was reconstituted in 1 ml 50 mM ammonium acetate buffer, pH 5.5, with a final concentration of DNA of 80 µg mL^{-1}.

4.3.4 HPLC-UV-ECD analysis of 8-oxoG formation

Samples were reconstituted in 100 µl 10 mM NaOH, followed by addition of 900 µl 50 mM ammonium acetate, pH 5.5 and separated by RP HPLC using a Varian ProStar HPLC system with Varian ProStar 230 Solvent Delivery Module and Varian ProStar 310 UV-VIS Detector. The eluent composition was 50 mM ammonium acetate/85 mM acetic acid buffer, pH 4.6: ACN (98.8:1.2) through a Phenomenex Onyx RP C_{18} Monolith 4.6 x 100 mm column, equipped with Ultra C_{18} 4 x 10 mm guard column. The separation was carried out at 4.0 ml min^{-1} isocratic elution. G was detected using UV detection at 254 nm and any 8-oxoG formed was detected by electrochemical detection (ECD), using a BAS CC-4 electrochemical cell comprising of glassy carbon working electrode, stainless steel auxiliary electrode and Ag/AgCl reference electrode at a detection potential of +550 mV. ECD chromatograms were generated using a CHI 800B potentiostat and

accompanying software. UN-SCAN-IT digitising software was used to digitise integrator chromatograms, which were then imported into SigmaPlot 8.0 or MS Office Excel.

4.3.5 HPLC-MS/MS analysis of further oxidation products of G

Incubated samples were analysed by HPLC-MS-MS using an Agilent 1100 HPLC System with diode array detection coupled to a Bruker Daltonics Esquire 3000 LC-MS. Reconstituted samples were separated by HPLC using gradient elution through the Supelco Supelcosil LC-18 reversed phase column 5 μm 2.1 mm x 250 mm. Eluent A consisted of 10 mM ammonium acetate buffer pH 5.5. Eluent B was 50/50 methanol/water. A flow rate of 0.2 ml/min was used with a linear gradient of 0-10% B from 0-22 min, 10-0% B from 22-25 min. DNA bases and oxidation products were also detected by UV detection at 210, 254 and 280 nm. Mass spectrometric analysis was carried out at an ionisation temperature of 350 ^{o}C and at an ionisation potential of +15 V unless otherwise stated.

4.4 RESULTS AND DISCUSSION

4.4.1 HPLC-UV-ECD determination of 8-oxoG

Control experiments showed no detectable formation of 8-oxoG on incubation in the absence of any metal and also in the absence of the H_2O_2. This was indicative that any damage caused to G with the metal-H_2O_2 mixture was indeed caused by some variation of the Fenton reaction, mediated by the metal involved.

Peaks were quantitated using Origin 6.0. The chromatogram was exported from the CHI 800B software to Origin 6.0 and the peak was isolated, fitted to a Gaussian curve using the analysis option, and the area and height of the peak of interest were noted.

Co was incubated for a total incubation time of 20 min. The 8-oxoG had a retention time of approximately 29-30 seconds. The analysis was allowed to run for a longer time period than this, in order to detect the formation of other, longer retained oxidation products that may have been detected by HPLC-UV-ECD. No late eluting impurities or other products formed on incubating G with Co(II)Fenton reagents were detected.

The results observed for Co induced damage to DNA via a Fenton-like reaction demonstrate a significant initial formation of 8-oxoG, which further reacts instantaneously producing only minute quantities of 8-oxoG thereafter. Fig. 4.1 illustrates the formation of 8-oxoG at 0 min, and overlaid chromatograms illustrating no formation at 5, 10 and 20 min.

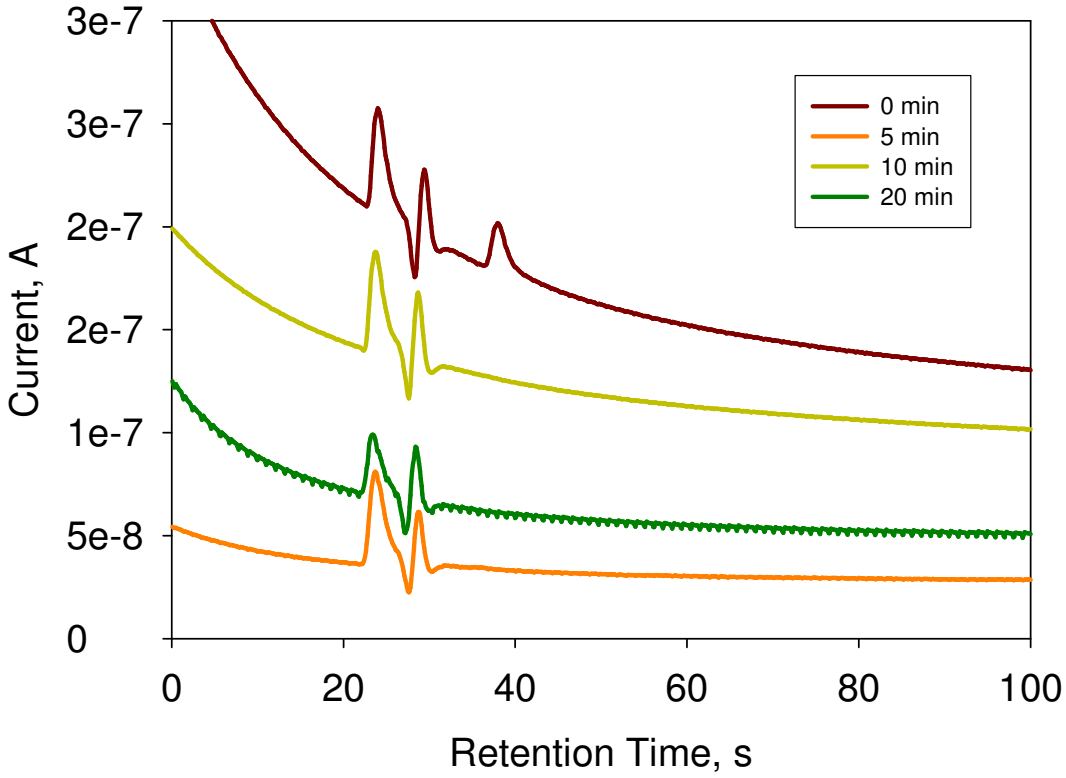

Fig 4.1: Overlay of HPLC chromatograms with ECD illustratsing the formation of 8-oxoG from G on incubation at 37 ^{o}C with 1.5 mM $CoSO_4$ and 50 mM H_2O_2. The 0, 5, 10 and 20 min. samples are shown here. Separation was carried out with 50 mM ammonium acetate/85 mM acetic acid buffer, pH 4.6:ACN (98.8:1.2). Detection was at +600 mV vs. Ag/AgCl, with 4.0 ml min^{-1} through an Onyx Phenomenex C_{18} column of 100 mm x 4.6mm I.D. and split prior to the ECD detector, so that 0.7 ml min^{-1} went to detector; the run time was 100 seconds.

Fig. 4.2 shows the concentration of 8-oxoG that was formed over the entire course of the incubation period. The quantity formed at the beginning of the incubation period was greater than the concentrations formed in the latter minutes, and therefore the inset in Fig. 4.2 illustrates the small quantities that were formed in the time after the degradation of the initial formation.

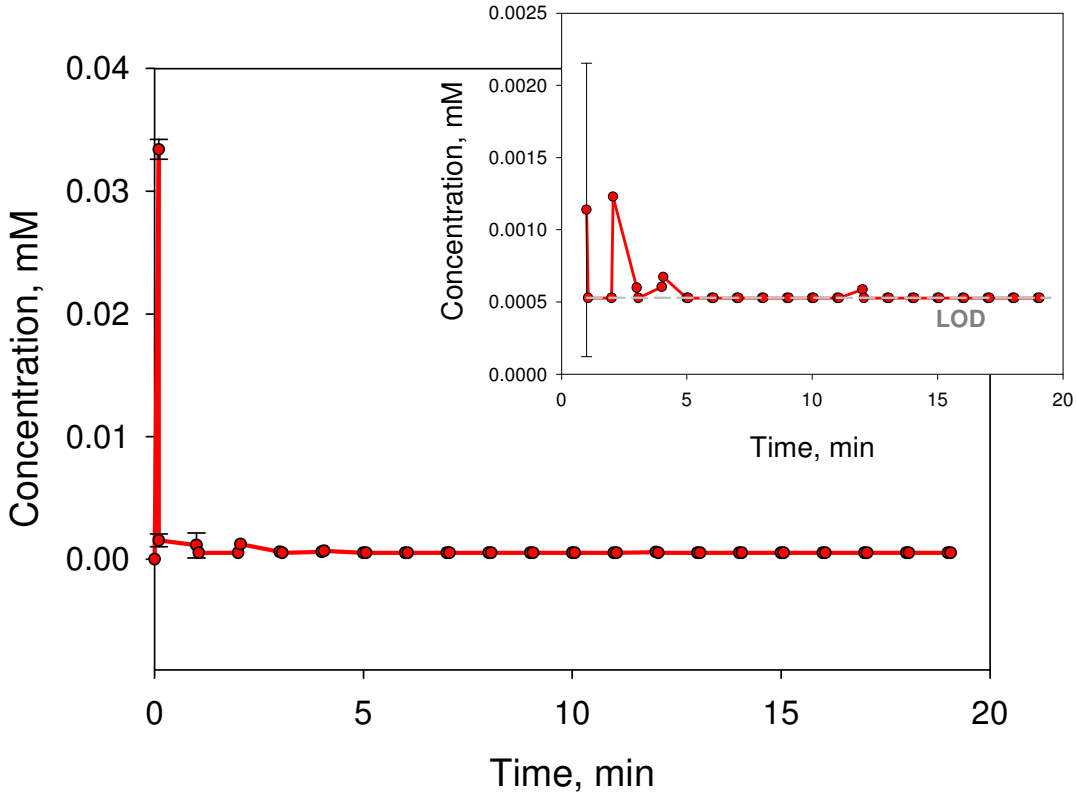

Fig 4.2: 8-oxoG concentration as a function of time, after incubation of free G with 1.5 mM $CoSO_4.7H_2O$ and 50 mM H_2O_2 Fenton reagents at 37 ^oC. The mean of the injections of each of the samples is taken. Separation and detection conditions as per Fig 4.1 (N=3). Inset shows the concentration of 8-oxoG formed from 1 min without the first two initial samples of the graph.

.

There was a series of small oscillations noted in the 2 and 4 min. samples, though for most of the incubation period, there was very little 8-oxoG formed after 5 min, with one final small oscillation at 12 min above the signal to noise ratio. For Co, there was definite formation of 8-oxoG at the beginning of the study. This decreased after the second 0 min. sample, which was taken approximately 5 s after the first sample. This sudden decrease was evidence of an almost immediate further oxidation of the 8-oxoG that was formed. There were very low concentrations of 8-oxoG formation over the course of the experimental incubation period, at or below the LOQ of 0.5 μM. These small concentrations are also in an erratic formation pattern. In reference to the kinetics of the reaction, the high initial concentration of 8-oxoG formed suggests that this Co(II)-Fenton-like reaction had a fast initiation, resulting in a burst of ·OH, or other free radical species. This ·OH formation could then have caused an almost instantaneous formation of 8-oxoG from G with a fast reaction rate, and subsequent rapid oxidative attack on the 8-oxoG to form a non-retained or a non-electrochemically active species. The speed at which this initial peak formation occured suggests that there was no major induction period involved here in the kinetics of the reaction, *i.e.* the Cobalt-Fenton reaction had a very fast reaction rate.

Zn showed very little 8-oxoG formation over the course of its incubation period with G and H_2O_2, though of the 8-oxoG that was formed, there was a definite oscillatory pattern observed. Fig 4.3 illustrates the observed 8-oxoG peak that was formed from G on incubation with the Zinc Fenton reagents, and it was clear that there was some formation, though the amount formed was not quantifiable.

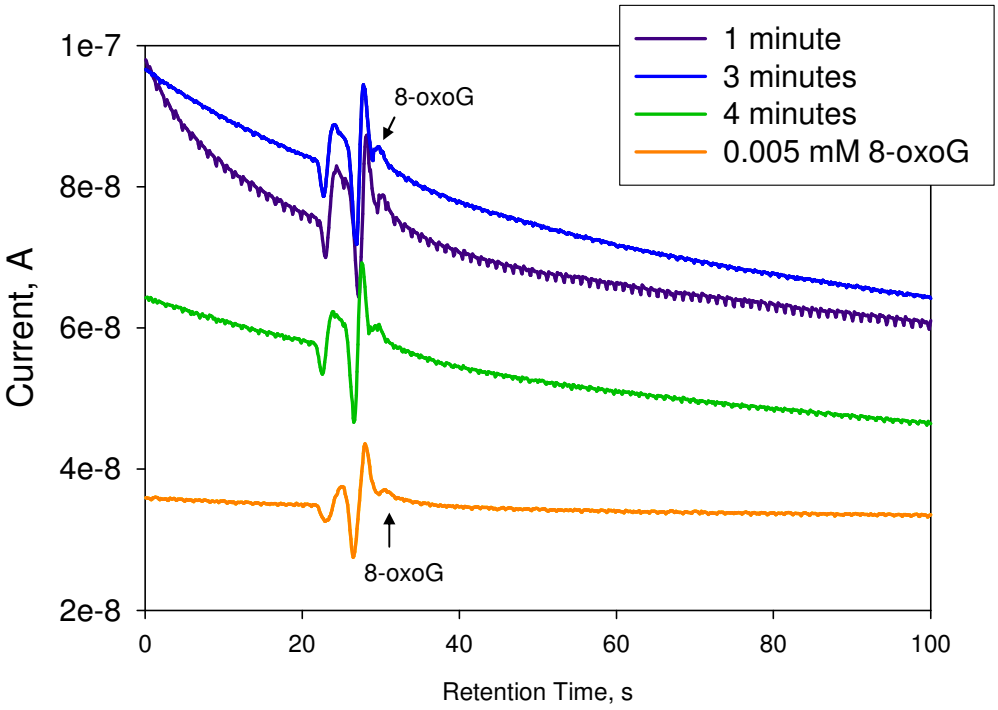

Fig 4.3: Overlay of HPLC chromatograms with ECD illustrating the formation of 8-oxoG from G on incubation at 37 ^{o}C with 1.5 mM $ZnSO_4$ and 50 mM H_2O_2. Min. 1, and 4 of a 19 min. incubation period and a peak marker 0.005mM 8-oxoG are shown. Separation and detection conditions as per Fig 4.1.

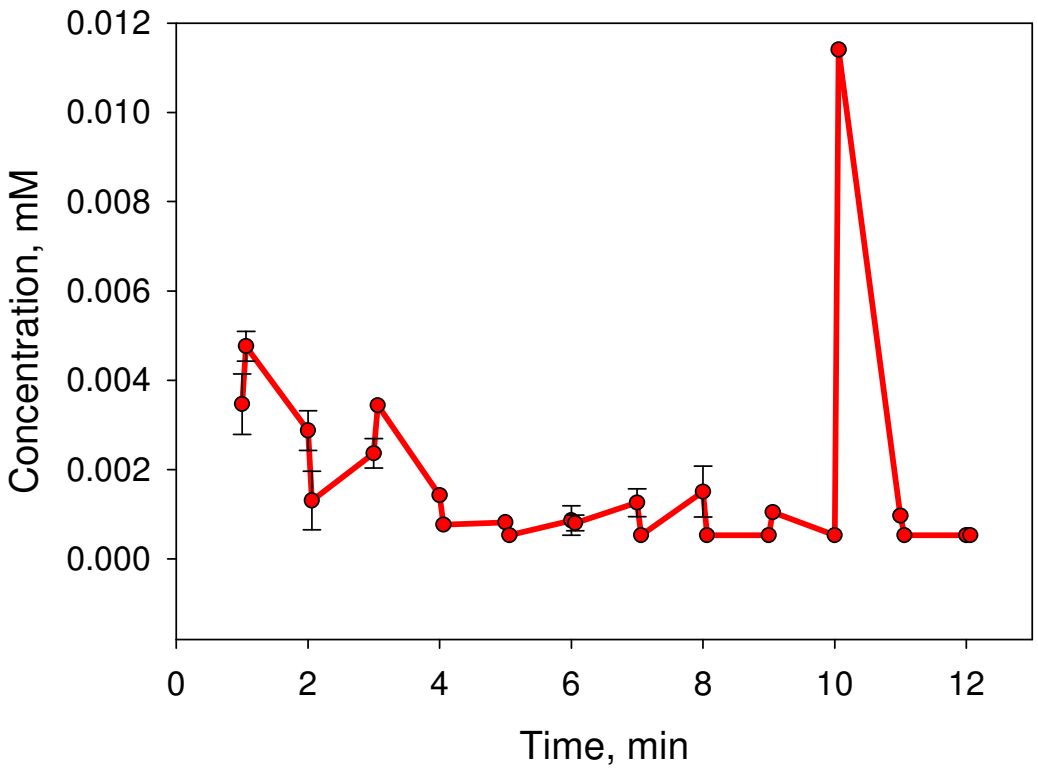

Fig 4.4: 8-oxoG concentration as a function of time, after incubation of free G with 1.5 mM $ZnSO_4.7H_2O$ and 50 mM H_2O_2 Fenton reagents at 37 ^oC. The mean of the injections of each of the samples is taken (N=3).

The concentration of Zn was quantified and was monitored over the incubation time period, as illustrated in Fig. 4.4. There was a sporadic burst of 8-oxoG formation observed again here, with a distinct increase in concentration of 8-oxoG at 11 min. This formation of 8-oxoG was of low concentration, but did continue to form oscillation-like patterns over the course of the incubation period. This illustrates that the reaction was occurring by a similar mechanism to that of the Ni incubation, albeit at smaller concentrations.

Cd incubations showed a general pattern of low erratic formation with a jump in concentration at min. 7 of the incubation period. Fig. 4.5 illustrates the chromatograms obtained at 1, 3, 6, 7 and 10 min, which clearly showed the formation of 8-oxoG, most noticeably at 3 and 7 min.

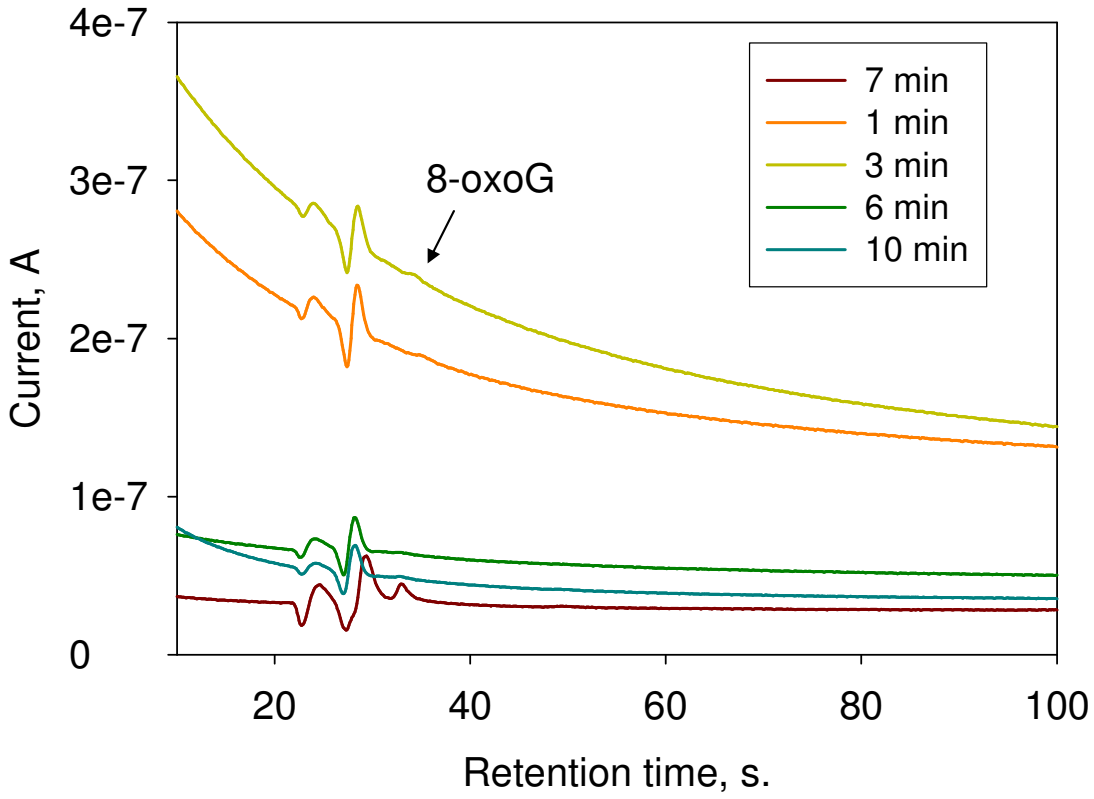

Fig 4.5: ECD Chromatograms illustrating the lack of formation of 8-oxoG from G on incubation at 37 ^{o}C with $CdSO_4$ and H_2O_2. The 1, 3, 6, 7, and 10 min. samples are shown here. Separation and detection conditions as per Fig 4.1. The run time was 100 s.

The largest burst at 7 min. was detected for both the first and second 7 min. sample, although there was a decrease in concentration at the second sample, taken approximately 5 s after the first.

Over the course of the rest of the Cd-Fenton incubation period, there was a definite intermittent formation of 8-oxoG detected that at much lower concentrations than that of the 7 min. sample. Fig 4.6 indicates the concentration of

8-oxoG formed are in the range LOD to 0.02 mM until 7 min. when the concentration dramatically increased momentarily to over 0.1 mM. At 3 and 13 min. there were two smaller, but noticeable increases in concentration, which quickly decreased.

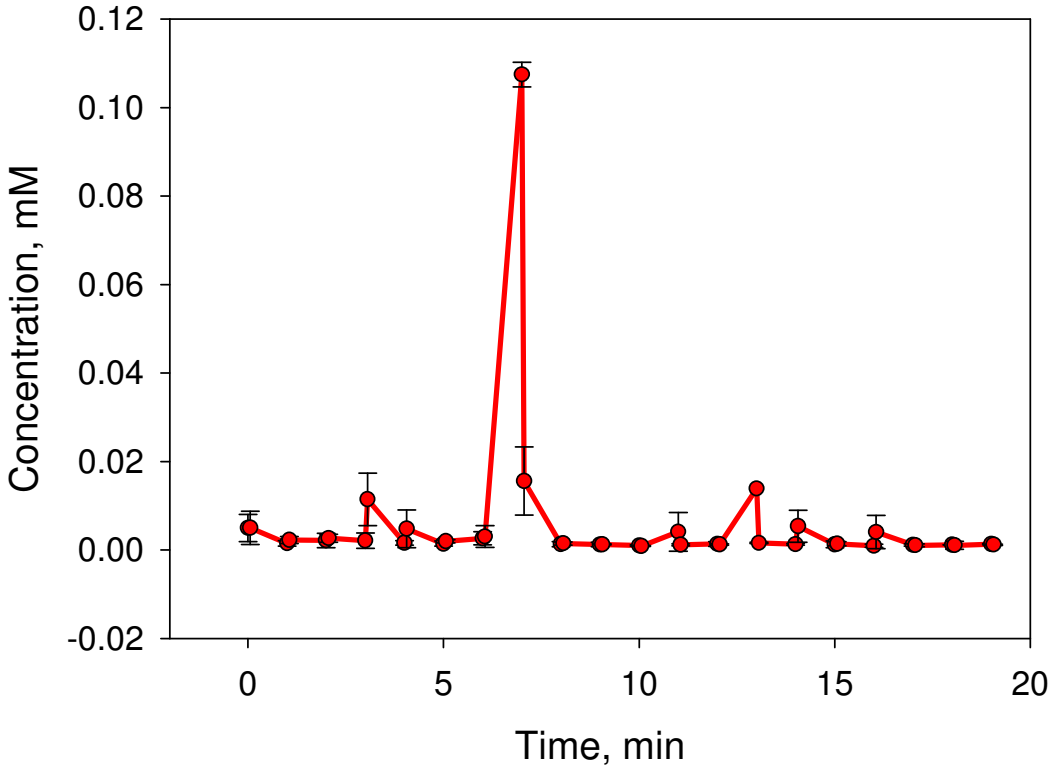

Fig 4.6: 8-oxoG concentration as a function of time, after incubation of free G with 1.5 mM $CdSO_4$ and 50 mM H_2O_2 Fenton reagents at 37 ^oC. The mean of the injections of each of the samples is taken (N=3).

The alkali earth metal, Mg, as discussed previously, has the ability of complexing with biomolecules, but cannot change oxidation states from its Mg(II) oxidation state and it exists only as its 2+ ion. It can not, therefore, participate in the Fenton reaction, which involves the oxidation of the metal to a higher oxidation state, for example Fe(II) to Fe(III). This is evident from the results observed in this study. There was no 8-oxoG formation at all observed over the course of the 19 min. incubation. The first 6 min. are illustrated in Fig. 4.7. This experiment could also be considered as a further control study, as it indicates that the transition metal-Fenton, or at least a transition metal Fenton-like reaction is involved in the generation of 8-oxoG.

The results obtained in this study are enlightening, in that they give an insight into the mechanisms of oxidative damage by transition metals Co, Cd, Zn and alkali earth metal, Mg. Each of these ions can co-ordinate and form complexes with biomolecules, as indicated above. The transition metals are also able to vary oxidation states, and therefore in the conditions of the Fenton reaction, could potentially be $^{\cdot}OH$, or other potent ROS generators.

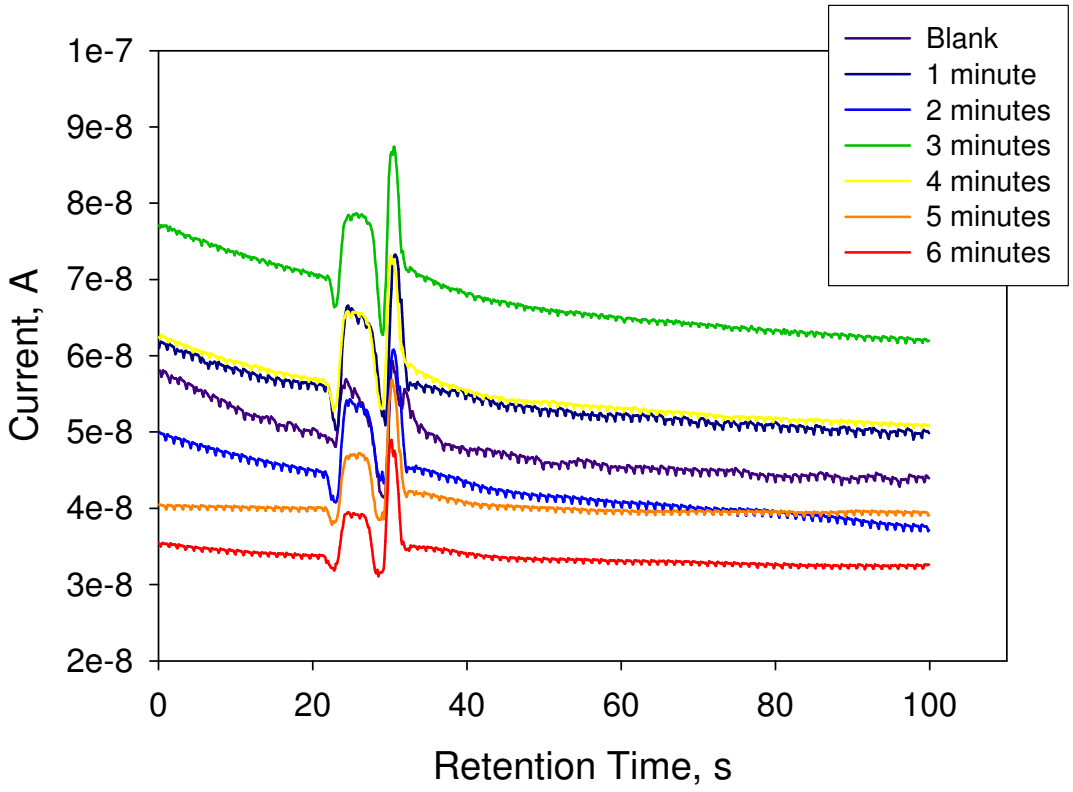

Fig 4.7: Chromatograms illustrating the lack of formation of 8-oxoG from G on incubation at 37°C with $MgSO_4$ and H_2O_2. Separation and detection conditions were as per Fig 4.1.

The amount of 8-oxoG generated, although low, does oscillate or form in erratic patterns. The results also illustrate that there is a definite link between a transition metal catalysed Fenton decomposition of H_2O_2 and the formation of 8-oxoG. Control studies using HPLC-UV-ECD showed that there was no detectable formation of 8-oxoG in the absence of the H_2O_2, nor was there any in the absence of the metal. The Mg- H_2O_2 mix also showed no formation of the G oxidation product, which also confirmed that it was the variation of oxidation states of the transition metals that caused the formation of the ·OH in this reaction. With respect to the

kinetics of the respective reactions, it was evident that the "oscillatory", or erratic nature of the formation of 8-oxoG from G was dependent upon the metal involved, and hence the rate of formation of the ROS involved.

The erratic formation of 8-oxoG is also indicative that the product is not a final product, but an intermediate, and therefore is not suitable as a biomarker of DNA damage by oxidation. It is, therefore, vital to determine potential, more stable, biomarkers for the determination of this type of damage to DNA, with a view to their use as biomarkers of disease.

4.4.2 HPLC-MS and HPLC-MS/MS determination of 8-oxoG further oxidation products from free G

The results obtained in the HPLC-UV-ECD are indicative that for each of the transition metals involved in this study, 8-oxoG is formed in an erratic manner, involving formation followed by further reaction. In order to give an insight into the mechanisms of oxidative DNA damage by each of the transition metals Co, Cd, Zn and Mn, a mass spectrometric analysis was undertaken.

$CoSO_4$ was incubated with G and H_2O_2 over 120 min. of incubation time with samples taken immediately and after 10, 20, 30, 40, 60 90 and 120 min. The samples were analysed by HPLC-MS with a uracil internal standard. The formation of oxGH, GH, Sp and 8-oxoG were analysed. These were analysed as they had previously been detected from Ni in chapter 2. A product at *m/z* 156 was formed.

There was no detected peak corresponding to Sp (*m/z* 184) or 8-oxoG (*m/z* 168) determined. The formation of this peak at 156 is illustrated in Fig. 4.8.

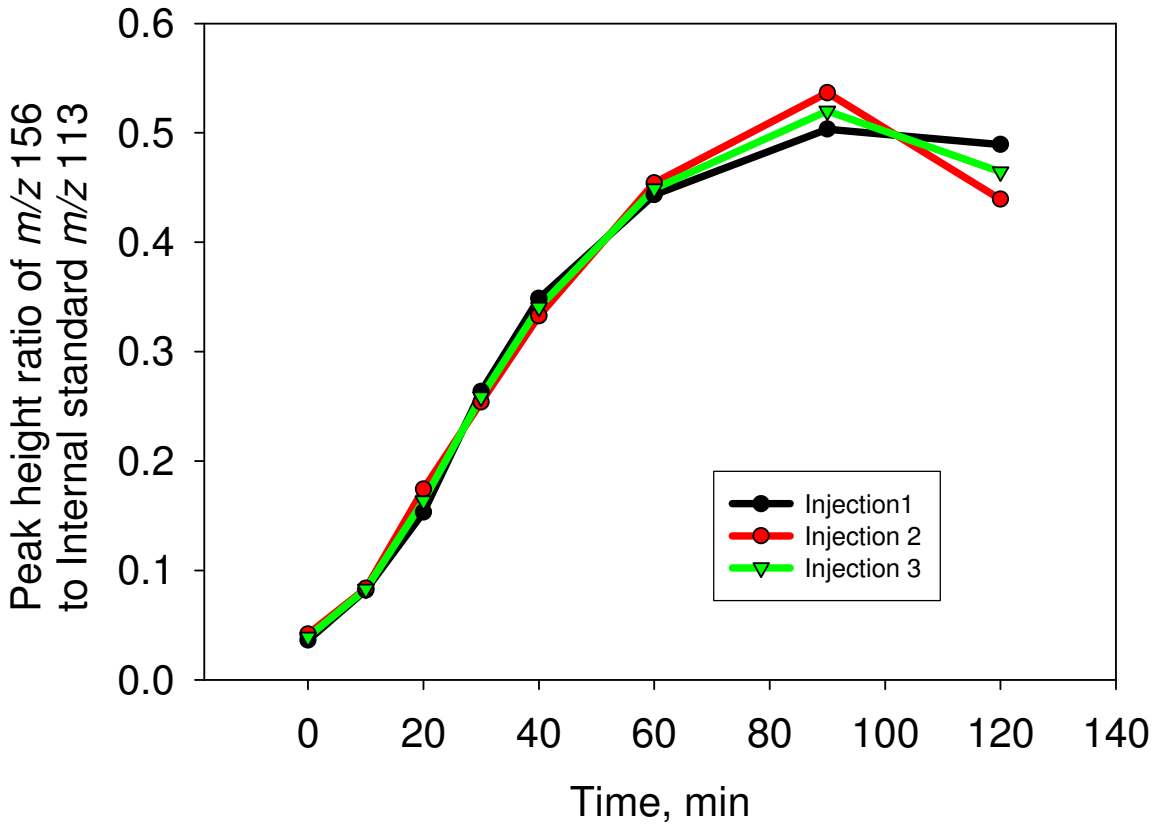

Fig 4.8: Formation of Product of m/z156 from Guanine on incubation with 1.5 mM $CoSO_4$ and 50 mM H_2O_2 at 37 ^oC with internal standard Uracil (112 g mol^{-1}). The ionisation potential used was +15 V (N=3).

The mass spectrum fragmentation pattern shown in Fig. 4.9 corresponds to that illustrated previously for oxGH by this laboratory for Ni(II) induced damage to G as discussed in Chapter 2.

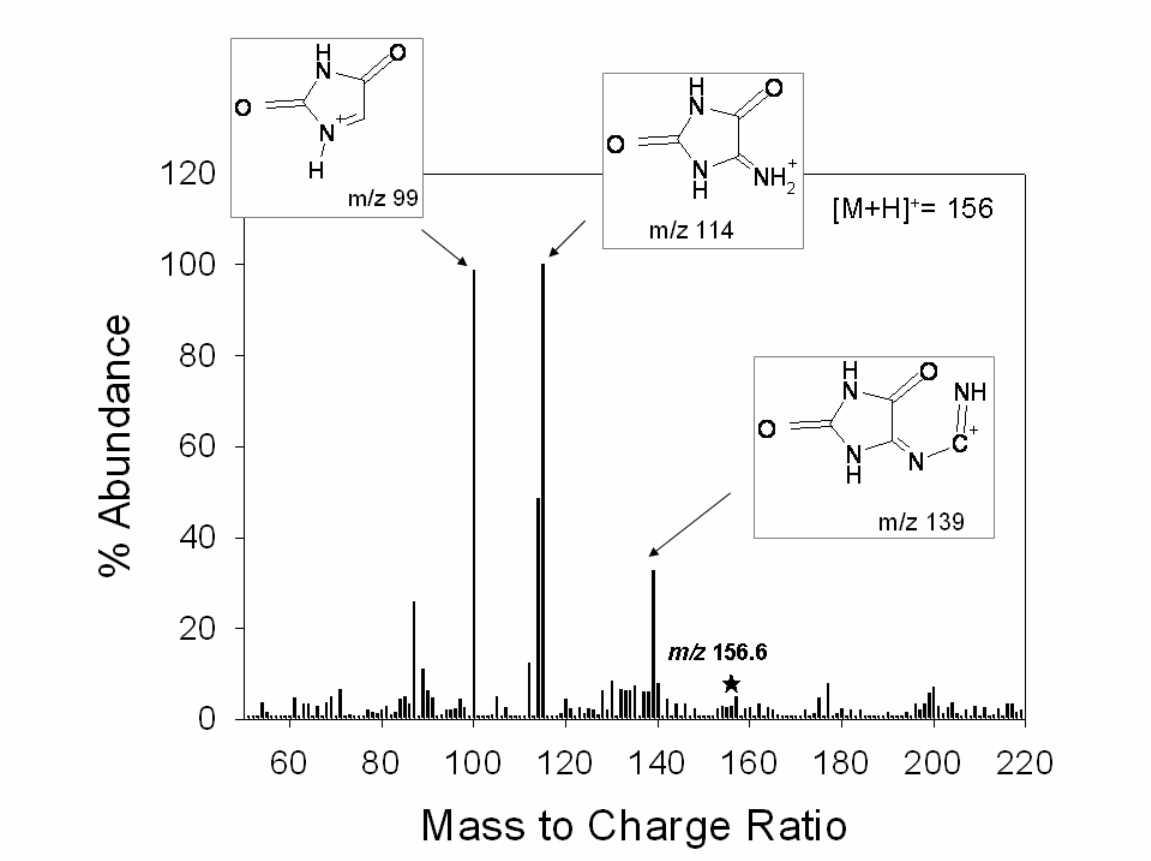

Fig 4.9: Mass Spectrum for the fragmentation pattern for peak at m/z 156, illustrating [M+ – 17] and [M+ – 43] peaks. This mass spectrum is from a sample of G incubated with 1.5 mM $CoSO_4$ and 50 mM H_2O_2 after 20 m in at 37 ^oC. The ionisation potential used was +15 V.

A negative ionisation potential of -15 V was then applied and the formation of peaks at *m/z* 154, 113 and 131 was noted. The formation of these products is

illustrated in Figs. 4.10, 4.11 and 4.12, respectively. In this experiment, the Co-Fenton reagents were incubated for 1 hour. The peak at *m/z* 154 corresponds to positive mode MS formation of *m/z* 156.

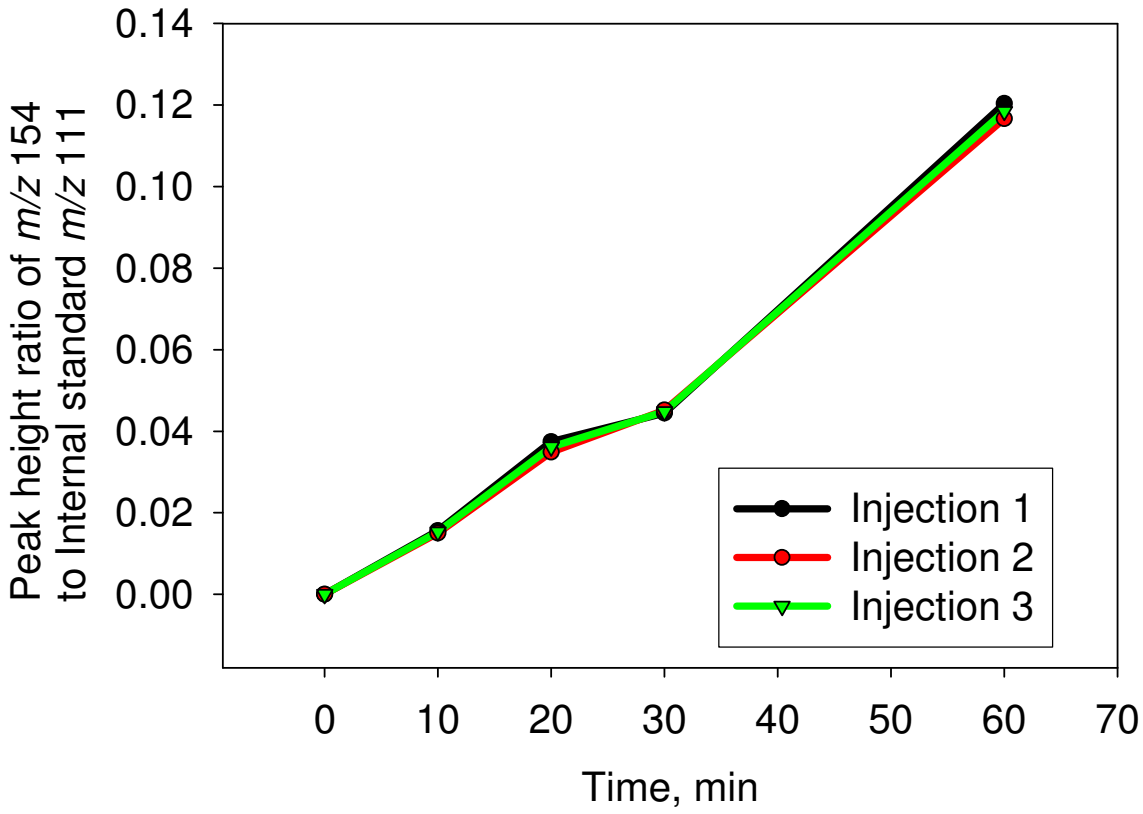

Fig 4.10: Negative MS formation of M/z 154 from G incubated with 1.5 mM $CoSO_4$ and 50 mM H_2O_2 at 37 ^{o}C. The ionisation potential used was -15 V (N=3).

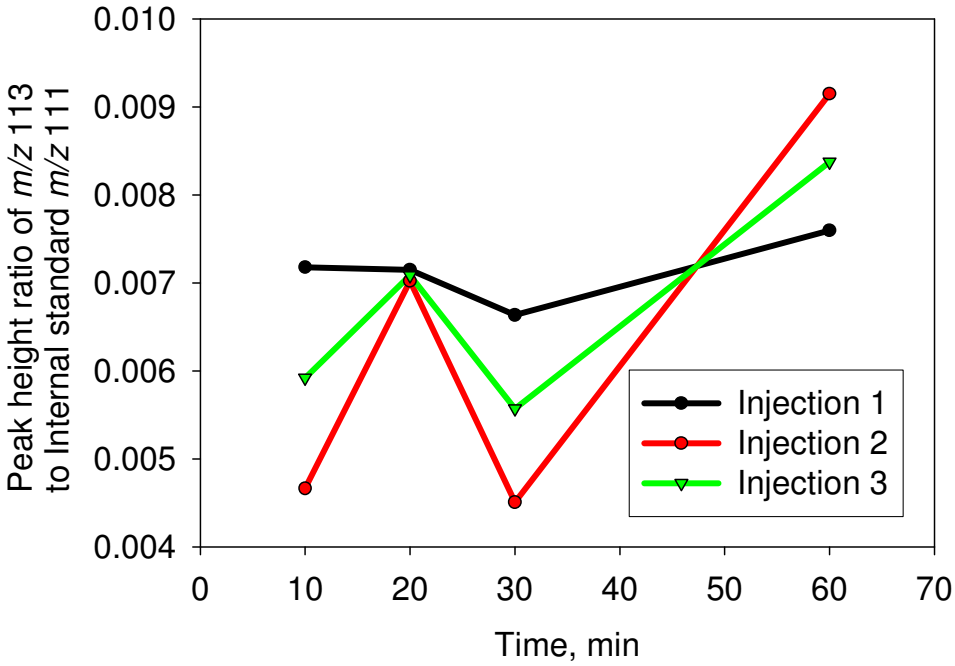

Fig 4.11: Formation of Product of m/z 113 from Guanine on incubation with 1.5 mM $CoSO_4$ and 50 mM H_2O_2 at 37 ^oC, with internal standard U (112 g mol^{-1}). The ionisation potential used was -15 V (N=3).

Repeat experiments, resulted in a transient formation of *m/z* 113 and 131. This may be from the degradation of the product after reconstitution of the sample prior to injection. In some cases, the sample may have been reconstituted at least 8 hours before analysis. The half-life of the precursor product, oxGH, or GH is 8 hours, and therefore after this time, it is expected that it can break down into its degradation products, Pa and Oa [45]. The levels of both *m/z* 113 and *m/z* 131 were too low in order to obtain an accurate mass spectrum in order to elucidate structural data.

The formation of the oxGH, at *m/z* 156.6 (and negative *m/z* 154), however, increases in a steady and repeatable pattern over time. This along with its long half life, means it is still ideal for use as a biomarker and a means of determining the extent of damage to G caused by metal mediated oxidative stress.

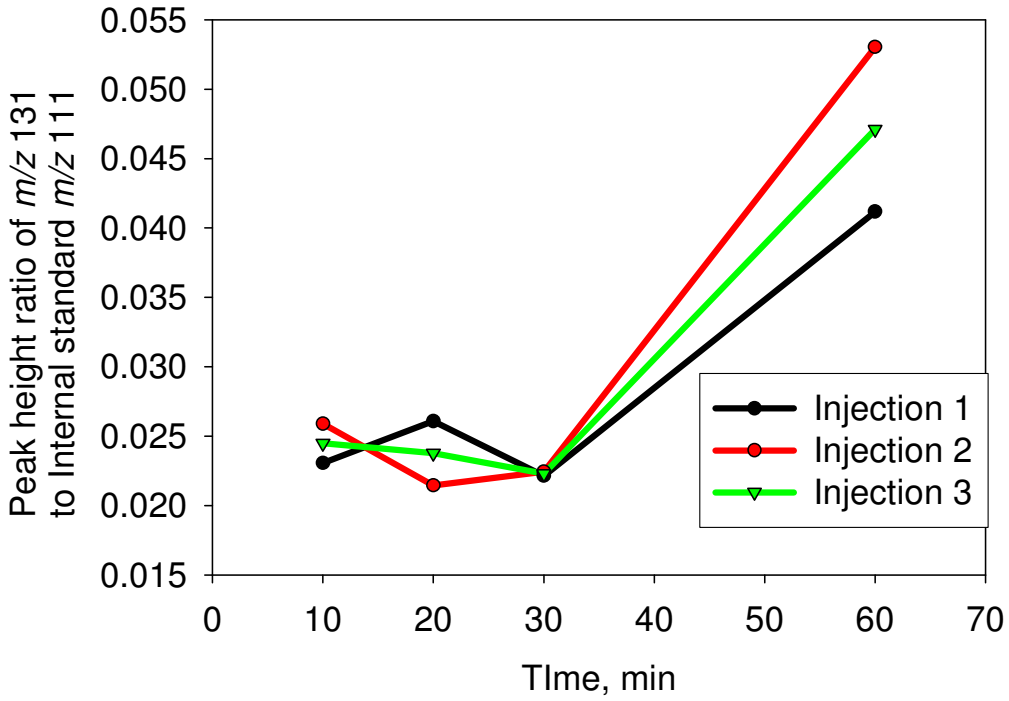

Fig 4.12: Formation of Product of m/z 131 from Guanine on incubation with 1.5 mM $CoSO_4$ and 50 mM H_2O_2 at 37 ^oC, with internal standard U (112 g mol^{-1}). The ionisation potential used was -15 V (N=3).

$MnSO_4$ salt was also investigated in the MS study for comparison to the other metals. It was incubated in a similar manner with G and H_2O_2 over 90 min. of incubation time with samples taken immediately and after 10, 20, 30, 40, 60 and 90 min. The samples were analysed by HPLC-MS with a U internal standard and ionisation potential of +15 V. The formation of oxGH, Sp and 8-oxoG were again

analysed. The product at *m/z* 156 was again determined. Sp, was not detected in this experiment. There was, again, no Sp or 8-oxoG detected.

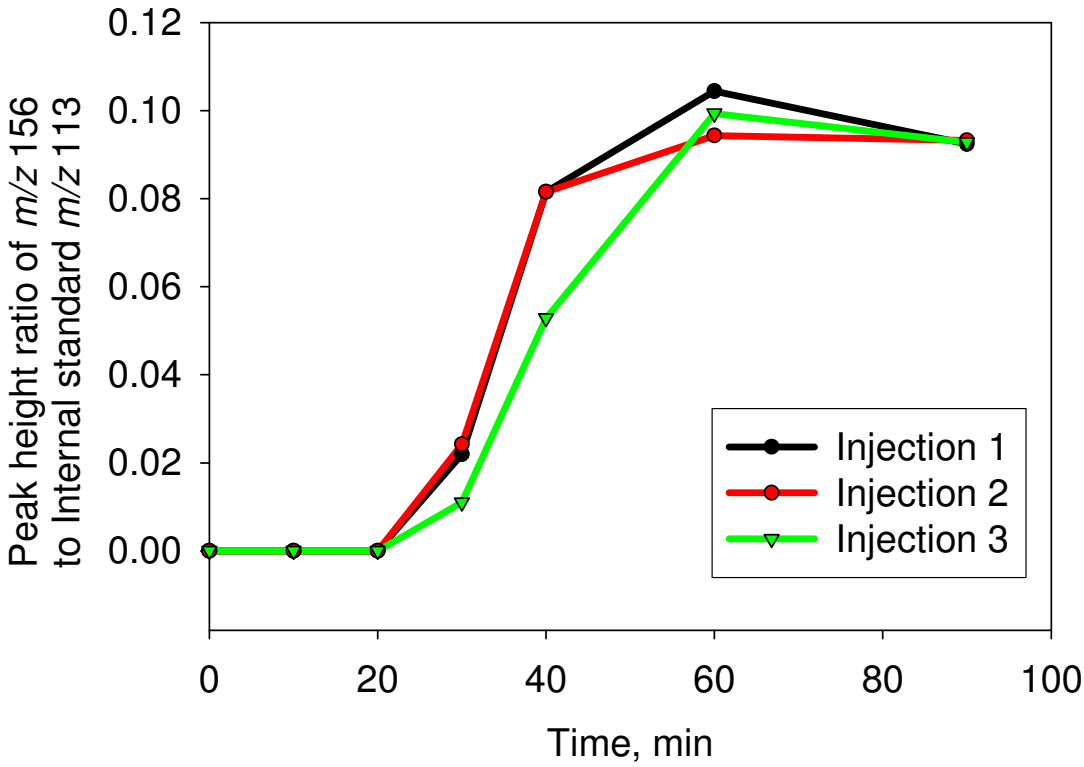

Fig 4.13: Formation of Product of m/z 156 from G on incubation with 1.5 mM $MnSO_4$ and 50 mM H_2O_2 at 37 ^oC with internal standard U (112 g mol^{-1}). The ionisation potential used was +15 V (N=3).

A MS/MS Scan for the peak at *m/z* 156 was carried out, and once again was comparable to that obtained for Ni and for Co, discussed in Chapter 2, and earlier in this Chapter. Negative ionisation mass spectrometric analysis was also carried out though there was no formation of products at *m/z* 113 and 131 detected in these samples. The product at *m/z* 154 was detected, corresponding to the *m/z* 156 in the positive scans.

$CdSO_4$ salt was incubated and analysed by HPLC-MS as per Co and Mn with samples taken immediately and after 10, 20, 30, 40, 60 and 90 min. The formation of oxidised oxGH, Sp and 8-oxoG were again analysed. Once again, Sp and 8-oxoG were not detected.

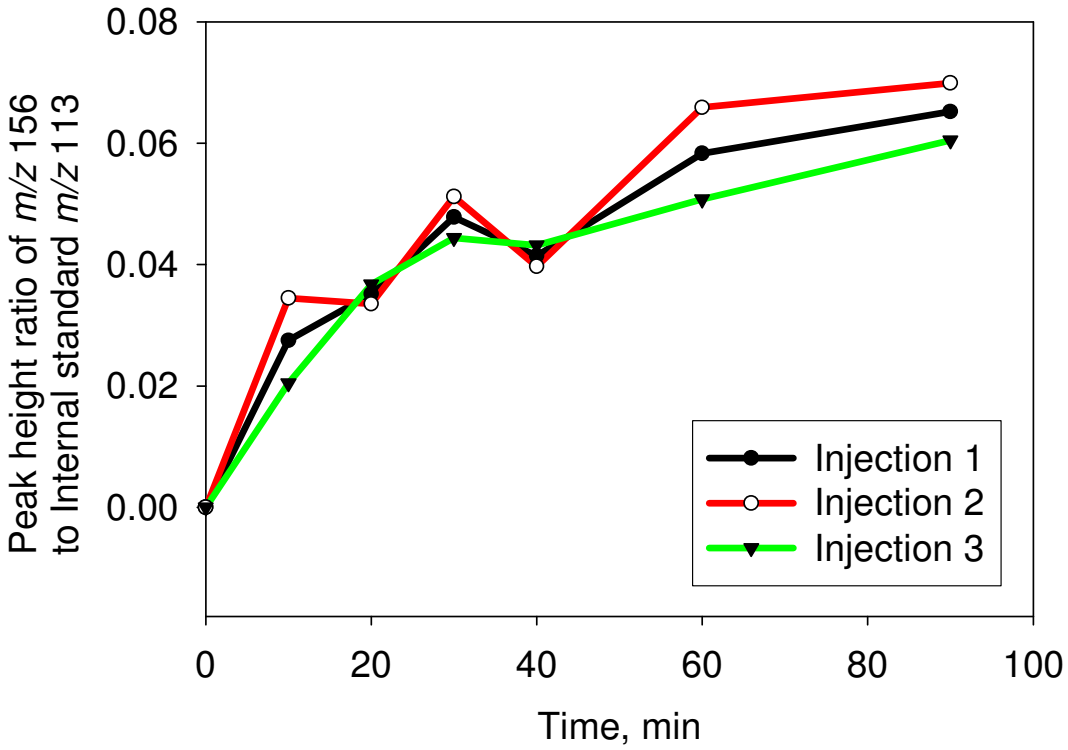

Fig 4.14: Formation of Product of m/z 156 from G on incubation with 1.5 mM $CdSO_4$ and 50 mM H_2O_2 at 37 ^{o}C with internal standard U (112 g mol^{-1}). The ionisation potential used was +15 V (N=3).

Zn again showed the formation of this *m/z* 156 peak; however, concentrations were lower again. Cd and Zn incubations showed the lowest levels of formation, which were comparable to control incubations. Therefore, it is impossible to speculate whether this formation was due to the Fenton-like reaction

or due to artifactual, or baseline damage to G in the reaction sample. The concentration of *m/z* 156 product appeared greater than the controls in the Mn and of higher concentration again in the Co incubations.

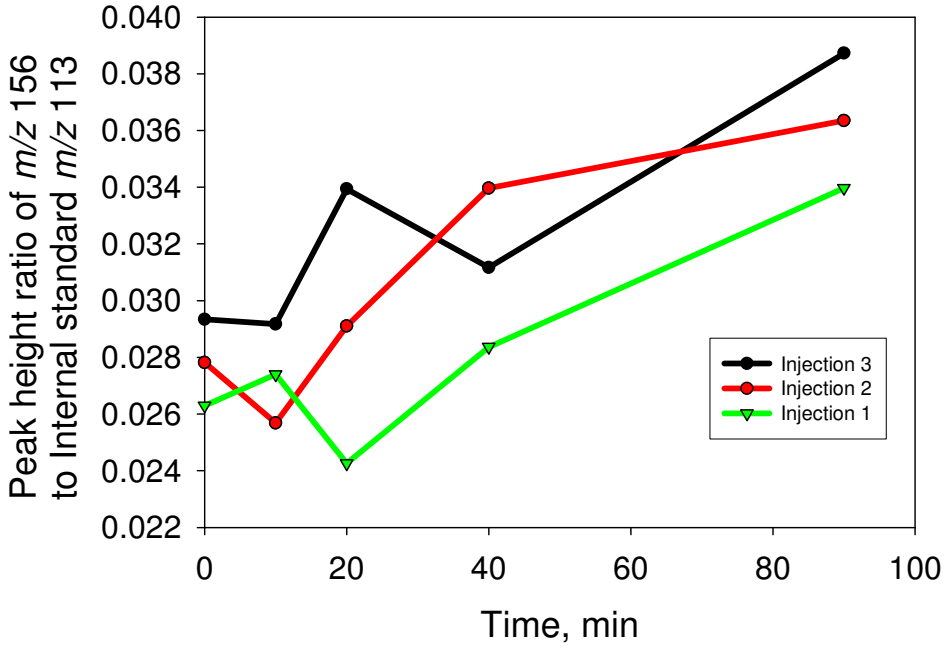

Fig 4.15: Formation of Product of m/z 156 from G on incubation with 1.5 mM $ZnSO_4$ and 50 mM H_2O_2 at 37 ^{o}C, with internal standard U (112 g mol^{-1}). The ionisation potential used was +15 V (N=3).

4.4.3 HPLC-MS and HPLC-MS/MS analysis of 8-oxoG further oxidation products from G in DNA

The study formation of these adducts from free G is important as it gives us an insight into the pathway of damage that is occurring from metal induced oxidative stress. These results, therefore, are a good indication that it is important to determine if this type of damage can occur in G in the DNA backbone. Experiments

were performed in a similar manner to the free G experiments using Calf Thymus DNA in place of G. The DNA was incubated with each of the transition metals Co, Mn, Cd, Zn and also Ni over an incubation period and DNA damage adducts were analysed. The formation of a peak was detectable at both *m/z* 158 and 159. This may be indicative of GH formation, similar to that detected from Ni induced damage in DNA, as described in Chapter 2.

The formation of the peak at 158/159 was analysed on incubation with Cobalt and is illustrated below in Fig 4.16. This is indicative that GH or a GH like substance was formed from Co induced damage.

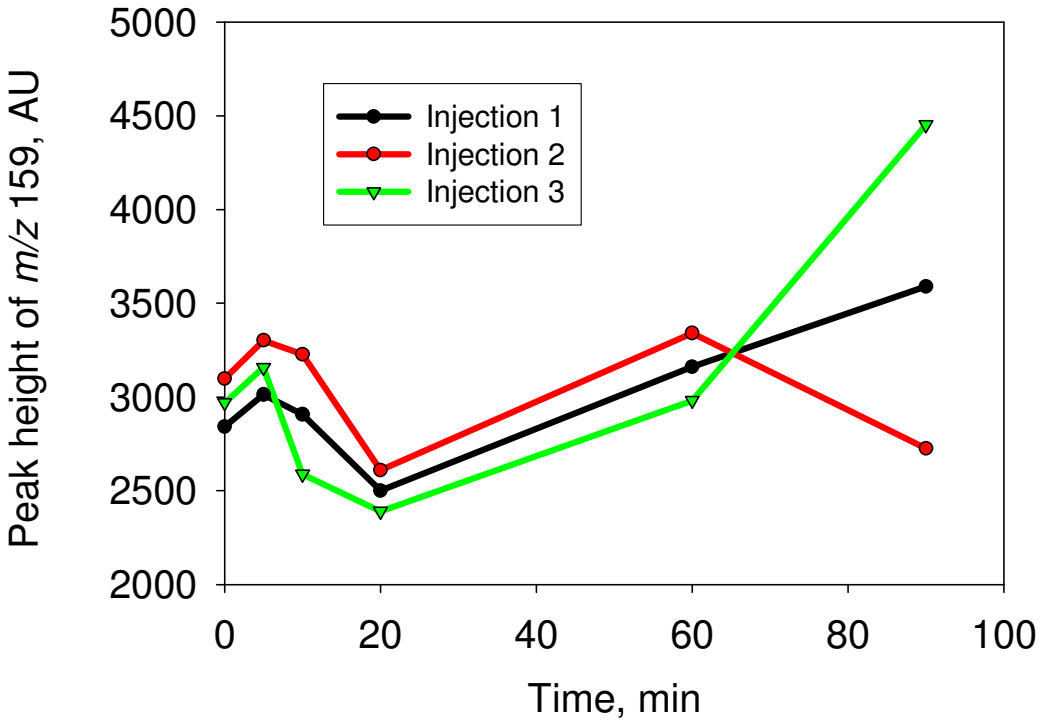

Fig 4.16: Formation of Product of m/z 159 from G in DNA on incubation with 1.5 mM $CoSO_4$ and 50 mM H_2O_2 at 37 ^oC . The ionisation potential used was +15 V (N=3).

In order to elucidate the structure of this compound of *m/z* 158/159, a MS/MS examination of the peak in question was undertaken. The resulting spectrum is shown in Fig.4.17. The spectrum was analysed at both *m/z* values, and showed identical fragmentation patterns, suggesting that the *m/z* 159 peak may have been due to a double protonation of the molecular ion.

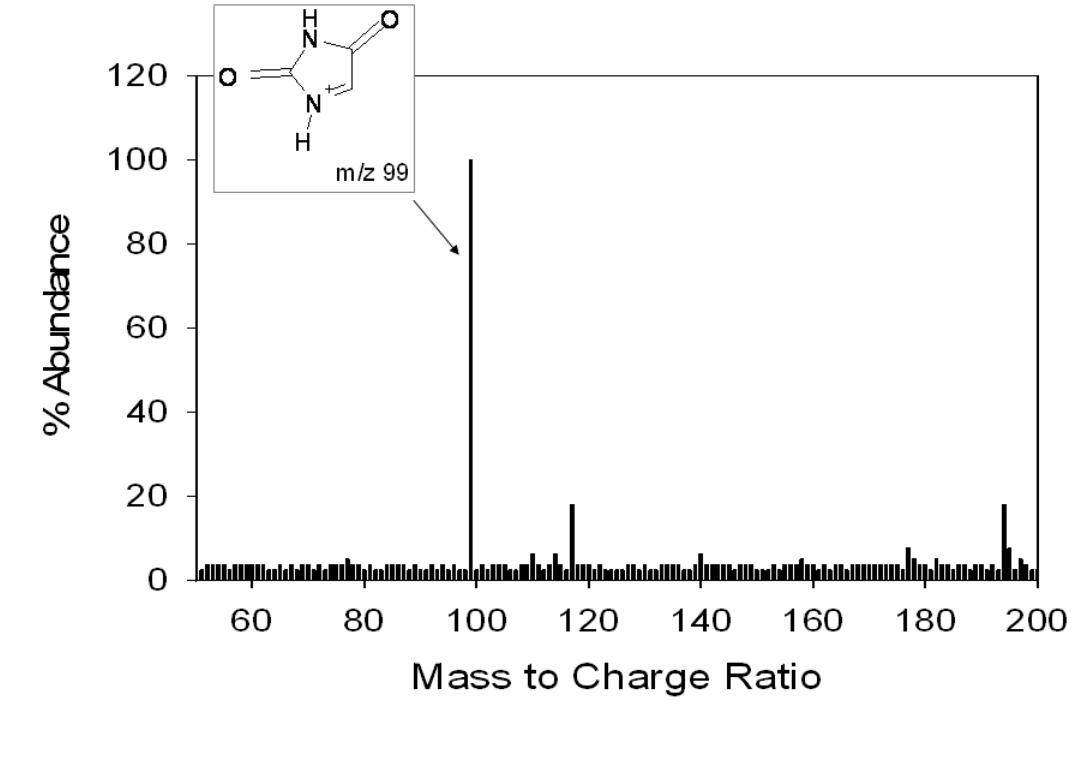

Fig 4.17: MS/MS of peak at m/z 159 from G incubated with 1.5 mM $CoSO_4$ and 50 mM H_2O_2 at 37^{o}C, illustrating fragmentation pattern, This mass spectrum was taken from the sample after 30 min. of incubation and the ionisation potential was +15 V.

The formation of a peak at *m/z* 113 was also noted and the formation was monitored over the entire incubation period with Co. The concentrations were below the LOQ of the system, and therefore could not be analysed further to obtain structural information.

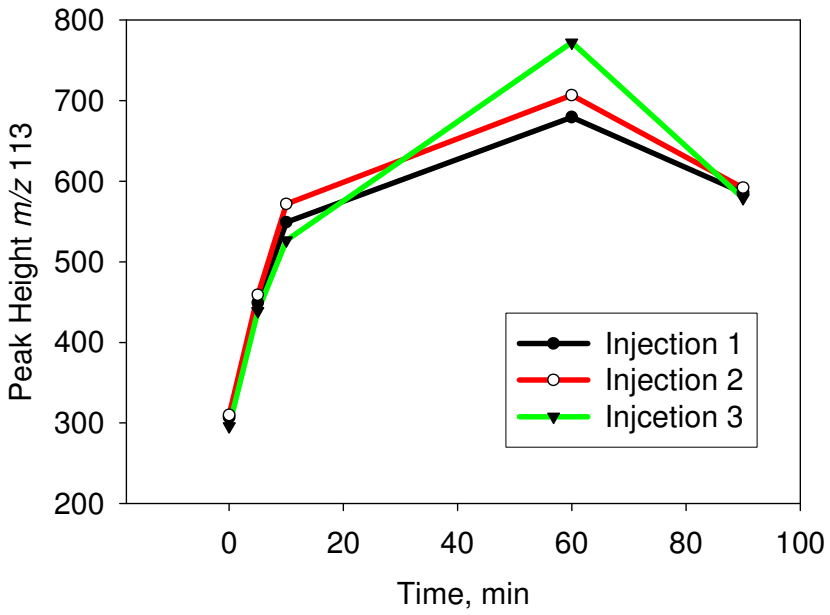

Fig 4.18: Formation of Product of m/z 113 from G in DNA on incubation with 1.5 mM $CdSO_4$ and 50 mM H_2O_2 at 37 ^oC . The ionisation potential used was set to -15 V (N=3).

Each of the metals examined showed levels of the peaks at both *m/z* 158, suspected to correspond to GH. There was very little, if any, *m/z* 168, corresponding to 8-oxoG, present in quantifiable levels present in the samples. Any detectable amount that was present was transient, as expected due to its ease of further oxidation, and apparent oscillatory formation noted in previous experiments. The concentration of 8-oxoG was also low in the initial HPLC-ECD experiments, in

comparison to previous work on Ni and also Fe and Cu [44], and therefore it would be expected that the level obtained was below the LOQ of the system. The fact that there is a breakdown of oxGH and GH to give low levels of *m/z* 113 could lead to an indication of the complete pathway of oxidation of G, as indicated in Fig 4.19 [45].

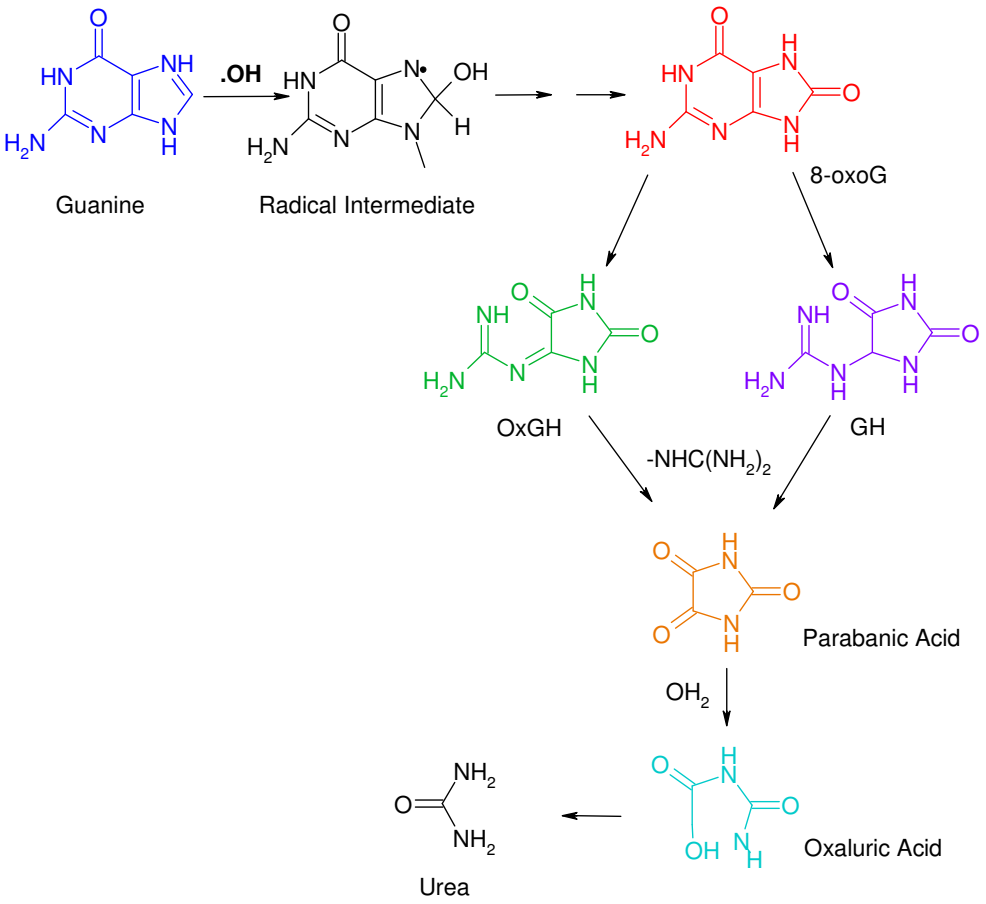

Fig 4.19: Oxidation pathway for the oxidation of G by transition metal-Fenton Systems [45].

The determination of oxidation products of 8-oxoG is vital in order to be able to determine the fate of DNA during oxidative stress. When the pathway has

been fully elucidated, the final products of DNA oxidation can be used as biomarkers of damage, and because of the range of products that have been discovered to date, it may be possible to determine the origin of the stresses that have caused the damage, as well as the extent of the damage.

Again, it is clear that the extent of the damage caused is dependent upon the transition metal involved. The levels of the oxGH formed are very dependent on the metal in question. Co produces 4.5 times the amount of oxGH than Mn after a 60 min. incubation. Mn in turn produces more oxGH than Cd and Zn, which show extremely low levels compared to the control incubations. Table 2.1 in Chapter 2 illustrates the available oxidation states for each of the first row transition metals and cadmium. This table illustrates the ability of the transition metals to change oxidation states.

4.5 CONCLUSION

This study was performed in order to determine if each of the transition metals Cd, Co, Mn, Zn and Mg could cause damage to DNA in a similar Fenton-like manner to that of Fe, Cu and Ni, as has been shown previously [44]. The study showed that there was a similar mechanism of generation of 8-oxoG from G from each of the transition metal-induced Fenton-like reactions for Cd, Co, Ni and Zn. The formation of 8-oxoG was again indicative of its role as an intermediate in the oxidation of G. Mg, as it cannot alter oxidation states and remains as a doubly charged cation did not generate 8-oxoG. 8-oxoG's ease of further oxidation was again evident in the study of Co, Cd and Zn oxidation of G.

The investigation described here has shown the formation of oxGH from free G and GH from G in DNA for Co and Mn, as has been shown previously for Ni. Cd and Zn did not show traces of these lesions above the level of controls. Both Cd and Zn are in the same group of the periodic table, and these results were indicative that both these react in a similar way. The formation of oxGH and GH adducts was in a steady, non-oscillating or erratic pattern, indicating their suitability and potential to be used as biomarkers of oxidative damage to DNA induced by Co, Mn, Ni, Fe and Cu. This will require further *in vivo* analysis but is a crucial step toward determining a biomarker for diseases such as cancer and neurodegeneration with a goal to fully elucidate the mechanisms and metabolism of these diseases within the body.

Given the differences between the concentrations of 8-oxoG formed and in the rates of formation and oxidation of 8-oxoG, it seems unlikely that the same

reaction takes place here for all transition metal-mediated DNA damage. The possibility that the transition metals generate different ROS needs to be investigates further. This will give a more comprehensive insight into the mechanisms of transition metal-mediated oxidative damage to DNA.

4.6 REFERENCES

1. Halliwell, B. and Gutteridge J.M.; Free Radicals in Biology and Medicine, 2nd edition, Clarendon Press; New York, *Oxford University Press*, **1989**.
2. Wisemann, H; Halliwell, B.; *Biochemistry Journal*; 313; **1996**, 17-29.
3. Kiyosawa, H; Suko, M.; Okudaira, H.; Murata, K.; Miyamoto, T.; Chung, M.H.; Kasai, H.; Nishimura S., *Free Radical Research Communications,* 11; **1990**, 23-27.
4. Loft, S.; Deng, X.S.,;Tuo; J.; Wellejus, A.; Sorensen, M; Poulsen, H.E; *Free Radical Research*, 29; **1998,** 525–39.
5. Loft, S.; Thorling, E.B.; Poulsen, H.E.; *Free Radical Research,* 29; **1998**, 595–600.
6. Asami, S.; Manabe, H.; Miyake, J.; Tsurudome, Y.; Hirano, T.; Yamaguchi, R.; Itoh, H.; Kasai, H.; *Carcinogenesis*; 18; **1997**, 1763–1766.
7. Cooke M.S., Olinski, R., Evans, M.D., *Clinica Chimica Acta,* 365; **2006**: 30-49.
8. Kawanishi, S; Hiraku, Y; Oikawa, S; *Mutation Research,* 488; **2001**, 65-76.
9. Halliwell, B.; Aruoma, O.I.; *FEBS Letters,* 281; **1991,** 9-19.
10. Steenken, S.; Jovanovic, S.Y.; *Journal of the American Chemical Society,* 119; **1997,** 617-618.
11. Cadet, J.; Delatour, T.; Douki. T.; Gasparutto, D,.;Pouget, J.P.; Ravanat,J.L.; Sauvaigo, S.; *Mutation Research: Fundamental and Molecular Mutagenesis,* 424; **1999**, 9-21.

12. Graf, E.; Mahoney, J.R.; Bryant, R.G., Eaton J.W.; *Journal of Biological Chemistry,* 259; **1984**, 3620-3624.

13. H. J. H. Fenton, *Journal of the Chemical Society*, **65**, 1894, 899.

14. Gutteridge, J.M.C.; Maidt, L.; Poyer, L.; *Biochemical Journal,* 269; **1990**, 169-174.

15. Breen A.P., Murphy J.A., *Free Radical Biology and Medicine,* 18; **1995**, 1033-1077.

16. Valavanidis, A.; Vlahoyianni, T.; Fiotakis, K.; *Free Radical Research*, 39; **2005**, 1071-1081.

17. Jarup, L.; Berglund, M.; Elinder, C.G.; Nordberg, G.; Vahter, M.; *Scandinavian Journal of Work, Environment and Health*, 24; **1998**, 1-51.

18. Jarup L.; *British Medicine Bulletin,* 68; **2003**, 167-182.

19. Aifen, T.; Elinder, C.G.; Carisson, M.D.; Grubb, A.; Hellstrom, L.; Persson, B.; Petterson, C.; Spang, G.; Schutz, A.; Jarup, L.; *Journal of Bone and Mineral Research*. 15; **2000**, 1579-1586.

20. Navas-Acien, A.; Selvin, E.; Sharett, A.R.; Calderon-Aranda, E.; Subergeld, E.; Guallar E.; *Circulation: Journal of American Heart Association,* 110; **2004,** 3195-3201.

21. Elinder, C.G.; Lind, B.; Kjellstrom, T.; Linnman, L.; Friberg, L.; *Archives of Environmental Health*, 31; **1976**, 292-302.

22. Bulbul, M.; Coker, C.; Orivural, B.; *Journal of Trace Elements in Medicine and Biology*, 17; **2003**, 51-55.

23. Wolnik, K.A., Friche, F.L.; Capar, S.G.; Meyer, M.W.; Duane Satzger, M.R., Nonan, E.; Gaston, C.M.; *Journal of Agricultural Food Chemistry* 33; **1985**, 1987.

24. Wolnik, K.A.; Fricke, F.L.; Capar, S.G.; George L. Braude, G.L.; Meyer, M.W.; Satzger, R.D.; Bonnin, E.; *Journal of Agricultural Food Chemistry*, 31; **1983,** 1240-1244.

25. Hossain, Z.; Huq, F.; *Journal of Inorganic Biochemistry*, 90; **2002**, 85-96.

26. DeBoeck, M.; Kirsch-Volders, M.; Lison, D.; *Mutation Research*; 533; **2003,** 135-152.

27. Burgos, M.G.; Rainbow, P. S.; *Estuarine, Coastal and Shelf Science*, 47; **1998**, 603-620.

28. Martin, P.T.; Mazumdar, S.U.; Chauduri, S.; *Journal of Inorganic Biochemistry*, 19; **1983**, 237-246.

29. Terron, A.; Fiol, J.J.; Garcia-Raso, A.; Bercelo-Oliner, M.; Moreno, V.; *Co-ordination Chemistry Reviews*, 25; **2007**, 1973-1986

30. Velasco-Ryenold, C.; Navarro-Alarcon, M.; Lopez-G, H.; Serrana, D.L.; Perez Valero, V.; Lopez-Martinez, M.C.; *Food Chemistry*, 109; **2008**, 113-121.

31. Pennington, J.A.T.; Young, B.; *Journal of Food Composition and Analysis*, 3; **1990**, 166-184.

32. Ljung, K.; Vahter, M.; *Environmental Health Perspectives*, 115; **2007**, 1533-1538.

33. Quintanar, L.; *Inorganica Chimica Acta,* 361; **2008**, 875-884.

34. Bowler, R.M.; Gysens, S.; Diamond, E.; Nakgawa, S.; Drezgic, M.; Roels, H.A.; *NeuroToxicology*, 17; **2006**, 315-326.

35. Racette, B.A.; McGee-Minnich, L.; Moerlein, S.M.; Mink, J.W.; Videen, T.O.; Perlmutter, J.S.; *Neurology*, 56; **2001**, 8-13.

36. Halliwell, B. and Gutteridge J.M.;,Free Radicals in Biology and Medicine, 4th edition, Clarendon Press; New York, *Oxford University Press*, **2007**.

37. Stredrich, D.L.; Stokes, A.H.; Worst, T.J.; Freeman, W.M.; Johnson, E.A.; Lash, L.H.; Aschner, M.; Vrana, K.E.; *Neurotoxicology*, 25; **2004**, 543-553.

38. Taylor, M.D.; Erikson, K.M.; Dobson, A.W.; Fitsanakis, V.A.; Dorman, D.C.; Aschner, M.; *Neurotoxicology*, 27; **2006**, 788-797.

39. Wolf, F.I.; Maier, J.A.M.; Nasulewicz, A.; Feillet-Coudray, C.; Simonacu, M.; Mazur, A.; Citadini, A.; *Archives of Biochemistry and Biophysics*, 458; **2007,** 24-32.

40. Ford, E.S.; Mokdad, A.H.; *Journal of Nutrition*, 133; **2003**, 2879-2882.

41. Eichhorn, G.L.; Shin, Y.A.; *Journal of the American Chemical Society*, 90; **1968**, 7323-7328.

42. Cavalieri, L.F.; *Journal of the American Chemical Society*, 74; **1952**, 1242-1247.

43. Petrov, A.S.; Lamm, G.; Pack, G.R.; *Journal of Physical Chemistry*, 106; **2002**, 3294-3300.

44. White, B.; Smyth, M. R.; Stuart, J. D.; Rusling, J. F.; *Journal of the American Chemical Society;* 125; **2003**, 6604-6605.

45. Gimisis, T.; Cismas, C.; *European Journal of Organic Chemistry*, 6; **2006**, 1351-1378.

46. Cotton, F.A.; Wilkinson, G.; *Basic Inorganic Chemistry*, **3rd Edition**, J. Wiley Publishers, New York, USA, **1995**.

47. Cotton, F.A.; Wilkinson, G.; Murrillo, C.A.; *Advanced Inorganic Chemistry*, **6th Edition**, J. Wiley Publishers, New York, USA, **1999**.

5 DETERMINATION OF THE REACTIVE OXYGEN SPECIES INVOLVED IN TRANSITION METAL INDUCED OXIDATIVE DAMAGE TO DNA

5.1 INTRODUCTION

The level of oxidative stress that the human body is subjected to results in DNA undergoing thousands of oxidative stresses per day. The term oxidative stress implies an imbalance in the level of oxidants as a ratio to antioxidants, leading to oxidative damage in cells, whether this is to proteins, lipids, RNA or DNA or their components [1-6]. The ROS that are implicated in oxidative damage to DNA, including singlet oxygen, superoxide, the peroxyl radical and ·OH have been previously discussed in detail in Chapter 1.

Classically in the literature, ·OH has been implicated as the ROS of interest in Fenton chemistry, but there has been speculation for some of the metals that have been studied, that there is a metal-oxygen complex involved, or by other ROS such as singlet oxygen ($^1O_2$) [7-9]. There is, therefore, a need for the accurate determination of the correct ROS that is involved in these metal-induced Fenton-like reactions.·OH is the most reactive ROS that is generated *in vivo*. Its high reactivity is attributed to its high electrophilicity, high thermochemical reactivity as well as its production near to DNA *in vivo*. It reacts with all known biomolecules. It acts by adding to DNA as well as abstracting H atoms [10, 11].

It is important to determine if it is, in fact, ·OH which causes the erratic formation of 8-oxoG from G and the subsequent further oxidation of 8-oxG that has been observed in the previous Chapters for all the transition metals studied.

·OH is difficult to detect directly, due to its extreme reactivity. Electron paramagnetic resonance (EPR) is a method generally used for radical detection, and has been used in order to determine ·OH. Fenton reaction generated ·OH gives a

distinct pattern of a quartet of lines with a ratio of 1:2:2:1 in EPR, illustrated in Fig 5.1 [12]. This method is accurate but can be difficult to interpret and is expensive; it also cannot be used to gain an *in vivo* determination of ·OH. Therefore simpler, more indirect methods are generally used in the determination of ·OH, both *in vitro* and *in vivo*.

Fig 5.1: Electron paramagnetic resonance spectrum for ·OH. (Reproduced from Freinbichler *et al.*[12]).

An indirect ·OH assay that has been used frequently is the HPLC determination of salicylate and products of its reaction with ·OH. HPLC can be used to detect 2, 3- and 2, 5-dihydroxybenzoate, and quantitation of these compounds may lead to the determination of quantities of ·OH production (Scheme 5.1). This method would be also beneficial to the determination of the ROS produced in the Fenton reactions investigated. The ·OH production can be monitored over time in order to analyse the kinetics of the metal-Fenton reactions [13].

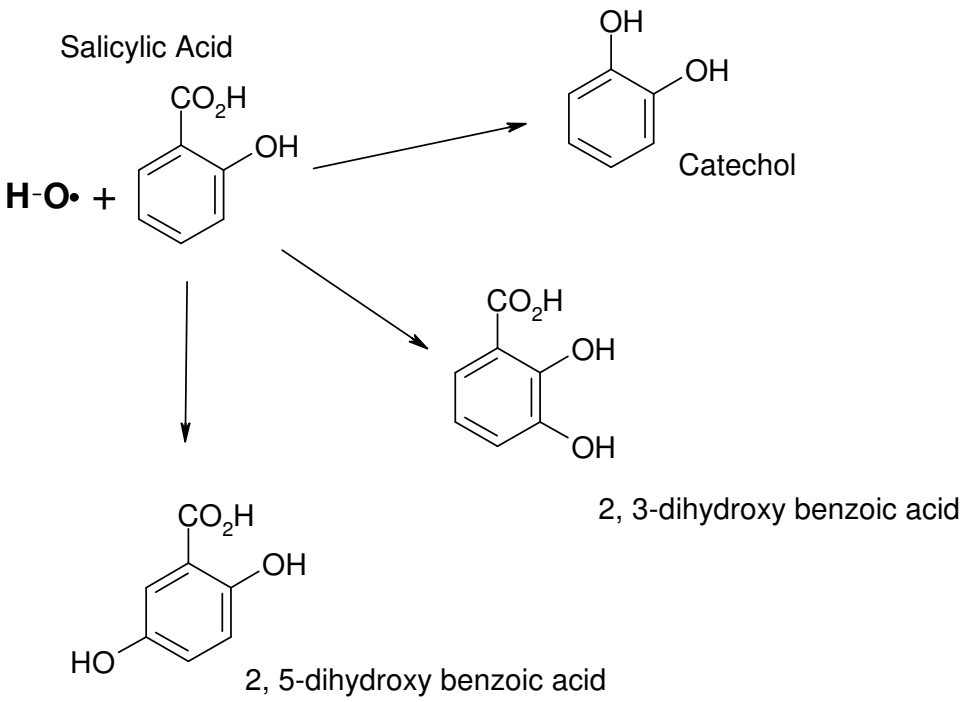

Scheme 5.1: Reaction of ·OH with salicylic acid to form catechol, 2, 3 – dihydroxybenzoic acid, 2,5-dihydroxybenzoic acid [13].

The main drawback of this reaction is the quantitation of ·OH is subject to error. For accurate determination of ·OH concentration, all three products must be analysed. For cellular analysis, salicylic acid and its product, 2, 5-dihydroxybenzoic acid are present in basal cell samples, and therefore it is difficult to determine the true extent of ·OH attack on applying a stress, thus adding to possible over estimation. The use of high concentrations of the trap can also influence biological processes, and thus it is not a good choice for *in vivo* studies [14, 15].

A better method of determination of ·OH is through the use of a similar scavenger, 4-hydroxybenzoic acid (4-HBA), which on specific reaction with ·OH

produces a single compound, 3, 4-dihydroxybenzoic acid (3,4-DHBA). This means that all ·OH reacted can be accounted for by the determination of a single product. 3, 4-DHBA is electrochemically active [16]. The electrochemistry of the two products were investigated by Hu *et al.*, who noted that the product, 3,4-DHBA, had a peak oxidation potential which was sufficiently different to the 4-HBA, and therefore, the 3,4-DHBA can be analysed independently of its precursor, without prior separation [17]. The peak potentials at which 4-HBA and 3, 4-DHBA were oxidised were 0.83 V and 0.27 V, respectively. This experiment was carried out on a homemade carbon disk electrode against a Ag/AgCl reference electrode, therefore, by scanning between 0.0 and 0.6 V, Hu *et al.* were able to determine the formation of 3, 4-DHBA and utilise this formation to determine the concentration of ·OH that reacted with the precursor. This method was applied to the determination of the formation of ·OH via the Fe(II)-catalysed Fenton reaction [17].

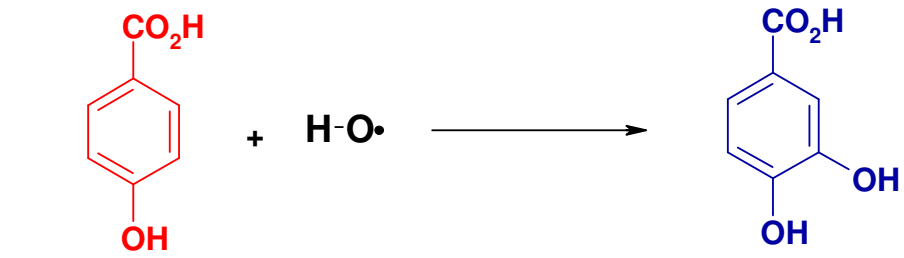

4-Hydroxybenzoic Acid **3, 4-Dihydroxybenzoic Acid**

Scheme 5.2: Reaction of ·OH with 4-hydroxybenzoic acid to form 3,4-dihydroxybenzoic acid [17].

5.2 SCOPE OF THE RESEARCH

HPLC with UV and ECD can be used to determine 4, HBA and 3,4-HBA in order to monitor of the formation of ˙OH. Because they were separated, both 4-HBA and its hydroxylation product 3,4-DHBA could be detected. The use of a separation technique is important for *in vivo* analysis in particular as it allows for separation of the compounds from complex biological matrices [12, 18, 19]. The determination of the ROS involved in the transition metal induced G oxidation was also vital in understanding the mechanism behind transition metal-induced DNA damage. This research to date suggested Fenton-like reactions were involved due to the nature of the DNA damage that occurred from a number of transition metals, but it was important to determine if it was in fact the ˙OH that was causing the damage. This study employed the use of HPLC-UV-ECD method in order to determine 3, 4-DHBA formation from the radical scavenger 4-HBA. The potential was set so that 4-HBA concentration was also monitored. This therefore allowed for the study of transition metal-mediated Fenton reactions, thus allowing for an insight into the ROS that is involved in DNA damage by Zn, Cd, Ni, Co, Mn, Cu and Fe.

5.3 EXPERIMENTAL

5.3.1 Materials

The DNA base, G (G0381, ≥99%), 7,8-dihydro-8-oxoG (R288608), cadmium sulphate hexahydrate (481882, 99.999%), cobalt(II) sulfate heptahydrate (C6768, 99%), iron(II) sulphate, copper (II) sulfate, 4-hydroxybenzoic acid and 3, 4-dihydroxybenzoic acid were purchased from Sigma-Aldrich (Tallaght, Dublin, Ireland). Magnesium sulfate heptahydrate and LC-MS grade methanol were purchased from Riedel-de Haen (99.5-100.5%, <0.001% Fe), and zinc sulfate heptahydrate from Fluka (96500 95-103%, </= 0.0005% Fe). Ethanol and methanol were purchased from Labscan Ltd. (Dublin, Ireland). Deionised water was purified using a MilliQ system to a specific resistance of greater than 18 MΩ-cm. All HPLC buffers and mobile phases were filtered through a 47 mm, 0.45 μm polyvinylidene fluoride (PVDF) micropore filter prior to use. Fresh solutions of all standards were prepared weekly.

5.3.2 Incubation of 4-HBA with transition metal-Fenton reagents

Unless otherwise stated, for HPLC-UV-ECD, a 4 mM solution of 4-HBA, prepared in deionised water, was incubated at 37 ^{o}C in stirred solution with 1.5 mM of the metal salt of interest and 50 mM solution of hydrogen peroxide (H_2O_2), as described in Chapter 2 for G incubations. Samples were quenched in ethanol and dried under N_2 flow.

5.3.3 HPLC-ECD analyis of 3, 4-DHBA and 4-HBA

Samples were reconstituted in 1 mL 50 mM ammonium acetate and separated by RP HPLC using a Varian ProStar HPLC system with Varian ProStar 230 solvent delivery module and Varian ProStar 310 UV-VIS detector. The eluent composition was, 50 mM ammonium acetate/85 mM acetic acid buffer, pH 4.6: methanol (90:10) through a Phenomenex 4.6 x 100 mm Onyx RP C_{18} monolith column, equipped with Ultra 4 x 10 mm C_{18} guard column.

The separation was carried out at 2.0 ml min^{-1} isocratic elution, with post UV detection flow spitting resulting in 0.35 ml min^{-1} eluent to the ECD system. ECD detection, using a BAS CC-4 electrochemical cell comprising of glassy carbon working electrode, stainless steel auxiliary electrode and Ag/AgCl reference electrode at a detection potential of +900 mV. ECD chromatograms were generated using a CHI 800B potentiostat and accompanying software. UN-SCAN-IT digitising software (Silk Scientific Corporation) was used to digitise integrator chromatograms, which were then imported into SigmaPlot 8.0 or MS Office Excel.

5.4 RESULTS AND DISCUSSION

5.4.1 HPLC-UV-ECD methodology

HPLC-UV was used initially to ensure separation of the two components, 4-HBA and 3,4-DHBA. Three mobile phase compositions were compared. The mobile phase compositions of 50 mM ammonium acetate/85 mM acetic acid buffer, pH 4.6:methanol in ratios of 60:40, 70:30 and 90:10 were investigated. The results from an injection of a 1 mM mix of 4-HBA and 3,4-DHBA at a flow rate of 1.0 ml min^{-1} were analysed. Table 5.1 shows retention time, peak width at half height ($W_{1/2}$), efficiency and resolution for the separations using 50 mM ammonium acetate/85 mM acetic acid buffer, pH 4.6: Methanol in the ratios of 60:40, 70:30, and 90:10 at 1 ml min^{-1} and compares these results to a 90:10 composition at 2 ml min^{-1}. As expected, the reduction in methanol concentration in the eluent led to an increased retention for each compound. Retention at the higher flow rates were comparable to that of the highest methanol concentration for 3,4-DHBA and comparable to the 70:30 composition for 4-HBA. The 90:10 composition at 1 ml min^{-1} resulted in broadened peaks with large peak widths, which was resolved by increasing the flow to 2 ml min^{-1}. The peak efficiency for 3,4-DHBA decreased with decreasing methanol concentration; however, with an increase in flow rate, the number of theoretical plates increased from 1146 to 3253. The 4-HBA peak efficiency was comparable for each of the mobile phase compositions and remained comparable with an increase in flow rate with the 90:10 composition. The resolution was acceptable for all compositions but showed an increase with

decreasing mobile phase organic content, and increased to 7.751 with the higher flow rate.

Parameter		Eluent Composition*			
	Component	60:40 1 ml min^{-1}	70:30 1 ml min^{-1}	90:10 1 ml min^{-1}	90:10 2 ml min^{-1}
Retention Time	3,4-DHBA	1.844	2.070	3.355	1.655
(min)	4-HBA	2.123	2.690	5.345	2.620
Peak Width $_{1/2}$	3,4-DHBA	3.8	4.6	14.0	4.1
(s)	4-HBA	4.2	4.9	8.8	4.7
Efficiency	3,4-DHBA	4701	4042	1146	3253
	4-HBA	5100	6016	7364	6203
Resolution		2.465	4.613	6.169	7.751

Table 5.1: HPLC Parameters for the separation of 3,4-DHBA and 4-HBA through an Onyx Phenomenex C18 monolith column of dimensions 100 mm X 4.6mm ID, with eluent composition 50 mM ammonium acetate/85 mM acetic acid buffer, pH 4.6:methanol* at flow rates of 1 and 2 ml min^{-1}.

The 50 mM ammonium acetate/85 mM acetic acid buffer, pH 4.6:methanol (90:10) mobile phase was selected at 2 ml min^{-1} as it showed separated peaks, with comparable efficiencies and $W_{1/2}$ to the higher solvent concentrations, but generated less organic solvent waste.

In order to couple the HPLC-UV system to ECD detection, the same flow splitting T-piece discussed in Chapter 3, Section 3.3.2.3 was used. With 2 ml min^{-1} flowing from the HPLC through the T-piece, 0.35 ml min^{-1} went to the ECD detector with 1.65 ml min^{-1} to waste.

ECD was optimised by varying the potential in the range of 100 mV to 1 V vs. Ag/AgCl. The resulting chromatograms and hydrodynamic voltammograms (HDVs) are illustrated in Figs 5.2 and 5.3. 3,4-DHBA was not detected below 300 mV vs. Ag/AgCl, and 4-HBA was detected only above 800 mV. It was determined that the optimum voltage to be used was 900 mV.

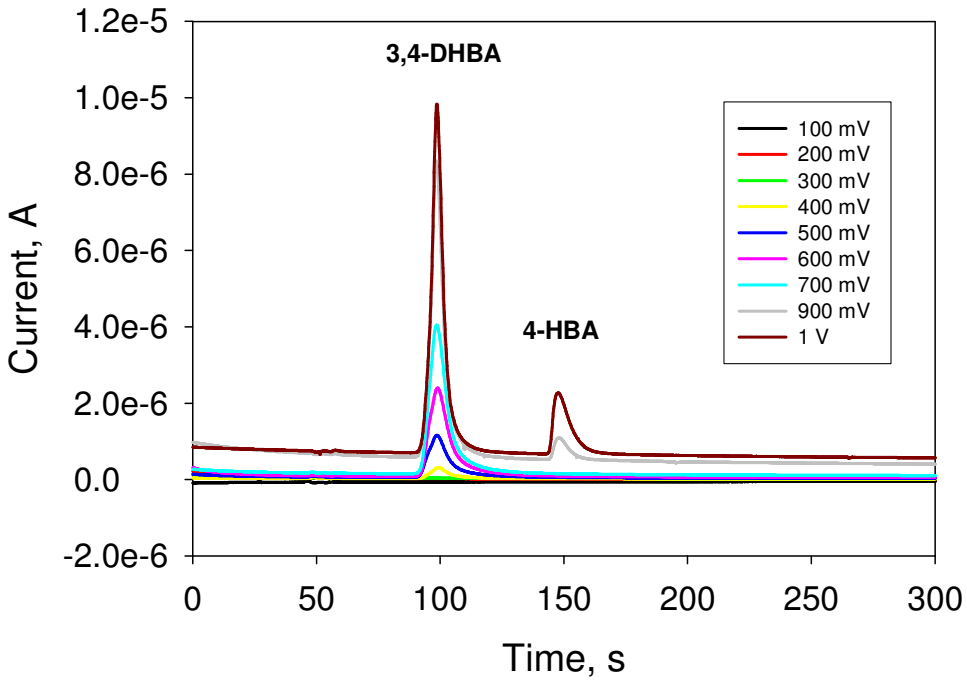

Fig 5.2: HPLC separation with ECD of 3,4-DHBA and 4-HBA illustrating the increase in peak height with increase of detection voltage vs. Ag/AgCl. Separation was carried out using a 50 mM ammonium acetate/85 mM acetic acid buffer, pH 4.6:methanol (90:10) on a Phenomenex 4.6 x 100 mm Onyx RP C_{18} column with ECD. The flow rate from the HPLC was 2 ml min^{-1} and to the ECD was 0.35 ml min. after splitting post UV detection.

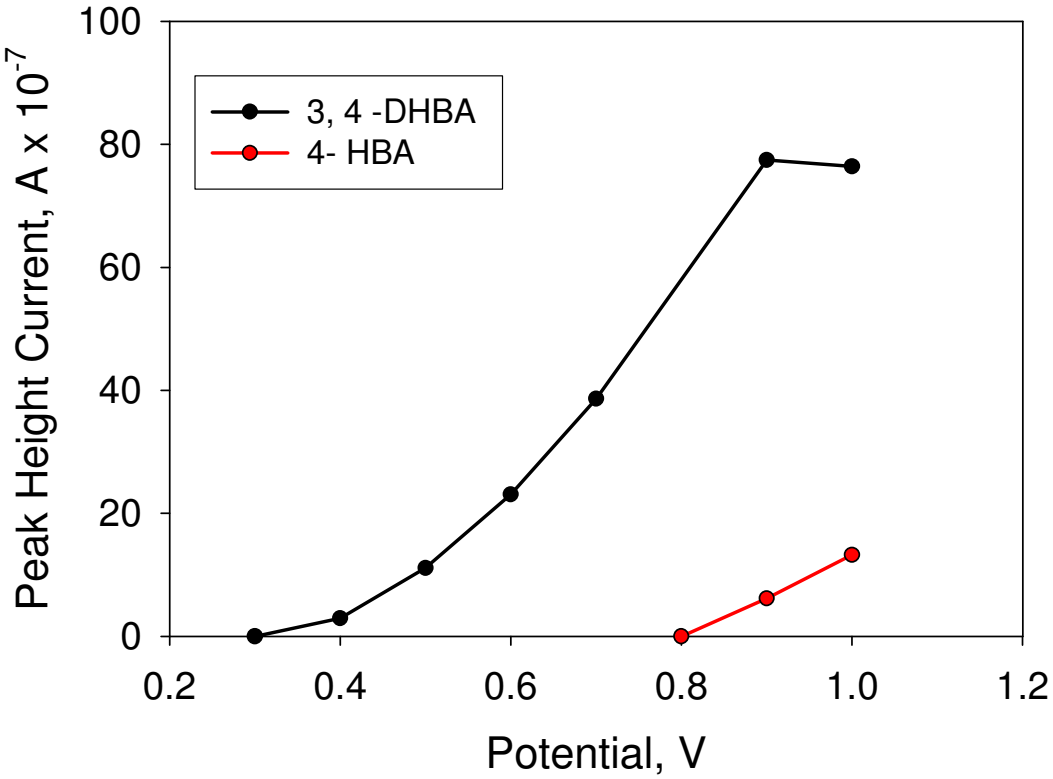

Fig 5.3: Hydrodynamic voltammogram illustrating the peak height current against change in potential for 3,4-DHBA in the range of +300 mV to +1V vs. Ag/AgCl. Separation and detection conditions as described in Fig 5.2.

A calibration curve for ECD of 3,4-DHBA was constructed in the range of 10 nM to 1 µM with a correlation coefficient of 0.9958, indicating good linearity. Below 10 nM, the graph was no longer linear. The limit of detection of the assay was approximately 100 pM (3 times S/N), though the limit of quantitation was 10 nM (determined from calibration curve). This is shown in Fig 5.4. The ECD calibration curve for 4-HBA in the mM range gave a correlation coefficient of 0.95.

The UV LOD for 3,4-DHBA was 0.1 µM (3 times S/N) and the LOQ was 0.3 µM, which was much higher than that of the ECD detection.

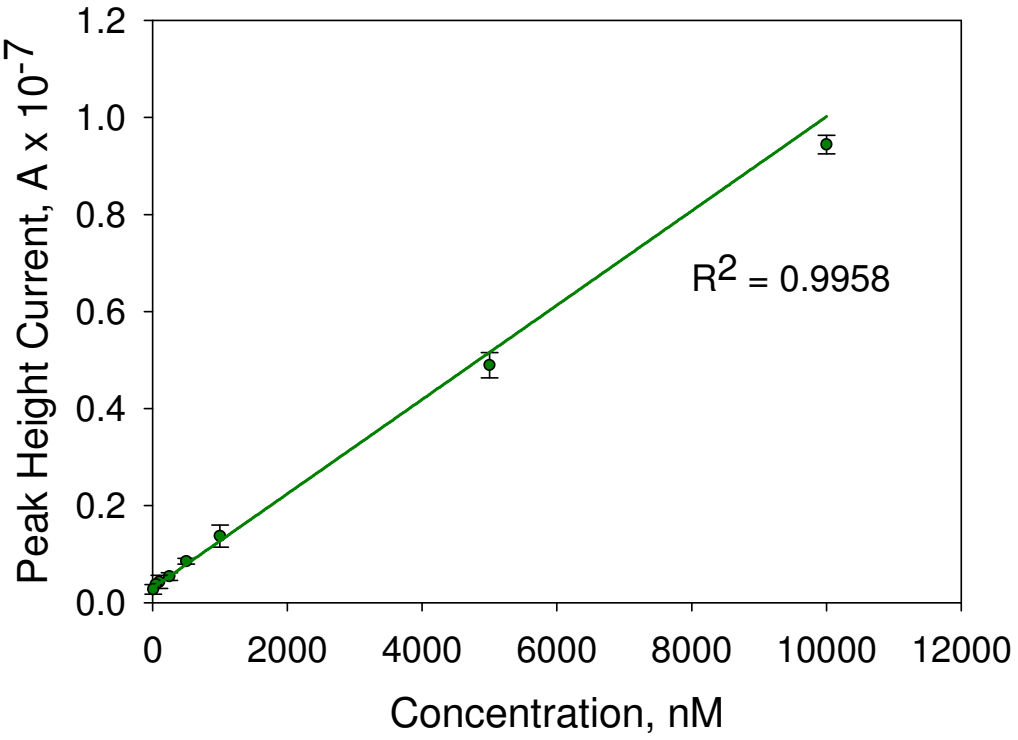

Fig 5.4: HPLC- ECD calibration curve for 3,4-DHBA in the range of 10 nM to 1 µM, at 0.9 V vs. Ag/AgCl. Separation and detection conditions as described in Fig 5.2.

This method was subsequently applied to attempt to detect the generation of $^{\cdot}OH$ from transition metal-Fenton reactions, discussed in Section 5.2.2, by analysing the formation of 3,4-DHBA from 4-HBA.

5.4.2 Determination of ·OH formation from transition metal-Fenton reactions

5.4.2.1 Fe-Fenton Reaction

This study was undertaken in order to determine if the ·OH was the ROS generated by each of the metals Fe, Cu, Ni, Co, Mn, Cd and Zn, suspected to take part in transition metal-mediated oxidation of DNA. Each of the metals in turn was incubated with 4-HBA and the other Fenton reactant H_2O_2. The formation of 3,4-DHBA from 4-HBA was analysed for each of the reactions.

Control incubations showed no decrease in the 4-HBA concentration during incubation. The control incubation with no metal and H_2O_2 shown in Fig 5.5 illustrates this. Over a 20 min. incubation, the concentration of 4-HBA remained constant. There was some formation of 3,4-DHBA detected at the initial stage of the incubation at a concentration of 1 μM. The control incubations, therefore, are indicative that any decrease in 4-HBA was due to the metal under investigation.

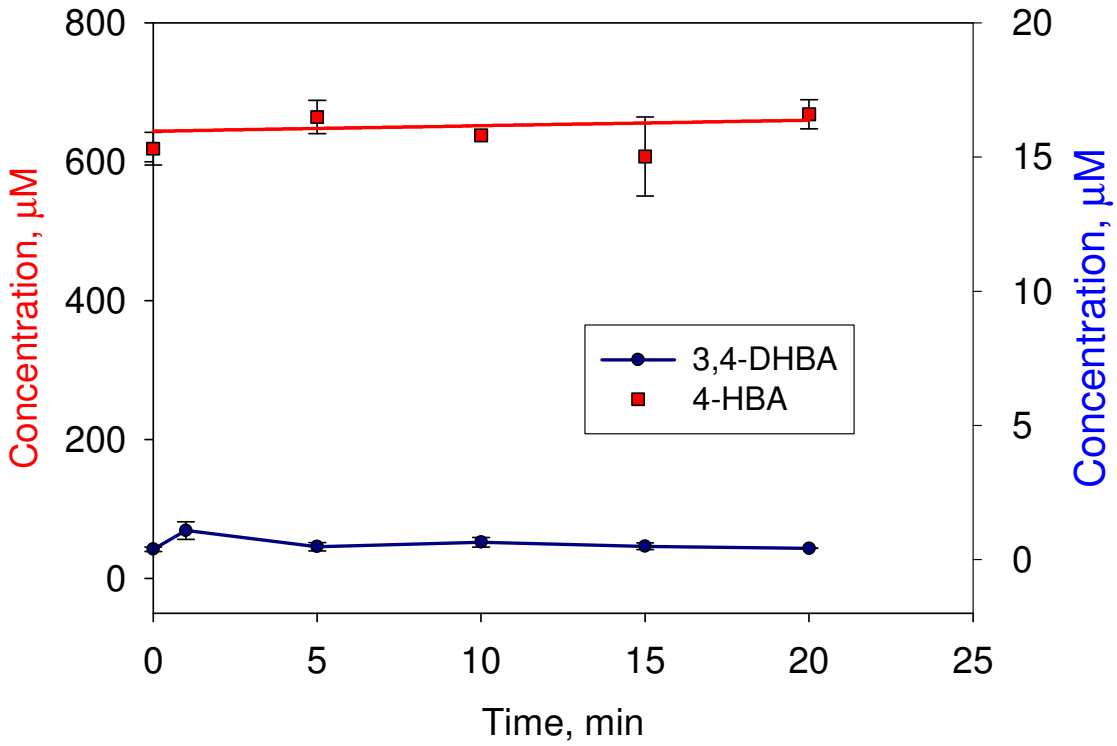

Fig 5.5: Graph of concentration of 3,4-DHBA and 4-HBA after control incubation of 4-HBA with H_2O_2 and no metal salt at 37 ^oC. Separation and detection conditions as described in Fig 5.2. The reaction was quenched in 1 ml ethanol, dried under N_2 flow and reconstituted in 1 ml 50 mM ammonium acetate buffer pH 5.5. Samples taken in at 0, 1, 5, 10, 15 and 20 min, and injected in triplicate. Standard deviations shown are of N = 3.

Fig 5.6 shows chromatograms for samples of 4-HBA taken after 0, 3, 30, 60, and 90 s after incubation with 1.5 mM $FeSO_4$ and 50 mM H_2O_2 with the initial formation of 3,4-DHBA. The sample prior to reaction with the Fenton mixture shows the small background concentration of the 3,4-DHBA and clearly illustrates

the 4-HBA (grey dashed line). It is very evident that 3 s after addition of the reactants, there was significant 3,4-DHBA formation.

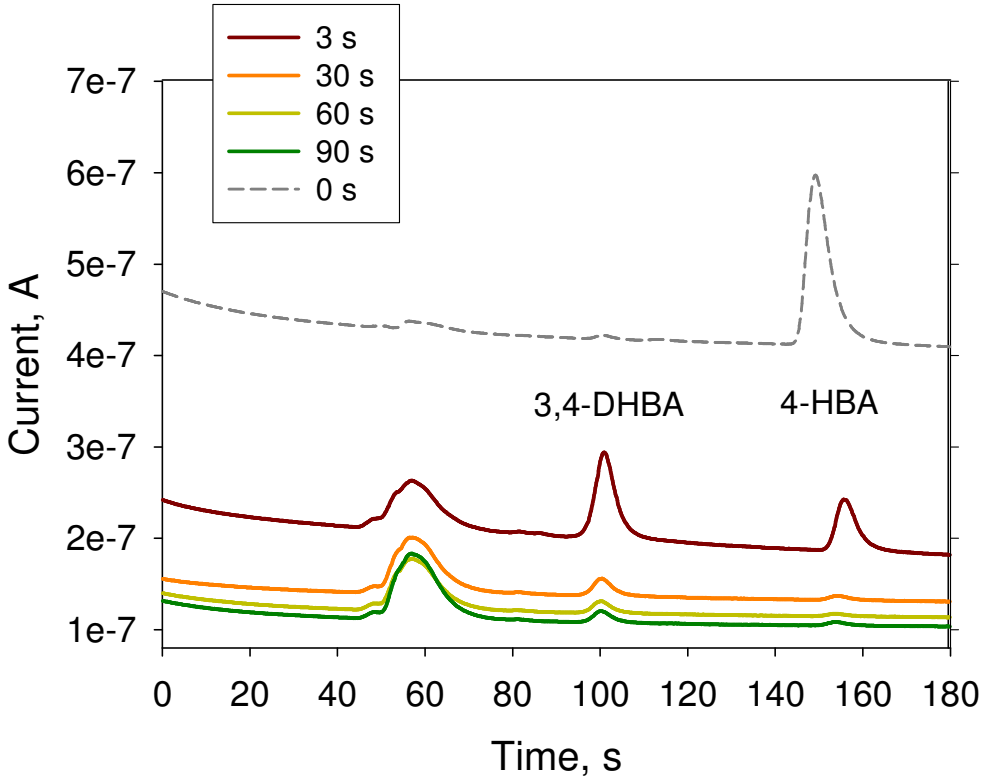

Fig 5.6: HPLC chromatograms with ECD illustrating the formation of 3,4-DHBA from 4-HBA on $FeSO_4$ and H_2O_2 at 37 ^{o}C. Separation and detection conditions as described in Fig 5.2. The reaction was quenched in 1 ml ethanol, dried under N_2 flow and reconstituted in 1 ml 50 mM ammonium acetate buffer, pH 5.5. Samples were taken and after 3, 30, 60 and 90 s. 0 s sample chromatogram is offset by 3 e^{-7} Amps.

The formation of 3,4-DHBA from 4-HBA on incubation with Fe-Fenton reagents is indicative that $^{\cdot}$OH is involved here. The 3,4-DHBA moiety appears to also be susceptible to $^{\cdot}$OH, though this could be expected as it is more easily

oxidised than 4-HBA, as discussed previously. Generally, the 3,4-DHBA is used in *in vivo* studies where it is removed immediately from the site of 4-HBA oxidation by microdialysis, for example, and therefore is adequate for this use. In this instance; however, it was almost certainly further oxidised. The product of 3,4-DHBA oxidation was not electrochemically active. The concentration of 4-HBA and 3,4-DHBA over the 90 s incubation period is shown in Fig 5.7. Most of the 4-HBA oxidation by ROS occurred between adding the reagents to the 4-HBA and taking the first sample reaction mixture, after 3 s. This oxidation continued between the initial sample and the 30 s sample.

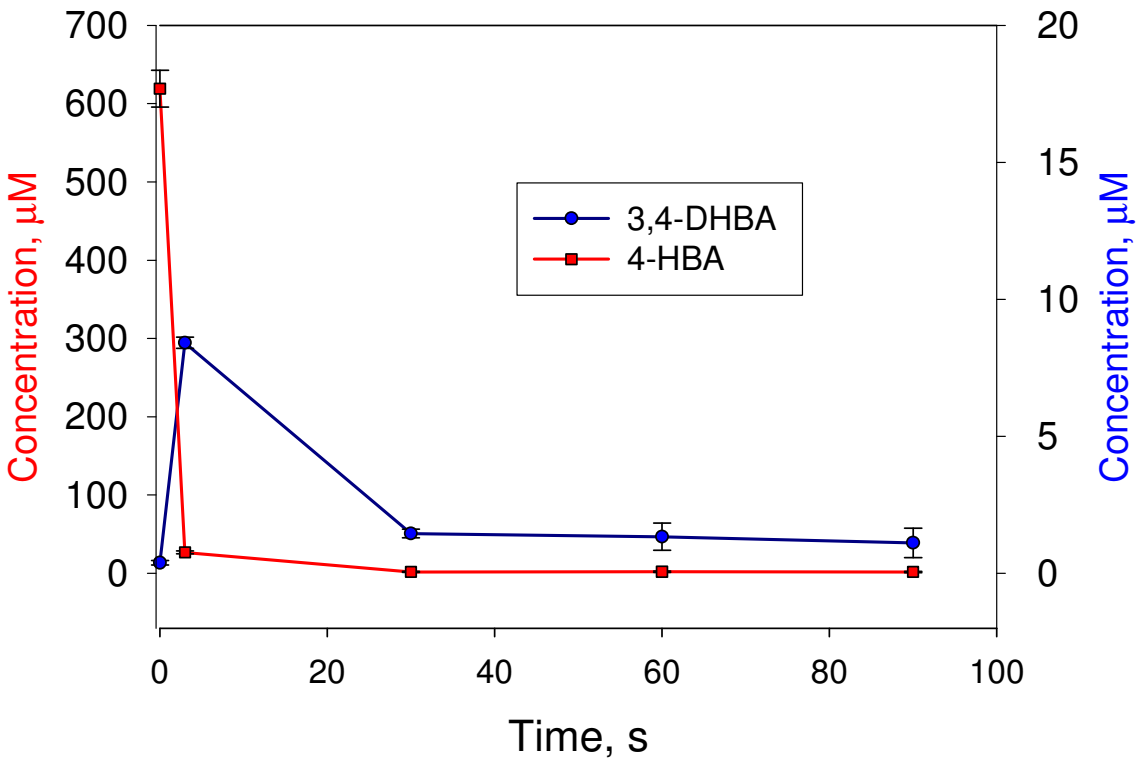

Fig 5.7: Effect of the Fe-Fenton reaction on the concentrations of 3,4-DHBA and 4-HBA after incubation of 4-HBA with 1.5 mM $FeSO_4$ and 50 mM H_2O_2 at 37 ^oC. Separation and detection conditions as described in Fig 5.2. The reaction was quenched in 1 ml ethanol, dried under N_2 flow and reconstituted in 1 ml 50 mM ammonium acetate buffer, pH 5.5. Samples were taken immediately, and after 30, 60 and 90 s. (N=3)

A further experiment was performed in order to analyse the damage that occurred in between 3 s and 30 s sample. This consisted of a repeat of the experiment with samples taken at 0, 2, 6, 10, 14, 18, 22, 24, and 26 s. The results, in Fig 5.8 show a similar rapid decrease in concentration of 4-HBA indicating that it was immediately used up at the very start of the reaction. The 3,4-DHBA on the

other hand, did show a detectable decrease over the first 26 s of the reaction. This appears to confirm that the ·OH produced in the Fe-Fenton reaction which reacted to produce the 3,4-DHBA, also reacted with this product over time, especially as the concentration difference between the reactant and product decreased.

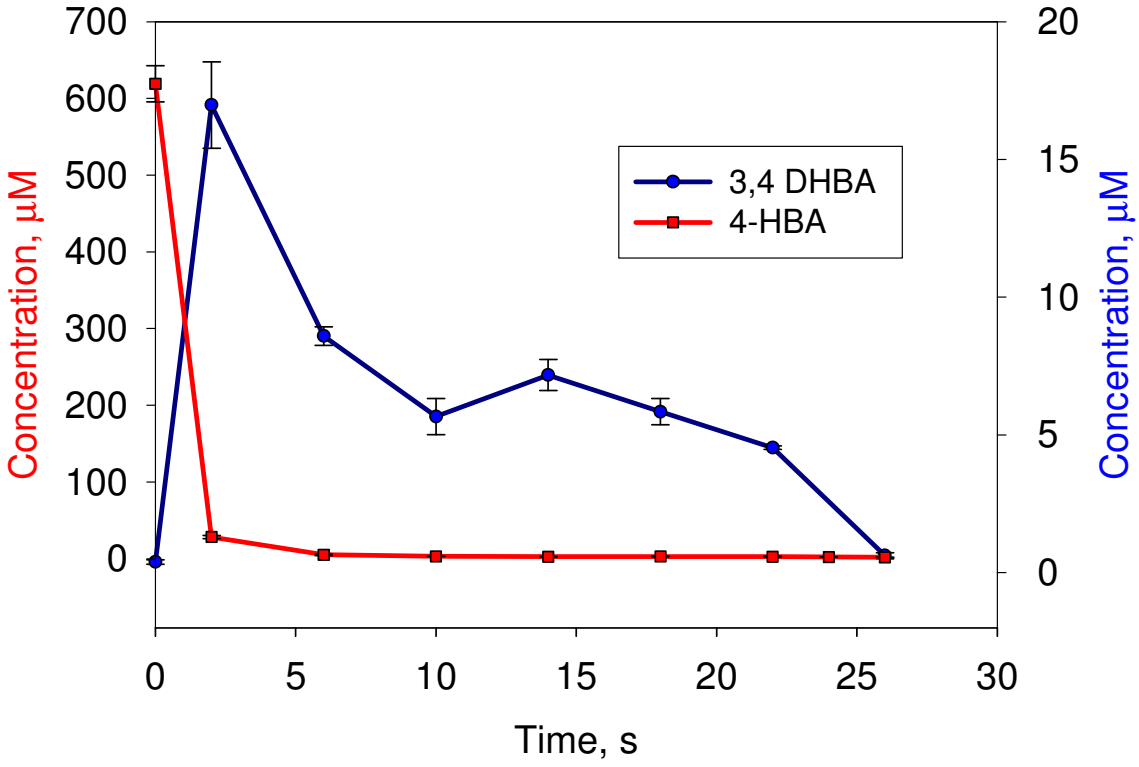

Fig 5.8: Illustration of concentration of 3,4-DHBA and 4-HBA after incubation of 4-HBA with $FeSO_4$ and H_2O_2 at 37 ^oC. Separation and detection conditions as described in Fig 5.2. The reaction was quenched in 1 ml ethanol, dried under N_2 flow and reconstituted in 1ml 50 mM ammonium acetate buffer pH 5.5. Samples taken after 2, 6, 10, 14, 18, 22, 24 and 26 s. (N=3)

5.4.2.2 Effect of G moiety on Fe-Fenton interaction

In order to determine the effect of the presence G moiety on the production and consumption of the ·OH that was produced in the Fe-Fenton reaction, a 5 mM G and 2 mM 4-HBA mixture was used and the reaction repeated under the same conditions with Fe-Fenton reaction. There was a very different reaction profile for the incubation. The reaction profile observed in this experiment gave a very low concentration of 3,4-DHBA formed, close to the LOQ of the assay. A decrease in concentration of the 4-HBA was also noted, however, this was not immediate, such as that of the previous experiment, but was over the course of the 20 min. incubation. G also showed a decrease in concentration over the 20 min. incubation period, as detected by UV absorbance.

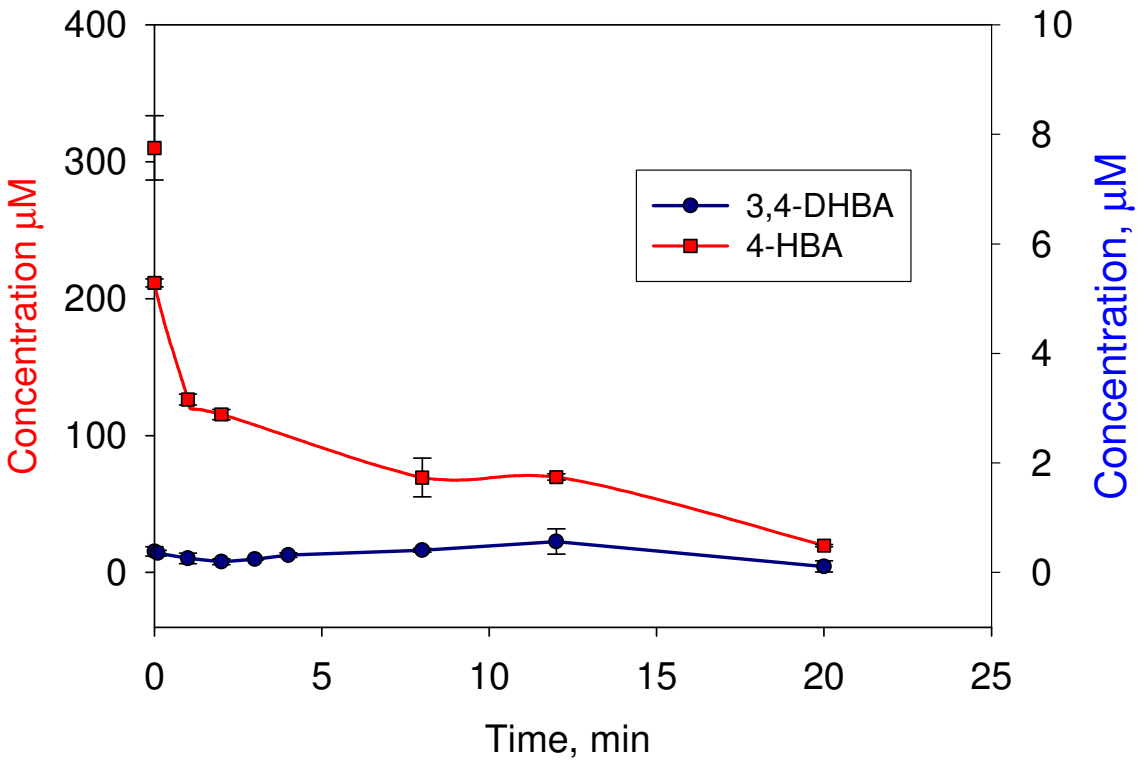

Fig 5.9: Graph illustrating concentration of 3,4-DHBA and 4-HBA after control incubation of 2mM 4-HBA and 5mM G with H_2O_2 and Fe SO_4 at 37 ^oC. Separation and detection conditions as described in Fig 5.2. Samples were injected in triplicate. The reaction was quenched in 1 ml ethanol, dried under N_2 flow and reconstituted in 1 ml 50 mM ammonium acetate buffer, pH 5.5. Standard deviations shown are of N = 3.

The non-detectable formation of 3,4-DHBA could suggest that there was only a minute amount formed and it itself was subjected to oxidation by ˙OH. There was a much slower decrease in the amount of 4-HBA over the 20 min. reaction period, which suggested that there was a direct competition of 4-HBA and G. Fe (II) has the ability to complex G at the N7 position [20] and therefore this may have

caused competition between G and the other reactants in the mixture, ultimately resulting in a much slower degradation of the 4-HBA in the solution via the Fenton reaction. The proximity of Fe to the G moiety meant that any ·OH formed would react with G. G was in excess here with respect to the 4-HBA concentration.

Therefore, it was deduced that in the presence of G, 4-HBA was not a suitable radical scavenger in this experiment. Also, due to the nature of the analysis, the formation of 8-oxoG could not be analysed accurately. At a fixed potential of 0.9 V, both G and 8-oxoG were oxidised, and as they were not separated, the 8-oxoG could not be specifically detected. It was therefore impossible to determine if the 4-HBA had any other effect or reactivity with 8-oxoG, G or any other radicals formed in this reaction. Because of the interfering effect of G in the reaction of 4-HBA with the metal of interest, this experiment was not repeated for the other metals. The metals were compared solely on their interaction with 4-HBA alone.

5.4.2.3 Ni, Co, Cu, Cd, Mn and Zn -Fenton reactions

4 mM 4-HBA was incubated with each of $NiSO_4$, $CoSO_4$, $MnSO_4$, $CuSO_4$, $CdSO_4$ and $ZnSO_4$ and 50mM H_2O_2 at 37 ^oC. The concentration of both 4-HBA and 3,4-HBA were plotted in a similar fashion to Fe, though the results are very different. The Fe incubations showed that within the first 30 s of the reaction, there was an almost complete degradation of all of the 4-HBA to form 3,4-DHBA, followed by what was probably further reaction of the product. The other metals, Ni, Co, Mn, Cd and Zn, did not show this spontaneous and rapid degradation of the 4-HBA. Instead, for Ni, Co, Cd and Cu over a 20 min. period, the concentration of

4-HBA appeared to drop in a steady slow rate over the 20 min. Fig 5.10 shows the reaction profile for Ni.

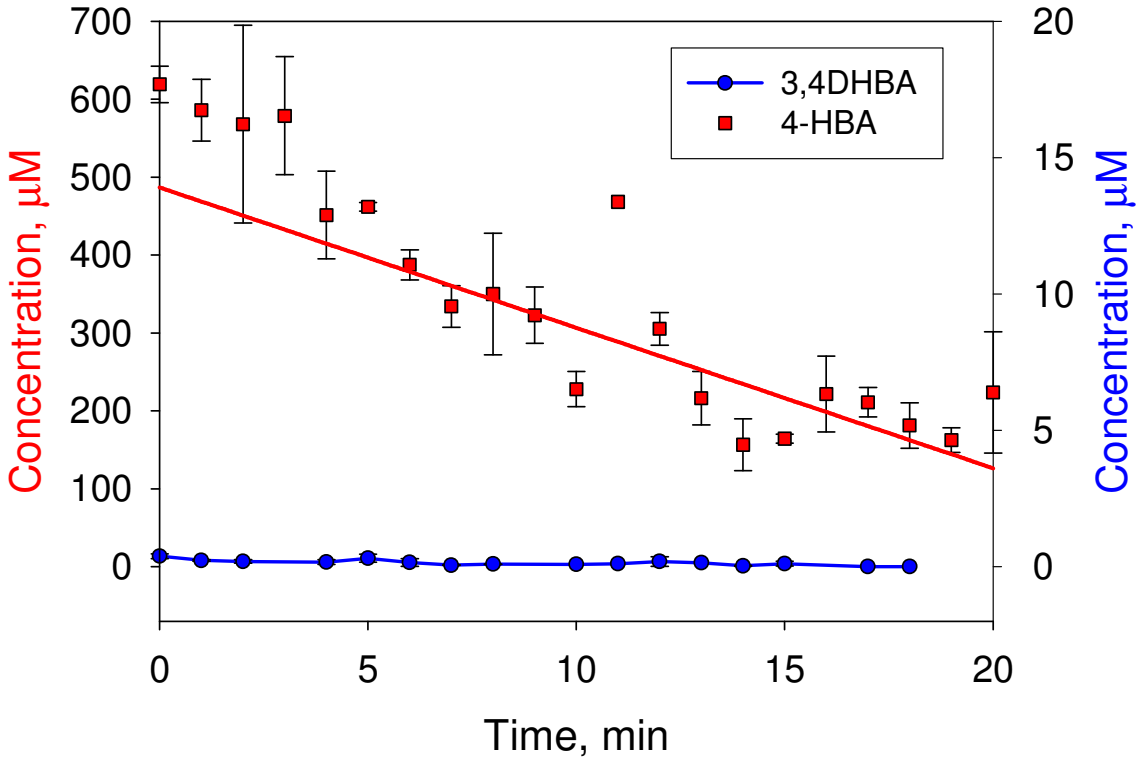

Fig 5.10: Plot of concentration of 3,4-DHBA and 4-HBA after incubation of 4-HBA with $NiSO_4$ and H_2O_2 at 37 ^oC. HPLC analysis was carried out at 2 ml min^{-1} and ECD at 0.9 V vs. Ag/AgCl. The reaction was quenched in 1 ml ethanol, dried under N_2 flow and reconstituted in 1 ml 50 mM ammonium acetate buffer pH 5.5. Samples taken in duplicate at every min. from 1- 20 min, and injected in triplicate. Standard deviations shown are of N = 6.

The concentration of 3,4-HBA was very low, in the low nM range, and in the case of Co, was below the limit of quantitation of the system. It was therefore assumed that over the course of these incubations, very little if any 3,4 DHBA was

formed from the ROS involved. None the less, there was a definite decrease in the concentration of 4-HBA over the time, indicating that the Ni and Co were involved in some reaction with the 4-HBA leading to its degradation over time, albeit slowly.

Cd and Cu also showed a decrease in concentration of the 4-HBA, although at slower rates than Co and Ni, indicating that there was a similar degradation reaction occurring. The concentration of 3,4-DHBA was again close the LOQ over the course of the incubation period. Cu is known to produce $^1O_2$ or a $^1O_2$–like product in Fenton like reactions, and these results therefore indicated that it is possible that Cd, Co and Ni are also involved in a similar $^1O_2$ producing reaction [7-9].

$MnSO_4$ and $ZnSO_4$ were also incubated in a similar manner. They did not show such a decrease in 4-HBA. There was an initial decrease in the 4-HBA concentration, but this recovered over the remainder of the incubation period. The concentration of 4-HBA and 3,4-DHBA from the Zn incubation is shown in Fig 5.11.

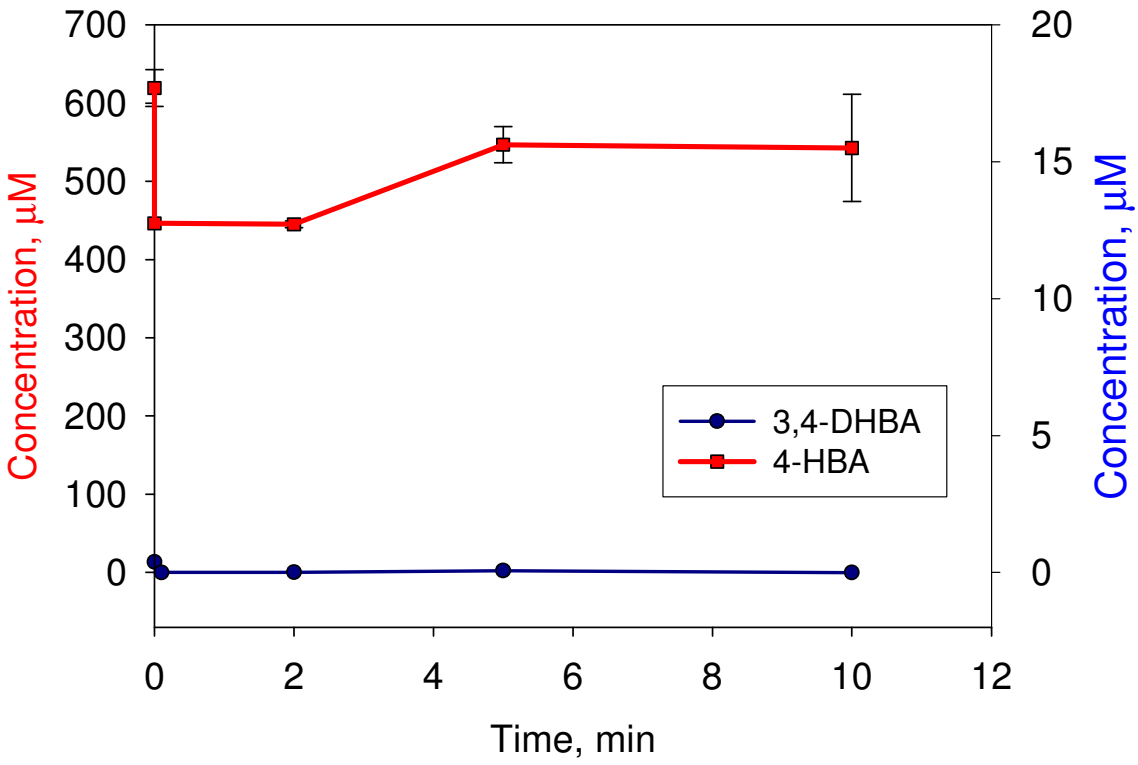

Fig 5.11: Plot of concentration of 3,4-DHBA and 4-HBA after incubation of 4-HBA with $ZnSO_4$ and H_2O_2 at 37 ^oC. HPLC analysis was carried out at 2 ml min^{-1} and ECD at 0.9 V vs. Ag/AgCl. The reaction was quenched in 1 ml ethanol, dried under N_2 flow and reconstituted in 1 ml 50 mM ammonium acetate buffer pH 5.5. Samples were injected in triplicate. Standard deviations shown are of N = 3.

This may be indicative that the ROS was not ·OH, and the ROS that was produced reacted in a different manner to ·OH. Another possibility is that the metal itself was interacting weakly with 4-HBA in such a way to diminish its ECD properties, thus causing the initial drop in concentration. The magnitude of the 4-HBA peak then increased over time, which may be indicative of the metal-4-HBA

interaction weakening. This may have been caused by stirring the solution. Again, for most of the incubation period, the concentration of 3,4-DHBA was below the LOQ of the system, and therefore it was not possible to plot the concentration of the product accurately. The level produced, if any, was too low for accurate determination, unlike that produced in the Fe incubation, and therefore it can be assumed that the oxidation by Mn and Zn was not due to ·OH, but by a different mechanism or by a different ROS.

From the results obtained in this study, there is evidence that each of the metals appears to react differently, though there appears to be three distinct groups. Fe is a definite ·OH generator, as illustrated by the formation of 3,4-HBA from the reaction of 4-HBA with Fe-Fenton reagents. The second group is composed of Ni, Co, Cd and Cu, which all caused a slow degradation of the 4-HBA over time, though little or no 3,4-DHBA was detected. Due to the nature of oxidative damage by Cu to DNA, it could be speculated that each of these metals produced $^1O_2$, a $^1O_2$– like product, or another ROS [7-9]. The third group consists of Mn and Zn, where an initial decrease in 4-HBA concentration followed by a slow recovery over time could indicate that a week interaction between the metal and the 4-HBA occurred. Transition metals have the ability of complexing organic molecules such as benzoic acids, at the carboxylic group [21-22]. As a result, this could be the reason for the slow degradation over time. Zn appears to have the weakest interaction with such molecules, therefore recovery in 4-HBA with Zn and Mn could be indicative that the interaction here is weak [23]. These weak interactions may diminish the electrochemistry of the 4-HBA initially and as the weak

interactions are broken, the concentration of free 4-HBA recovered over the rest of the experiment.

5.5 CONCLUSION

·OH is classically presumed as the ROS involved in transition metal-fenton reactions. This study confirmed that the ·OH is formed from Fe-Fenton reaction [1]. The other transition metals, Co, Cu, Ni, Cd, Mn and Zn investigated however, showed a very different reaction profile to that of Fe. Co, Cu, Ni, Cd, also, in turn showed a different profile from Zn and Mn.

The Fe-Fenton reaction caused massive burst of ·OH formation which was evident from decrease in 4-HBA and initial increase in 3,4-DHBA followed by further reaction. This was not evident when G was in competitive reaction with the 4-HBA, suggesting that alternative means such as ESR [7, 12] should be applied to the analysis of the ·OH production in G oxidation. The analysis did, however, give an insight into the comparable reactivity of the transition metals.

The Co, Ni, Cd and Cu-Fenton reactions caused a slow decrease in concentration of 4-HBA over the course of the incubation. This could indicate the involvement of a low concentration of ·OH or may be due to another radical species, for example $^1O_2$ or a $^1O_2$– like species, which has been speculated for Cu-induced oxidative damage [7-9]. Metal complexation with the benzoic acid may also have occurred over the incubation period. The relative rate of decrease of each of the metals was different, with Ni showing a faster decrease in 4-HBA concentration than Co. The level of 3, 4-DHBA formed was at the LOQ of the assay for all of these metals.

Essential metals, Mn and Zn [7], both induced an initial decay in 4-HBA concentration, with subsequent recovery. This may have been caused by a weak interaction of the metal with the 4-HBA moiety, followed by the breakdown of this interaction over time. Also, no 3,4-DHBA was detected over the course of the analysis suggesting that no damage detectable by this particular assay occurred from Mn and Zn-mediated oxidation.

The results indicate that the metals involved display differences in their mechanisms of oxidative damage and ROS production. They can be divided into three groups where Fe is the only $^{\cdot}OH$ producer, Co, Cd, Cu and Ni all produce a similar ROS which can damage 4-HBA, and Mn and Zn did not display any oxidation of 4-HBA.

5.6 REFERENCES

1. Halliwell, B. and Gutteridge J.M.;,Free Radicals in Biology and Medicine**, 2nd Edition**, Clarendon Press; New York, *Oxford University Press*, **1989**.
2. Wisemann, H; Halliwell, B.; *Biochemistry Journal*; 313; **1996**, 17-29.
3. Kiyosawa, H; Suko, M.; Okudaira, H.; Murata, K.; Miyamoto, T.; Chung, M.H.; Kasai, H.; Nishimura S.; *Free Radical Research Communications.* 11; **1990**, 23-27.
4. Loft, S.; Deng, X.S.,; Tuo; J.; Wellejus, A.; Sorensen, M; Poulsen, H.E; *Free Radical Research*.; 29; **1998,** 525–39.
5. Loft, S.; Thorling, E.B.; Poulsen, H.E.; *Free Radical Research,* 29; **1998**, 595–600.
6. Asami, S.; Manabe, H.; Miyake, J.; Tsurudome, Y.; Hirano, T.; Yamaguchi, R.; Itoh, H.; Kasai, H.; *Carcinogenesis*; 18; **1997**, 1763–1766.
7. Halliwell, B. and Gutteridge J.M.; Free Radicals in Biology and Medicine, **4th Edition**, Clarendon Press; New York, *Oxford University Press*, **2007**.
8. Bales, B.C.; Kodama, T.; Weledji, Y.N.; Pitié, M.; Meunier, B.; Greenberg, M.M., *Nucleic Acids Research*, 33; **2005**, 5371-5379.
9. Keyer, K.; Strohmeier Gort, A.; Imlay, J.A.; *Journal of Bacteriology*, 117; **1995** 6782-6790.
10. Pryor, W.A.; *Free Radical Biology and Medicine,* 4; **1988**, 219-233.
11. Ahmad, S.; *Oxidative Stress and Antioxidant defences in Biology*; Chapman and Hall Publishing, New York, **1995**.

12. Freinbichler, W.; Bianchi, L., Colivicchi, M.A.; Ballini, C.; Tipton, K.F.; Linert, W.; Della Corte, L.D.; *Journal of Inorganic Biochemistry* 102; **2008**, 1329-1333.

13. Grootveld, M.; Halliwell, B.; *Biochemical Journal*, 237; **1986**, 499-504.

14. Liu, M.; Liu, S.; Peterson, S.L.; Miyake, M.; Liu, K.J.; *Molecular and Cellular Biochemistry*, 235; **2002**, 379-385.

15. McCabe, D.R.; Maher, T.J.; Acworth, I.; *Journal of Chromatography B*, 691; **1996**, 23-32.

16. Ste-Marie, L.; Boismenu, D.; Vachon, L.; Mongomery, J,; *Analytical Biochemistry*, 241; **1996**, 67-74.

17. Hu, Y.L.; Lu, Y.; Zhou, G.J.; Xia, X.H.; *Talanta*, 74; **2008**, 760-765.

18. Marklund, N.; Clausen, F; Lewader, T.; Hillered, L.; *Journal of Neurotrauma*, 18; **2001**, 1217-1227.

19. Matteoa, D.V.; Pieruccia, M.; Giovanni, D.G.; Santoa, A.D.; Poggia, A.; Benigno, A.; Esposito, E.; *Brain Research*, 1095; **2006**, 167-177.

20. Noblitt, S.; Huehls, A.M.; Morris, Jr., D.L.; *Journal of Inorganic Biochemistry*, 101; **2007**, 536-542.

21. Griffith, W.P.; Noguiera, H.I.S.; Parkin, B.C.; Sheppard, R.N.; White, A.J.P.; Williams, D.J.; *Journal of the Chemical Society: Dalton Transactions*, 11; **1995**, 1775-1781.

22. Garg, B.S.; Sharma, R.K; Kundra, E.; *Transition Metal Chemistry*, 30; **2005**, 152-159.

23. Lee, J.Y.; Kim, J.W.; Lee, M.K.; Shin, H.J.; Kim, H.T.; Park, S.M.; *Journal of the Electrochemical Society*, 151; **2004**, C25-C31.

6 CONCLUSIONS AND FUTURE WORK

6.1 CONCLUSIONS

This thesis examined the oxidative damage to DNA mediated by various transition metals in the Fenton reaction. Analogous experimental procedures allowed for a direct comparison of results obtained for a spectrum of metal catalysts. The damage product 8-oxoG was analysed as a potential biomarker for this type of damage. The results clearly illustrated that not all of the transition metals initiate comparable levels of oxidative damage to DNA and that 8-oxoG, due to its own ease of oxidation, is not a suitable biomarker. Given this ease of oxidation, 8-oxoG oxidation products, so-called "final oxidation products" were also investigated in detail.

The erratic, almost oscillatory nature of 8-oxoG formation is not only visible for Fe and Cu [1], but in this study was also noted for Ni and Cd. Co showed an initial peak followed by no further 8-oxoG formation, while Zn and Mg showed little or no formation of 8-oxoG.

This investigation also highlighted that there was a major difference in the mechanisms of transition metal mediated oxidative damage to DNA, which is dependent on the metal involved.

Fe was previously shown to produce high levels of 8-oxoG in an oscillatory pattern over time. The 8-oxoG oxidation products observed at that point were GH and oxGH with steady formation over time [2]. The 4-HBA study carried out in this thesis confirmed that the Fe-mediated Fenton reaction produced $^{\cdot}OH$, suggesting this was the ROS involved in the high levels of oxidative damage to G.

Fe, Co, Ni and Cu all have partially filled d orbitals, and are therefore expected to exhibit high reactivities. Cu was also observed to cause an oscillatory formation of 8-oxoG as well as further oxidation products, GH and oxGH, similar to Fe [2]. Ni, Cd and Co, investigated here, all produced a similar oscillatory-type formation of 8-oxoG from G. Of these three metals, Ni generated the highest concentrations of 8-oxoG, although lower concentrations than Cu were observed. Co-mediated oxidation displayed an initial surge of 8-oxoG followed by very low concentrations over the rest of the incubation. Each of the respective metal's abilites to complex with biomolecules could have a major impact here. In the MS study in Chapter 2 and Chapter 4 of further oxidation products, oxGH and GH were identified for Ni and Co. Ni and Co gave a steady formation of oxGH from G over time, similar to Fe and Cu. Cd did not result in formation of these 8-oxoG oxidation products above the level observed in control samples. Though the products formed from oxidative damage to G by Cu, Ni, Co and Cd are similar to Fe, Chapter 5 indicates that the ROS involved in oxidative stress mediated by these metals is different to that of Fe. The reaction of H_2O_2 and each of Ni, Cu, Co and Cd with 4-HBA did not produce the $^{\cdot}OH$ reaction product 3,4-DHBA, unlike Fe. They did, however, cause a slow degradation of the 4-HBA over time suggesting the formation of a different ROS. Cu, for example, has been associated with a $^1O_2$ like or Cu-oxo species [3-5]. Each of the four metals, Ni, Cu, Co and Cd, participates in a similar 4-HBA degradation reaction, though at different rates. The similar reactions of Ni, Cu, Co and Cd with 4-HBA suggest that similar oxidation reactions

are occurring here; and comparing this with their profiles of G oxidation, the extent of oxidative damage to DNA appears to be in the order of Cu > Ni > Co > Cd.

Zn and Cd are in the same group in the periodic table, and so it would be assumed that both would react similarly, though this is not the case. Each of these metals has similarly filled d and s orbitals, with configurations of $3d^{10}$, $4s^2$ and $4d^{10}$ $5s^2$. They both caused 8-oxoG formation from G, though Cd appeared to react faster than Zn, but neither produced oxGH or GH above control sample levels. The difference in ROS formation that was observed is in agreement with other studies that have examined Cd or Zn-induced mutagenesis separately. Cd has been implicated in DNA damage due to its carcinogenesis, and displays a degradation of 4-HBA, presumably from some ROS production. Zn is not carcinogenic, however, but an essential dietary element. Zn displayed what is speculated to be an initial weak interaction with the 4-HBA which subsequently recovered over time [6-8]. Mn displayed a similar 4-HBA reaction profile to Zn, though did cause G oxidation, detected by the formation of oxGH using HPLC-MS/MS. It is assumed, therefore, that Mn does not generate an ROS that can be detected by reaction with 4-HBA, similar to Zn.

Table 6.1 summarises the results of Chapters 2-5 with respect to the differences between each transition metal investigated and the products that are formed from its reaction with G and 4-HBA.

	8-oxoG	oxGH	GH	↑[3,4-DHBA]	↓[4-HBA]
Fe	✓	✓	✓	✓	✓
Cu	✓	✓	✓	×	✓
Ni	✓	✓	✓	×	✓
Co	✓	✓	✓	×	✓
Mn	✓	✓	✓	×	×
Cd	✓	×	×	×	✓
Zn	✓	×	×	×	×

Table 6.1: Summary of Results of transition metal-Fenton-like reactions with G and with 4-HBA.

Cr was not investigated in this study as its mechanisms of carcinogenesis have already been extensively researched. Oxidative damage to DNA has been implicated among the mechanisms of Cr induced carcinogenesis, resulting in GH-like adducts [9, 10]. Oxo-atom transfer or electron abstraction is implicated in Cr oxidation of G, and not ·OH [11].

The HPLC-MS/MS study has also given vital information into the use of 8-oxoG as a biomarker of oxidative stress. While 8-oxoG is a product of G oxidation, it is also subjected to further oxidation and is easier than its precursor to oxidise. This study has highlighted its rapid further oxidation with temporal analysis of its formation and further oxidation to produce products that do not undergo such rapid

further oxidation. In cases of higher amounts of oxidation to DNA, it may be of more benefit to determine these further products in order to analyse the extent of the damage that has occurred in the DNA *in vivo*. GH and oxGH, therefore are good examples of biomarkers of oxidative stress, due to their steady accumulation over time, with no further oxidation and the fact that they also give an indication to the extent of which the DNA has been damaged.

The Fenton-like reactions of the various transition metals, Ni Cd, Co, Zn as well as Fe and Cu with DNA moieties G and 2'-dG will be influenced by a number of factors. The rates at which the different reaction rates occur need to be elucidated. The formation of $^{\bullet}OH$ from a Fenton-like reaction is implicated for Fe only, shown in these results. However, the results from the other metals are very different, which supports the recent speculation in the literature that for metals other than Fe there may be a potential formation other metal-oxo species, such as the suspected oxidative damage causing Cu-oxo complex [3]. It is also possible that $O_2^{\bullet-}$ or O_2^{2-} could be formed [4, 5].

It should be considered that all of the experiments that have been performed to date have been *in vitro*, and therefore it is important that this kind of metal induced damage is investigated *in vivo* also. The factors that will influence the *in vivo* reaction will be much more complex than that of the *in vitro* reaction. However, to gain an in depth understanding of the reactions occurring at a molecular level, it was necessary to conduct these analyses *in vitro*.

The cell has a vast array of preventative and repair mechanisms to prevent the destruction of DNA, and other vital biomolecules from oxidative stress, as well

as other stresses, which will affect the concentration of damaged DNA *in vivo*. These have been discussed previously in Chapter 1. Repair systems include nucleotide excision repair, recombinational repair [9], and base excision repair, involving the action of DNA glycosylases including base or lesion specific enzymes such as Guanine lesion specific OGG1. The cell also has a number of protective enzyme mechanisms. Various important antioxidant enzymes including superoxide dismutase, glutathione peroxidase, and catalase, are present and destroy various ROS in the system.

The effect of this particular type of oxidative stress, *e.g.* metal induced oxidative damage, should therefore be examined *in vivo*, in order to determine if the oxidation which has been observed *in vitro* can also occur in living cells. This type of examination should comprise of a cell culture study, subjecting the cells to metal induced oxidative stress, and investigating the effect of this stress on the cell.

6.2 FUTURE WORK

6.2.1 Cell culturing/Comet assay

Cell culturing and the Comet assay should be applied order to determine the effect of the ingested metal-Fenton reactions on DNA in cells, as opposed to *in vitro*. Erba *et al*. have described a method for exposing cells to Fe and determining the antioxidant effect of tea. The cells were grown, then subjected to 24 hour incubation with green tea. The cells were then washed and subjected to a 100 μmol Fe^{2+} solution and incubated for 2 hours [10]. The methodology used in this study could be applied to the study of each of the ingested metals to determine the effect

of ingestion of trace metals at various concentrations on the cell. The metal salt solution should be applied to the cell and incubated for a certain length of time. The length of time should be varied to determine if there is a similar pattern of DNA damage formed to that found using HPLC-ECD in previous studies.

The nature of the determination of damage to DNA means that the Comet assay is not able to specifically detect 8-oxoG formation or damage to specific nucleobases. Therefore, in order to determine this kind of damage, there should be another pretreatment step in order to break the DNA at specific damaged sites, where a specific enzyme would nick the DNA at particular sites that have been damaged. In order to detect 8-oxoG, the enzymes formamidopyrimidine DNA glycosylase (FapyG) and endonuclease III (Endo III) as well as human 8-oxoG DNA glycosylase (hOGG1) should be used to nick the DNA at all 8-oxoG lesion sites. Endo III and FapyG, however, are not 8-oxoG specific as they can also detect alkylated bases [11, 12]. This may present problems in ensuring the specificity of this method, and may lead to overestimation of the concentration of 8-oxoG in the sample. hOGG1, however, is 8oxoG specific, and therefore should give more accurate account of the concentration of damage.

6.2.2 Further reactive oxygen species analysis

Reactive oxygen species (ROS) have been previously discussed in detail in Chapter 1, and analysed in Chapter 5. There originally was an assumption that the $^{\cdot}OH$ was the ROS of interest here, but there has been speculation for some metals, most notably Cu, that have been studied, that there is another ROS metal-oxygen

complex involved [13]. The results obtained in the ROS study have supported this possibility for each of the metals Ni, Co, Cu, Mn, Cd and Zn as the pattern of oxidative damage to DNA was very different to that obtained for Fe. Future work should therefore include a determination of the nature of the ROS involved in their role in oxidative stress. This can be achieved in numerous ways.

·OH, the most reactive ROS that is generated *in vivo,* was determined to be the ROS involved in the Fe-Fenton reactivity. Its high reactivity is attributed to its high electrophilicity, high thermochemical reactivity as well as its production near to DNA *in vivo*. It acts by adding to DNA as well as abstracting H atoms [14, 15]. This is important as it sets Fe-induced oxidative stress apart from the other transition metals investigated.

It is also important to determine if the 8-oxoG oscillations observed in these transition metal experiments are caused by the redox capability of the metal involved, by the ROS involved, or by another means. Selectively producing ·OH and determining the extent of damage that is caused, as well as monitoring if ·OH alone can cause the "oscillatory" pattern, could lead to important information about the role of the ROS in the reaction system. The selective production of ·OH has been accomplished by Aveline *et al*. who manipulated the photochemistry of N-Hydroxy-2(1H)pyridine to selectively produce ·OH, as illustrated in scheme 6.1. The second pyridyloxyl radical shows little reactivity with DNA. G could be subjected to this ·OH and the damage caused can be monitored over time. These results could then be compared to results obtained from a Fe-Fenton reaction [16] and other metal mediated DNA damage profiles.

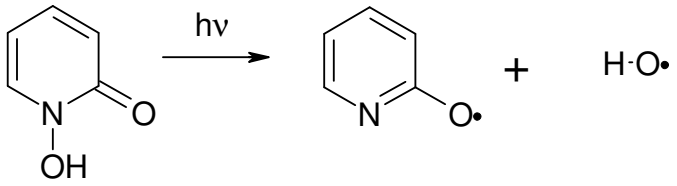

Scheme 6.1: Selective formation of ·OH from the photodecomposition of N-Hydroxy-2(1H)pyridine [16].

6.2.3 DNA oxidation products as biomarkers

The determination of a stable and detectable biomarker for oxidative damage to DNA is important in order to be able to learn about the mechanisms of this damage *in vivo* with a view to detecting initiation and early proliferation of important diseases. The identification of these biomarkers is therefore also important. This study has shown that in DNA, G results in a stable production over time of GH. The further study of this as an oxidation product is paramount.

G is not the only susceptible target of oxidation in DNA, however. The other 3 DNA bases are subjected to damage also, though G is generally used due to its ease of oxidation. (An exception to this is $^1O_2$, which only causes oxidative damage to G, due to its lower oxidation potential.) It is therefore important to analyse the damage caused to the other bases, in order to get a more complete picture of the damage caused to DNA by this type of oxidative stress. Preliminary results from the mass spectrometric study conducted in Chapter 4 show interesting and pursuable results for the oxidation of T. Thymine has been noted to undergo oxidative damage

in DNA. Cyclobutane dimers have been observed from radiation induced damage and thymine glycol (TyGly) from ROS induced damage to T [17-19].

The presence of TyGly is important for the determination of oxidative damage to DNA as it gives us a second parameter to assess in the analysis of oxidative stress. By looking at two lesions, oxGH/GH and TyGly, more can be learned about the type and the extent of damage that the DNA has undergone. Due to the nature of the implications of oxidative stress and its links with important modern diseases, it is very important to understand the mechanisms that cause and propagate such diseases. The presence of a biomarker for such damage is therefore vital, and the determination of more than one, could lead to a more thorough understanding of their modes of action.

The biomarkers GH and TyGly should be investigated *in vivo*, or in animal studies, with a goal to determine their role in oxidative stress and disease. Ultimately using these biomarkers in clinical studies as indicators of early signs of aging, disease, neurological stress and even inflammation could be of benefit in developing a more thorough understanding of these disorders, with a view to prevention or a cure.

6.2.4 Mechanistic studies

Significant studies investigating the mechanisms of oxidative damage to DNA have been discussed in Chapter 1. The various mechanisms; however, only detail the products that are formed, not the kinetics of these reactions as time

progresses, minute by minute, with various reactants and radical species constantly being formed, reacting further and being used up to form final stable products.

The oscillatory formation of 8-oxoG that has been noted in this study, suggests that there is a very intricate and complicated mechanism involved in the transition metal mediated Fenton oxidation of G. There are a number of various oscillatory and chaotic reactions which have been elucidated, such as the Belousov Zhabotinski (BZ) reaction, and the Brey Liebhafsky (BL) reaction, for example. By studying closely the mechanisms of these reactions, it should be possible to learn about the driving forces, the kinetics and what starting materials intermediate species are important for driving oscillatory and chaotic reactions, and therefore gain a better understanding of the mechanisms behind the erratic formation of 8-oxoG [20, 21].

A mathematical study of the model the Fenton mediated oxidation of G will allow it to be fitted against some oscillatory mechanisms such as the BZ and the BL reactions. The modelling of the oxidation mechanism involves designing experiments for measuring and stressing parameters of the reactions involved and determination of the effect that this has on the reaction kinetics, intermediate and product formation. Stressing parameters theoretically by modelling mathematically, may determine the optimal conditions for the reaction to occur with reproducible oscillations of 8-oxoG, and this can then be examined experimentally.

6.3 REFERENCES

1. Cotton, F.A.; Wilkinson, G.; Gaus, P.L.; *Basic Inorganic Chemistry*, **3rd Edition**, J. Wiley Publishers, New York, USA, **1995**.
2. White, B.; Smyth, M.R.; Stuart, J.D.; Rusling, J.F.; *Journal of the American Chemical Society*, 125; **2003**, 6604-6605.
3. Bales, B.C.; Kodama, T.; Weledji, Y.N.; Pitié, M.; Meunier, B.; Greenberg, M.M., *Nucleic Acids Research*, 33; **2005**, 5371-5379.
4. Keyer, K.; Strohmeier Gort, A.; Imlay, J.A.; *Journal of Bacteriology*, 117; **1995**, 6782-6790.
5. Halliwell, B.; Gutteridge, J.M.C.; Free Radicals in Biology and Medicine, **2nd Edition**, Clarendon Press, New York, Oxford University Press, **1989**.
6. Chater, S.; Douki, T.; Garrel, C.; Favier, A.; Sakly, M.; Melek, A.; *Comptes Rendus Biologies*, 31; **2008**, 426-432.
7. Hartwig, A.; *Toxicology Letters*, 102-103, **1998**, 235-239.
8. Filipic, M.; Hei, T.K.; *Mutation Research: Fundamental and Molecular Mutagenesis*, 546; **2004**, 81-91.
9. Codd, R.; Dillon, C.T.; Levina, A.; Lay, P.A.; *Coordination Chemistry Reviews*, 216; **2001**, 537-582.
10. Sugden, K.D.; Campo, C.K.; Martin, B.D.; *Chemical Research in Toxicology*, 14; **2001**, 1315-1322.
11. Slade, P.G.; Priestly, N.P.; Sugden, K.D.; *Organic Letters*, 9; **2007**, 4411-4414.
12. de Boer, J.; Hoejmaker J.H.J.; *Carcinogenesis*, 21; **2000**, 453-460.

13. Erba, D.; Riso, P.; Colombo, A.; Testolin, G.; *Journal of Nutrition*, 129; **1999**, 2130-2134.

14. Smith, C.C.; O'Donovan, M.; Martin, E.; *Toxicology*, 226; **2006**, 36.

15. Collins, A.; Gedik, C.M.; *FASEB Journal*, 19; **2005,** 882-84.

16. Bales, B.C.; Kodama, T.; Weledji, Y.N.; Pitié, M.; Meunier, B.; Greenberg, M.M., *Nucleic Acids Research*, 33; **2005**, 5371-5379.

17. Pryor, W.A.; *Free Radical Biology and Medicine*, 4; **1988**, 219-233.

18. Ahmad, S.; *Oxidative Stress and Antioxidant defences in Biology*; Chapman and Hall Publishing, New York, **1995**.

19. Aveline, B.M.; Kockevar, I.E.; Redmond, R.W.; *Journal of the American Chemical Society,* 118; **1996**, 10124-10133.

20. Cooke, M.S.; Lunec, J.; Evans, M.D.; *Free Radical Biology and Medicine*, 33; **2002**, 1601-1614.

21. Cadet, J.; Delatour, T.; Douki, T.; Gasparutto, D.; Pouget, J.P.; Ravanat, J.L.; Sauviago, S.; *Mutation Research: Fundamental and Molecular Mechanisms of Mutagenesis*, 424; **1999**, 9-21.

22. Douki, T.; Court, M.; Cadet, J; *Journal of Photochemistry and Photobiology B: Biology*, 54; **2000**, 145-154.

23. Scott, S.K.; *Chemical Chaos*, Oxford University Press, **1991**.

24. Scott, S.K.; *Oscillations, Waves and Chaos in Chemical Kinetics*, Oxford Chemistry Primers, **1994**.

7 APPENDICES

7.1Appendix 1a: MS PARAMETERS FOR POSITIVE ESI

Mode	
Mass Range mode	Std/Normal
Ion Polarity	Positive
Ion Source Type	ESI
Current Alternating Ion Pol	N/A
Alternating Ion Polarity	N/A
Detector & Block Vages	
Multiplier Vage	1750 V
Dynode Vage	7.0 kV
Scan Delay	500 µs
Skimmer 1 Block	0.0 V
Skimmer 2 Block	300.0 V
Tune Source	
Trap Drive	25.1
Skim 1	15.0 V
Skim 2	6.6 V
Octopole RF Amplitude	111.5 Vpp
Octopole Delta	2.74 V
Lens 1	-4.0 V
Lens 2	-64.4 V
Octopole	2.51 V
Capillary Exit	82.9 V
Cap Exit Offset	53.3 V
HV End Plate Offset	-638 V
Current End Plate	1108.97 nA
HV Capillary	4000 V
Current Capillary	98.882 nA
Dry Temp (measured)	354 °C
Dry Gas (measured)	8.01 l/min
Nebulizer (measured)	50.56 psi
Trap	
Scan Begin	50.00 m/z
Scan End	400.00 m/z
Averages	20 Spectra
Charge Control	On
ICC Target	50000
ICC Actual	59913
Accumulation time	100000 µs
Max. Accu time	100000 µs

MS/MS Manual Mode	
Fast Calc	On
ISTD	Off
MS/MS Automatic	
Auto MS/MS	Off
Rolling Averaging	
Rolling	Off
Compressed Spectra	
Compressed Spectra	Off

7.2Appendix 1b: MS PARAMETERS FOR NEGATIVE ESI

Mode	
Mass Range mode	Std/Normal
Ion Polarity	Negative
Ion Source Type	ESI
Current Alternating Ion Pol	N/A
Alternating Ion Polarity	N/A
Detector & Block Vages	
Multiplier Vage	1750 V
Dynode Vage	7.0 kV
Scan Delay	500 µs
Skimmer 1 Block	0.0 V
Skimmer 2 Block	-300.0 V
Tune Source	
Trap Drive	33.5
Skim 1	-15.0 V
Skim 2	-6.0 V
Octopole RF Amplitude	105.9 Vpp
Octopole Delta	-2.40 V
Lens 1	5.0 V
Lens 2	60.0 V
Octopole	-2.23 V
Capillary Exit	-82.9 V
Cap Exit Offset	-67.9 V
HV End Plate Offset	-638 V
Current End Plate	1452.47 nA
HV Capillary	4000 V
Current Capillary	89.366 nA
Dry Temp (measured)	355 °C
Dry Gas (measured)	8.01 l/min
Nebulizer (measured)	50.56 psi
Trap	
Scan Begin	50.00 m/z
Scan End	400.00 m/z
Averages	20 Spectra
Charge Control	On
ICC Target	50000
ICC Actual	6885
Accumulation time	100000 µs
Max. Accu time	100000 µs

MS/MS Manual Mode	
Fast Calc	On
ISTD	Off
MS/MS Automatic	
Auto MS/MS	Off
Rolling Averaging	
Rolling	Off
Compressed Spectra	
Compressed Spectra	Off

7.3 POSTER PRESENTATIONS

- **Responses to DNA Damage: Insights from Chemical, Biochemical, Structural Biology and Cellular Studies**

University of Sussex, Brighton, United Kingdom, 19 - 21 September 2005
"Generation of 8-oxoGuanine by carcinogenic metal Nickel"
Michele Kelly, Gillian Whitaker, **Blánaid White**, Malcolm R. Smyth

- **4nd Biennial Conference on Analytical Sciences in Ireland**

Dublin Institute of Technology, Kevin Street, Dublin 24, Ireland, 11-12 April 2006
"A study of the mechanisms of oxidative DNA damage by Nickel"
Michele Kelly, Gillian Whitaker, Blánaid White, Malcolm R. Smyth

- **ESEAC 2006. 11th International Conference on Electroanalysis**

National Engineering School for Chemistry and Physics, University of Bordeaux, Bordeaux, France, 6-10 June 2006
"*A study of oxidative DNA damage using electrochemical detection***"**
Michele Kelly, Blánaid White, Gillian Whitaker, Malcolm R. Smyth

- **Analytical Research Forum 2007**

University of Strathclyde, Glasgow, UK, 16 – 18 July 2007
"*Monolith HPLC-UV-ECD analysis of oxidative DNA damage***"**
Michele Kelly, Blánaid White, Malcolm R. Smyth

- **Oxidative Damage Workshop**

Dublin City University, 28 March 2008
"A study of oxidative DNA damage caused by ingested transition metals"
Michele Kelly, Blánaid White, Malcolm R. Smyth

- **Bioanalysis in Oxidative Stress**

University of Exeter, United Kingdom, 2-3 April 2008
"A study of oxidative DNA damage caused by ingested transition metals"
Michele Kelly, Blánaid White, Malcolm R. Smyth

7.4 ORAL PRESENTATION

- **Nucleic Acids Group Research Forum.**

University of Reading, United Kingdom, 6 July 2007.
"Detection of Oxidative DNA Damage from Ingested Metals"
Michele Kelly, Blánaid White, Malcolm R. Smyth

7.5 PUBLICATIONS

- Kelly, M.C.; Whitaker, G.; White, B.; Smyth, M.R.; **Nickel(II)-catalysed oxidative guanine and DNA damage beyond 8-oxoguanine***; Free Radical Biology and Medicine*, 42 (11), **2007**, 1680-1689.

- Kelly, M.C.; White, B.; Smyth, M.R.; **Separation of oxidatively damaged DNA nucleobases and nucleosides on packed and monolith C_{18} columns by HPLC-UV-EC**; *Journal of Chromatography B*, 863; **2008**, 181-186.

- Kelly, M.C.; White, B.; Smyth, M.R.; **Oxidative damage to DNA by transition metals Co, Mn, Zn and Cd**; *Manuscript in process*; **2008**.